FINAL RESEARCH REPORT

DYNAMIC RESPONSE OF THREE-DIMENSIONAL RIGID EMBEDDED FOUNDATIONS

NSF GRANT - NSF ENV 76-22632

PRINCIPAL INVESTIGATOR: J. ENRIQUE LUCO

OTHER PARTICIPANTS: GERALD A. FRAZIER
STEVEN M. DAY
RANDY J. APSEL

UNIVERSITY OF CALIFORNIA, SAN DIEGO

1978

50272-101

REPORT DOCUMENTATION PAGE	1. REPORT NO. NSF/RA-780499	2.	PB 296617

4. Title and Subtitle
Dynamic Response of Three Dimensional Rigid Embedded Foundations

5. Report Date
1978

6.

7. Author(s)
J.E. Luco, G.A. Frazier, S.M. Day, et al

8. Performing Organization Rept. No.

9. Performing Organization Name and Address
University of California, San Diego
Department of Applied Mechanics and Engineering Science
La Jolla, California 92093

10. Project/Task/Work Unit No.

11. Contract(C) or Grant(G) No.
(C)
(G) ENV7622632

12. Sponsoring Organization Name and Address
Applied Science and Research Applications (ASRA)
National Science Foundation
1800 G Street, N.W.
Washington, D.C. 20550

13. Type of Report & Period Covered

14.

15. Supplementary Notes

16. Abstract (Limit: 200 words)

This research focuses on the dynamic response of rigid three-dimensional foundations embedded in the soil and excited by external forces as well as by different types of seismic waves. The response of foundations to these types of excitations plays a key role in the evaluation of the response of structures to wind and earthquake loads. Two methods to obtain the dynamic response of foundations were developed and tested. The first method is based on performing a transient finite element analysis for a set of impulsive motions of the foundation. This method eliminates the nonphysical reflections from the model's boundaries, and is more efficient than other finite element analyses in the frequency domain. The second method is based on an integral equation formulation of the boundary-value problem which employs the Green's functions for layered viscoelastic media. The accuracy of both methods was tested by cross-comparison and by comparison with available analytical solutions. The effects that the geometry of the foundation, the contact conditions at the foundation-soil interface, the attenuation mechanisms in the soil, and the stratification of the soil have on the dynamic response of foundations have been studied in detail. The response of embedded foundations to different types of seismic waves has also been studied. Some of the techniques developed in the course of this project have permitted significant advances in the study of the dynamic response of piles and in related areas such as strong-motion and ocean bottom seismology.

17. Document Analysis a. Descriptors

Earthquakes
Dynamic structural analysis
Earthquake resistant structures
Seismic waves
Seismic surveys
Dynamic response
Pile structures
Greens function

b. Identifiers/Open-Ended Terms
Strong-motion seismology
Ocean bottom seismology
Rigid three-dimensional foundations

c. COSATI Field/Group

18. Availability Statement
NTIS

19. Security Class (This Report)

20. Security Class (This Page)

21. No. of Pages
108

22. Price
A06-A01

TABLE OF CONTENTS

TABLE OF CONTENTS
(continued)

ABSTRACT

The project was addressed to the study of the dynamic response of rigid three-dimensional foundations embedded in the soil and excited by external forces as well as by different types of seismic waves. The response of foundations to these types of excitations plays a key role in the evaluation of the response of structures to wind and earthquake loads.

Two methods to obtain the dynamic response of foundations were developed and tested. The first method is based on performing a transient finite element analysis for a set of impulsive motions of the foundation. This method eliminates the nonphysical reflections from the model's boundaries, and is more efficient than other finite element analyses in the frequency domain. The second method is based on an integral equation formulation of the boundary-value problem which employs the Green's functions for layered viscoelastic media. The accuracy of both methods was tested by cross-comparison and by comparison with available analytical solutions.

The effects that the geometry of the foundation, the contact conditions at the foundation-soil interface, the attenuation mechanisms in the soil, and the stratification of the soil have on the dynamic response of foundations have been studied in detail. The response of embedded foundations to different types of seismic waves has also been studied.

Some of the techniques developed in the course of this project have permitted significant advances in the study of the dynamic response of piles and in related areas such as strong-motion and ocean bottom seismology.

1. INTRODUCTION

1.1 Objectives of the Study

The dynamic force-displacement relationships for embedded foundations play an important role in the study of the dynamic response of foundations of vibratory machines as well as in the analysis of the interaction between structures and the soil for dynamic loads such as wind and seismic excitation.

Most of the limited information available on the dynamic response of embedded foundations is restricted to the case of external excitation, i.e. to external forces and moments acting on the foundation. While this information is sufficient to analyze the response of foundations of vibratory machines and the soil-structure interaction effects for wind loads, it does not allow a complete analysis of the soil-structure interaction problem under earthquake excitation. In the latter case it is necessary to determine, in addition, the dynamic response of the foundation to seismic waves propagating through the soil.

It is the objective of this study to analyze the dynamic response of the three-dimensional embedded foundations subjected to two types of excitation: (i) harmonic external forces and moments and (ii) seismic excitation represented by plane waves with harmonic-time dependence and various angles of incidence. In the model under consideration, the three-dimensional foundation is assumed to be rigid and embedded in a layered viscoelastic half-space representing the soil (Fig. 1.1). Two different types of boundary conditions are considered: welded contact between the foundation and the surrounding soil, and the case in which lateral separation exists between the foundation and the soil (Fig. 1.2).

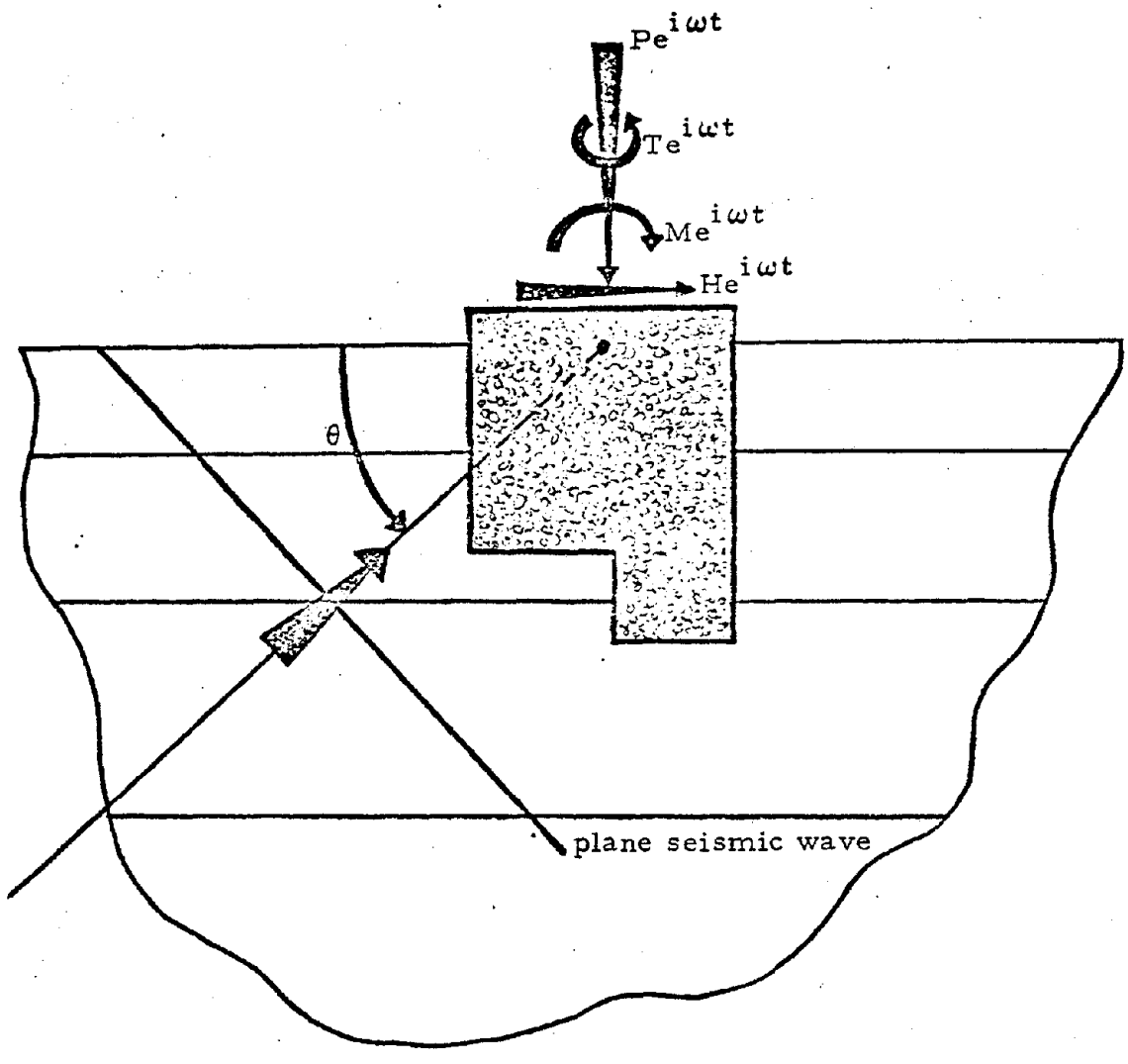

Figure 1.1. Description of the model and excitation

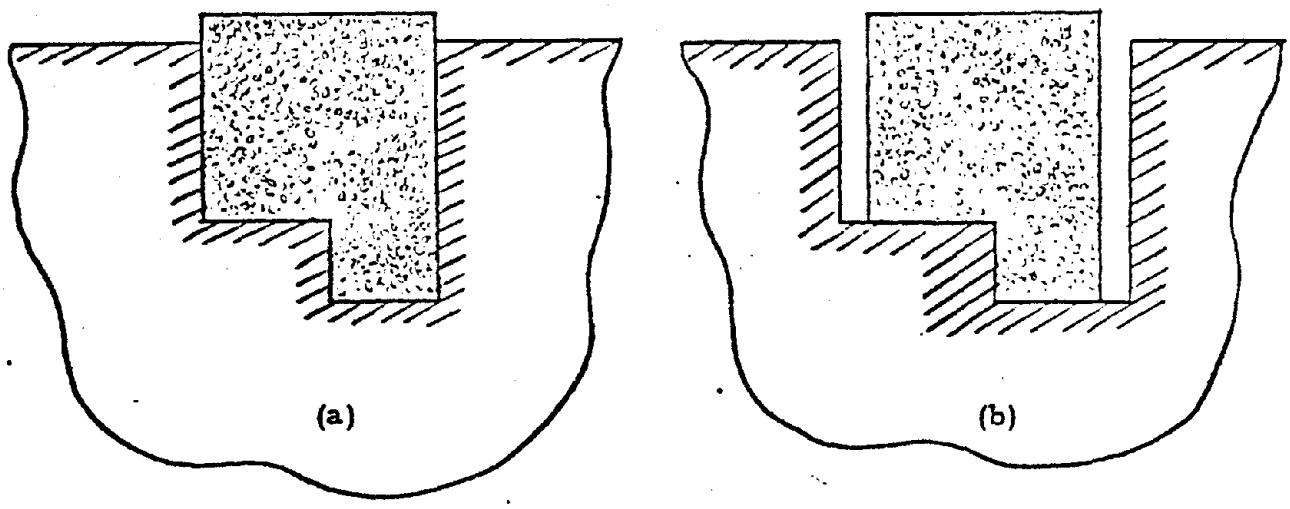

(a) Cast-in-place conditions;

(b) Free lateral conditions.

The problem of determining the harmonic dynamic response of embedded foundations to external forces and moments constitutes a mixed boundary-value problem in elasticity. Of main interest is the evaluation of the force-displacement relationship for the foundation, which, when expressed in matrix form, involves the impedance matrix for the foundation. A transient finite-element technique and an integral equation approach have been developed in the course of this study to obtain the impedance matrices for a variety of rigid embedded foundations. The results obtained by use of both methods have been validated by comparisons with each other and with available analytical solutions.

The dynamic response of embedded foundations to seismic excitation is analyzed through a sequence of three steps. First, the free-field ground motion in a horizontally layered soil is evaluated using analytical methods. Second, the diffracted field that results from the presence of the embedded foundation is obtained. In this step the foundation is assumed to be immovable, and the forces and moments required to keep the foundation fixed are evaluated. Both the transient finite-element technique and the integral equation approach are used to determine these "driving" forces and moments. In the third step, the response of the foundation to the "driving" forces is obtained. This step entails the use of the impedance matrix for the foundation together with the "driving" forces determined the second step. The response of the foundation obtained by this procedure is designated as "foundation input motion" and corresponds to one of the key elements involved in the evaluation of the dynamic response of structures to seismic excitation. It is important to mention that the impedance matrix and the foundation input motion are independent of

the characteristics of the superstructure and may then be used for different structural models or configurations.

The two methods developed to obtain the impedance matrices and the foundation input motion for three-dimensional embedded foundations will permit in the future a realistic assessment of the response of structures subjected to seismic excitation.

In the next section, a review of the state-of-the-art previous to this study is presented. The basic equations describing the dynamic response of rigid embedded foundations are presented in Section 2.1. Brief descriptions of the integral equation and finite-element techniques are presented in Section 2.2 and 2.3, respectively (complete descriptions may be found in Refs. I.1 and I.2). Chapter 3 is devoted to the presentation and results on the response of rigid embedded foundations subjected to external forces and moments. In particular, the effects of embedment are presented in Section 3.1, 3.2 and 3.3, the effects of material damping are described in Section 3.4, while the effects of lateral separation and of the layering are presented in Section 3.5 and 3.6, respectively. The response of foundations to seismic waves is discussed in Chapter 4. The response of different types of foundations to vertically incident waves are presented in Sections 4.1 and 4.3, while the corresponding results for horizontally incident SH-waves are presented in Sections 4.2 and 4.4. The conclusions arrived at are summarized in Chapter 5.

1.2 Review of the Literature

Complete analytical evaluations of the dynamic response of embedded foundations to external forces and moments have been reported only for simple models of the foundation. The two-dimensional antiplane vibrations of infinitely long rigid foundations have been studied by several authors: Luco [A1] and Trifunac [A2] have considered the case of a semi-circular cross section; Wong and Trifunac [A3], and Luco et al. [A4], studied the case of semi-elliptical cross sections; a method of solution for arbitrary cross sections has been presented by Wong [A5]; while Thau and Umek [A6], Dravinski [A7], and Dravinski and Thau [A8] have considered the case of rectangular cross sections. The two-dimensional plane-strain vibrations of a rigid foundation with rectangular cross section have been studied by Umek [A9], Thau and Umek [A10], Dravinski [A7] and Dravinski and Thau [A11]. Exact analytical solutions for three-dimensional embedded foundations are available only for axisymmetric foundations excited by an external torque: Luco [A12], and Apsel and Luco [A13] have studied the torsional response of a hemispherical and a semi-ellipsoidal foundation, respectively. The static torque-twist relation for a rigid cylinder embedded in an elastic medium has been obtained by Luco [A14].

Given the difficulties of obtaining exact analytical solutions, several approximate analytical approaches have been proposed. The best-known approximate methods may be classified as: the Baranov-Novak approach, Tajimi's approach, and Ohsaki's approach. In the first two procedures, it is assumed that the soil reactions at the base of the foundation are equal to those of a foundation placed on

the surface of the soil, while the lateral soil reactions are evaluated independently. In 1967, Baranov [B1] proposed that the lateral reactions may be evaluated by considering an independent layer surrounding the foundation. This layer in turn is represented by a series of infinitesimally thin independent layers. Compatibility between layers and the underlying half-space is satisfied only at the foundation and very far from it. This approach has been extensively used by Novak and associates [B2 - B8] to obtain the dynamic response of a rigid cylindrical foundation embedded in an elastic half-space. Tajimi's approach is based on the assumption that the reactions acting on the sides of the embedded foundation are equal to those of a layer resting on a rigid base located at a depth corresponding to the embedment depth. The vertical displacement at any point of the layer is neglected and only rocking motion of the foundation, represented by a circular cylinder, is considered [C1]. Tajimi's original work has been extended to consider coupled horizontal-rocking motion [C1 - C3], and to remove the rigid base condition [C4].

A more general approximate approach has been used by Ohsaki [D1] to determine the static force-displacement relation for a rigid foundation embedded in an elastic half-space. Ohsaki's approach consists of replacing the foundation by a set of concentrated forces distributed over the volume previously occupied by the foundation. The amplitudes of the concentrated forces are determined by imposing the boundary conditions on the contact area between the foundation and the soil. The integral equation approach used in this study corresponds to an extension of Ohsaki's method to the dynamic case.

The finite element method has been used in the past to determine the frequency response of cylindrical foundations embedded in an

elastic half-space and excited by external loads. Lysmer E1 , and Lysmer and Kuhlemeyer [E2] have studied the vertical response; Kaldjian [E3, E4], Waas and Lysmer [E5], and Waas [E6] have considered the torsional response; while Urlich and Kuhlemeyer [E7] and Kausel, et al. [E8, E9] have studied the coupled rocking and lateral vibrations of embedded foundations. In these studies, the solution was obtained in the frequency domain and special nonreflecting boundaries were used to avoid the problem associated with the finite size of the soil model. A different discrete representation of the soil, analogous to a finite difference scheme, has been used by Krizek, et al. [F1], and Parmelee and Weesakul [F2] to obtain plane-strain solutions for embedded foundation problems. The finite element approach used in the present study differs from the methods listed above in that a solution in time is obtained first in an attempt to eliminate the boundary effects while considerably reducing the cost of the analysis (refer to Section 2.3).

A reasonable number of experimental studies of the dynamic response of mebedded foundations to external loads have been conducted by various researchers [G1 - G9].

The number of studies devoted to the determination of the dynamic response of embedded foundations to seismic waves is quite limited, particularly for the case of three-dimensional foundations. Analytical studies have been conducted for two-dimensional antiplane [A1 - A8], and plane-strain models [A7, A9 - A11]. For three-dimensional models, only the torsional response for obliquely incident plane SH-waves has been obtained [A12, A13]. Tajimi's approximate approach has also been used to determine the response of a cylindrical foundation to vertically incident plan SH-waves [C1 - C4]. Although

the finite element method is used quite frequently to solve complete soil-structure interaction problems, no detailed finite element studies have been conducted on the response of embedded foundations to obliquely incident seismic waves.

2. STATEMENT OF THE PROBLEM AND METHODS OF SOLUTION

2.1 System Considered and Basic Equations

The system considered in the study is illustrated in Figs. 1.1 and 2.1. It consists of a rigid massless foundation of arbitrary shape bonded to a layered viscoelastic half-space. The bond between the foundation and the surrounding soil may be perfect, in which case the foundation is welded to the soil, or may be partial in the sense that separation may exists between the foundation and the soil. The viscoelastic medium consists, in general, of several parallel layers overlying a viscoelastic half-space. Each viscoelastic layer is characterized by a shear wave velocity β_i, a compressional wave velocity α_i, a density ρ_i, and attenuation constants $Q_{\beta i}$ and $Q_{\alpha i}$ for shear and compressional waves, respectively. In particular, the type of attenuation considered in such that the complex shear modulus is given by $G^* = \rho\beta^2(1 + 2i\xi)$ where the damping ratio for shear waves $\xi = (2Q_\beta)^{-1}$.

The foundation is excited by harmonic external forces having for resultant $(P_x, P_y, P_z)e^{i\omega t}$ acting at the origin of the coordinate system. The resultant moment of the external forces about the origin of the coordinate system is $(M_x, M_y, M_z)e^{i\omega t}$. The foundation may also be excited by seismic waves imping on the foundation with different angles of incidence. The objective of the study is to obtain the response of the foundation for both types of excitation.

It is convenient to consider first the case in which the foundation is excited by external forces and moments in absence of seismic excitation. The response of the rigid foundation to these forces and moments can be described by the motion $(\Delta_x, \Delta_y, \Delta_z)e^{i\omega t}$ of a

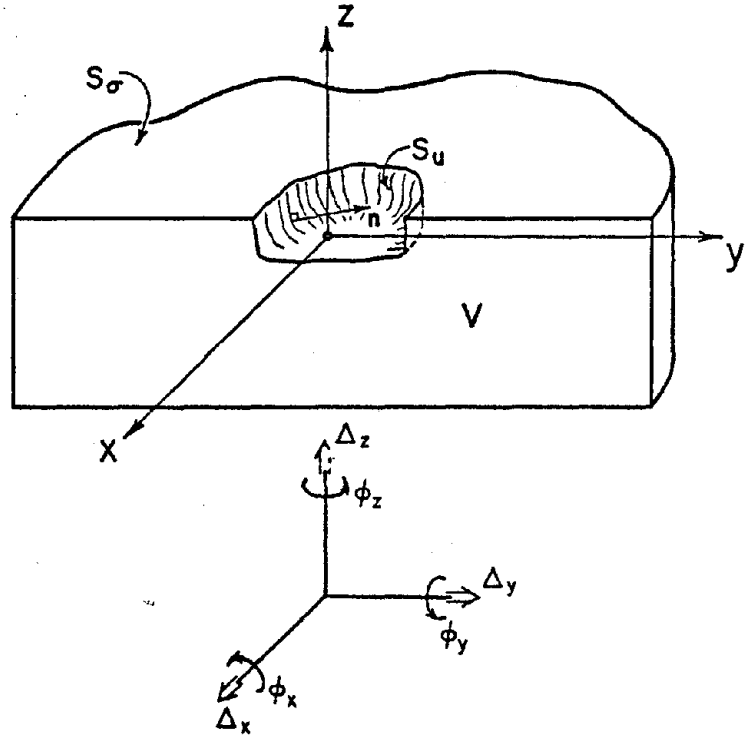

Figure 2.1. Problem geometry and coordinate system for analysis of embedded foundations.

reference point (origin of the system of coordinates in most cases) and by the rotation vector $(\phi_x, \phi_y, \phi_z)e^{i\omega t}$. The sign convention for the different components is illustrated in Fig. 2.1.

The relationship between the external forces and the motion of the foundation may be expressed in the form

$$\{\Gamma\} = [K(\omega)]\{\Delta\} \tag{2.1}$$

where $[K(\omega)]$ is the 6×6 impedance matrix, $\{\Gamma\}$ is the vector of generalized forces

$$\{\Gamma\} = (P_x, P_y, P_z, M_x, M_y, M_z)^T \tag{2.2}$$

and

$$\{\Delta\} = (\Delta_x, \Delta_y, \Delta_z, M_x, M_y, M_z)^T \tag{2.3}$$

is the vector of generalized displacements. The impedance matrix $[K(\omega)]$ which is frequency dependent completely characterizes the response of the foundation to external forces and moments. From Eq. (2.1) it is found that the motion of the foundation when excited by external forces in absence of seismic excitation is given by

$$\{\Delta\} = [K(\omega)]^{-1}\{\Gamma\} \tag{2.4}$$

where $[K(\omega)]^{-1}$ is the compliance matrix for the foundation.

The foundation motion due to seismic excitation in the absence of other external forces is denoted by $\{\Delta^*\}e^{i\omega t}$ and designated the "input motion." The input motion $\{\Delta^*\}$ depends on the geometry of the foundation and on the nature of the incident seismic disturbance.

In the general case, the total motion of the foundation is given by

$$\{\Delta\} = [K(\omega)]^{-1}\{\Gamma\} + \{\Delta^*\} \tag{2.5}$$

which can also be written in the form

$$\{\Gamma\} = [K(\omega)](\{\Delta\} - \{\Delta^*\}) \quad . \tag{2.6}$$

In the typical soil-structure interaction problem, the generalized external forces acting on the foundation correspond to the forces and moments that the superstructure exerts on the foundation. In this case, it is possible to write

$$\{\Gamma\} = \omega^2[M(\omega)]\{\Delta\} \tag{2.7}$$

in which $[M(\omega)]$ is a 6×6 "equivalent" mass matrix that depends on the characteristics of the superstructure.

Substitution from Eq. (2.7) into Eq. (2.6) leads to the following solution for the interaction problem

$$\{\Delta\} = ([I] - \omega^2[K(\omega)]^{-1}[M(\omega)])^{-1}\{\Delta^*\} \tag{2.8}$$

where $[I]$ denotes the 6×6 identity matrix. Equation (2.8) reveals that the soil-structure problem can be easily solved once the impedance matrix $[K(\omega)]$ and the foundation input motion $\{\Delta^*\}$ are known.

To determine the foundation input, it is convenient to refer to Eq. (2.5). This equation indicates that for the foundation to remain fixed ($\{\Delta\} = 0$) it is necessary to apply external forces

$$\{\Gamma^*\} = -[K(\omega)]\{\Delta^*\} \quad . \tag{2.9}$$

The force $-\{\Gamma^*\}$ is designated "driving" force. Equation (2.9) reveals that the foundation "input motion" $\{\Delta^*\}$ can be obtained if the forces necessary to keep the foundation fixed under the effects of the seismic excitation are evaluated. In this case, $\{\Delta^*\}$ is obtained from

$$\{\Delta^*\} = -[K(\omega)]^{-1}\{\Gamma^*\} \quad . \tag{2.10}$$

2.2 Integral Equation Method of Solution

To describe the integral equation method of solution, it is convenient to consider the general case of an intrusion occupying the volume V' embedded in a layered viscoelastic half-space occupying the volume V (Fig. 2.2). The interface between the intrusion and the surrounding medium is represented by the surface S.

Assuming harmonic time dependence of the type $e^{i\omega t}$, the Knopoff-de Hoop representation theorem applied to volume V leads to

$$\varepsilon(\vec{x})u_i(\vec{x}) = \int_S [G_{ji}(\vec{y}, \vec{x})\overset{\nu}{T}_j(\vec{y}) - \overset{\nu}{H}_{ji}(\vec{y}, \vec{x})u_j(\vec{y})]dS(\vec{y}) \qquad (i, j = 1, 2, 3) \qquad (2.11)$$

in which

$$\varepsilon(\vec{x}) = \begin{cases} 0 & \vec{x}\varepsilon V' \\ \frac{1}{2} & \vec{x}\varepsilon S \\ 1 & \vec{x}\varepsilon V \end{cases} \qquad (2.12)$$

In Eq. (2.11), $u_j(\vec{y})$ and $\overset{\nu}{T}_j(\vec{y})$ represent the displacement and traction components on $S(\vec{y}\varepsilon S)$, $G_{ji}(\vec{y}, \vec{x})$ represents the jth component of the displacement vector at point $\vec{y}\varepsilon S$ due to a concentrated point load at $\vec{x}$ acting in the i-direction, while $\overset{\nu}{H}_{ji}(\vec{y}, \vec{x})$ denotes the corresponding jth component of the traction vector at $\vec{y}\varepsilon S$ due to a concentrated point load at $\vec{x}$ acting in the i-direction. The normal $\vec{\nu}$ to the surface S is taken positive pointing into V'. In Eq. (2.11) and in the sequel, the summation convention over repeated indeces is adopted.

Assuming that the displacement vector $u_j(\vec{y})$ is known on the surface S (welded contact problem) and applying Eq. (2.11) to a point $\vec{x}\varepsilon V'$ leads to

$$\int_S G_{ji}(\vec{y}, \vec{x})\overset{\nu}{T}_j(\vec{y})dS(\vec{y}) = \int_S \overset{\nu}{H}_{ji}(\vec{y}, \vec{x})u_j(\vec{y})dS(\vec{y}) \quad (\vec{x}\varepsilon V', \ \vec{y}\varepsilon S) \quad . \qquad (2.13)$$

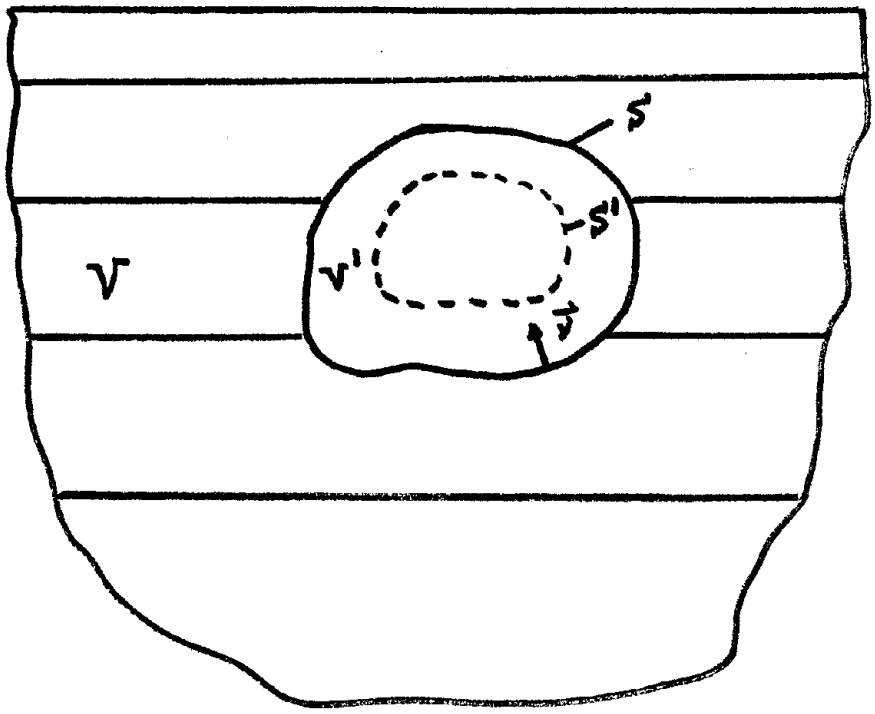

Figure 2.2. Description of the system and notation for the integral equation method.

Assuming that the Green functions G_{ji} and $\overset{\nu}{H}_{ji}$ are known, Eq. (2.13) corresponds to an integral equation in the unknown traction $\overset{\nu}{T}_j(\vec{y})$ on the surface S.

To solve Eq. (2.13), we propose to represent the unknown traction $\overset{\nu}{T}_j(\vec{y})$ by

$$\overset{\nu}{T}_j(\vec{y}) = \int_{S'} \overset{\nu}{H}_{jk}(\vec{y}, \vec{x}')F_k(\vec{x}')dS'(\vec{x}') \qquad (2.14)$$

where $F_k(\vec{x}')$ corresponds to an unknown distribution of forces on a surface S' internal to S.

Substitution from Eq. (2.14) into Eq. (2.13) leads to the following integral equation for $F_k(\vec{x}')$

$$\int_{S'} \hat{G}_{ij}(\vec{x}, \vec{x}')F_j(\vec{x}')dS'(\vec{x}') = \int_S \overset{\nu}{H}_{ji}(\vec{y}, \vec{x})u_j(\vec{y})dS(\vec{y}) \quad (x\varepsilon V') \qquad (2.15)$$

where

$$\hat{G}_{ij}(\vec{x}, \vec{x}') = \int_{S'} G_{ki}(\vec{y}, \vec{x})\overset{\nu}{H}_{kj}(\vec{y}, \vec{x}')dS(\vec{y}) \quad . \qquad (2.16)$$

It is easily proven that the kernel $\hat{G}_{ij}(\vec{x}, \vec{x}')$ is symmetric, i.e.

$$\hat{G}_{ij}(\vec{x}, \vec{x}') = \hat{G}_{ji}(\vec{x}', \vec{x}) \quad . \qquad (2.17)$$

Equation (2.15) constitutes, then, an integral equation with symmetric kernel in the unknown distribution of forces $F_j(\vec{x}')$, $\vec{x}'\varepsilon S'$. Once this equation is solved the tractions on the surface S may be obtained by use of Eq. (2.14).

Since the integral equation for the distributed forces $F_j(\vec{x}')$, $\vec{x}'\varepsilon S'$, depends linearly on the known displacement $u_j(\vec{y})$, $\vec{y}\varepsilon S$, and since the tractions $\overset{\nu}{T}_j(\vec{y})$, $\vec{y}\varepsilon S$, are linear functions of the distributed forces, it is possible to write formally

$$\overset{\nu}{T}_j(\vec{y}) = \int_S \hat{K}_{ji}(\vec{y}, \vec{y}')u_i(\vec{y}')dS(\vec{y}') \quad (\vec{y}\varepsilon S) \qquad (2.18)$$

where $K_{ji}(\vec{y}, \vec{y}')(\vec{y}, \vec{y}\varepsilon S)$ can be easily obtained once the general

solution of Eq. (2.15) is known.

In matrix form Eq. (2.18) can be rewritten as

$$\{\overset{\nu}{T}(\vec{y})\} = \int_S [\hat{K}(\vec{y}, \vec{y}')]\{u(\vec{y}')\}dS(\vec{y}')(\vec{y}\varepsilon S) \tag{2.19}$$

In the case in which the intrusion is rigid and excited by external forces applied on it, the displacement vector $\{u(\vec{y}')\}$ on the surface S can be represented in terms of the "generalized" displacement of the foundation $\{\Delta\}$ by

$$\{u(\vec{y}')\} = [\alpha(\vec{y}')]\{\Delta\} \tag{2.20}$$

where

$$\{\Delta\} = (\Delta_x, \Delta_y, \Delta_z, \phi_x, \phi_y, \phi_z)^T \tag{2.21}$$

is the 6×1 "generalized" displacement vector including the displacement $(\Delta_x, \Delta_y, \Delta_z)$ of the foundation as well as the rotation (ϕ_x, ϕ_y, ϕ_z) about the coordinate axes. The influence matrix $[\alpha]$, in the case of small rotations and in Cartesian coordinates is given by

$$[\alpha(\vec{y})] = \begin{bmatrix} 1 & 0 & 0 & 0 & z & -y \\ 0 & 1 & 0 & -z & 0 & x \\ 0 & 0 & 1 & y & -x & 0 \end{bmatrix} \tag{2.22}$$

where (x, y, z) are the coordinates of $\vec{y}\varepsilon S$.

The "generalized" force vector $\{\Gamma\}$

$$\{\Gamma\} = (P_x, P_y, P_z, M_x, M_y, M_z)^T \tag{2.23}$$

representing the total forces and moments that the intrusion exerts on the surrounding media can be obtained from

$$\{\Gamma\} = \int_S [\alpha(\vec{y})]^T \{\overset{\nu}{T}(\vec{y})\}dS(\vec{y}) \tag{2.24}$$

Substitution from Eqs. (2.19) and (2.20) into Eq. (2.24) leads to

$$\{\Gamma\} = [K(\omega)]\{\Delta\} \tag{2.25}$$

where $[K(\omega)]$ is the impedance matrix for the foundation obtained from

$$[K(\omega)] = \int_S \int_S [\alpha(\vec{y})]^T [\hat{K}(\vec{y}, \vec{y}')] [\alpha(\vec{y}')] dS(\vec{y}) dS(\vec{y}') \qquad (2.26)$$

Equation (2.26) provides a very efficient and general procedure to evaluate the impedance matrix for three-dimensional rigid foundations of arbitrary shape embedded in a layered visco-elastic half-space. In addition, the matrix $[\hat{K}(\vec{y}, \vec{y}')]$ connecting the displacements and tractions on the surface S of the foundation can be used to study the response of flexible foundations and may also be used to generate non-reflecting boundaries for finite element representation of the intrusion V'.

In the case in which the intrusion is excited by seismic waves, the forces and moments $\{\Gamma^*\}$ required to keep the foundation fixed under the action of seismic waves are obtained from

$$\{\Gamma^*\} = -\int_S \int_S [\alpha(\vec{y})]^T [\hat{K}(\vec{y}, \vec{y}')] \{u^f(\vec{y}')\} dS(\vec{y}) dS(\vec{y}') \qquad (2.27)$$

where $\{u^f(\vec{y}')\}$ denotes the free-field motion at the point y' on S. The free-field motion is obtained by considering the incident seismic wave and its reflection on the free-surface of the half-space.

The response of the foundation when subjected to the seismic waves in absence of other external forces is given by

$$\{\Delta^*\} = - K(\omega)^{-1} \{\Gamma^*\} \qquad (2.28)$$

where

$$\{\Delta^*\} = (\Delta_x^*, \Delta_y^*, \Delta_z^*, \phi_x^*, \phi_y^*, \phi_z^*)^T \qquad (2.29)$$

represents the "generalized" motion of the foundation (foundation input motion including translations and rotations). Equations (2.29) and (2.28) provide an efficient way of evaluating the foundation input for foundations of arbitrary shape embedded in a layered viscoelastic medium. The case of mixed boundary conditions on the interface S', as in the case of lateral separation, can be easily obtained by slightly modifying

the formulation just presented.

The integral equation method just described can also be used to study the scattering of seismic waves by canyons and valleys.

To complete the description of the integral equation approach it is only necessary to say that the integral equation (2.15) is solved numerically after reducing it to a system of linear algebraic equations by discretizing the surface integrals by use of quadrature formulae.

For the procedure described to become practical and general it was necessary to develop an efficient method to evaluate the Green functions G_{ij} and $\overset{\nu}{H}_{ij}$ for a layered viscoelastic half-space. A considerable portion of the research effort was directed at this task. The method developed has made possible not only the study of the response of embedded foundations but has also permitted a variety of studies in strong motion seismology and ocean bottom seismology.

2.3 Finite Element Method of Solution

Finite elements methods, one of the alternatives considered in this study, offer considerable potential for treating complex embedment conditions. However, to date this approach has not proven effective for reproducing analytical results. The basic limitation of finite element approaches stems from the inability of a numerical grid of finite extent to represent an extended earth. A significant improvement in the method occurred with the development of boundary conditions that remove seismic energy at the horizontal extremes of the grid. Lymer and Wass [E.10] implemented boundary conditions for simulating a horizontally unbounded medium acting in anti-plane strain, and Waas [E.11] and Kausel et al. [E.8] extended this procedure to a cylindrical geometry. No satisfactory conditions have been developed for allowing seismic energy to pass through the bottom boundary of the grid, however. As a result, finite element treatments fail to reproduce some aspects of analytical solutions, notably the radiation damping at low frequencies. It also appears that there is some confusion between incoming seismic waves and total wave motion, which includes incoming waves as well as scattered waves due to the presence of the structure. The procedure of specifying free-field particle motions along a grid boundary to simulate incoming waves neglects the presence of the scattered wave field.

This section describes a time domain finite element procedure for computing the response to seismic excitation of a three-dimensional, rigid foundation embedded in an elastic half-space. Because the analysis is performed in the time domain, the influence of grid boundaries is totally eliminated by completing the transient solution prior to the arrival of reflected waves from those boundaries. As an

intermediate step in determining the input motion to the foundation, the impedance matrix of the foundation is generated. The computed input motion and impedance matrix are sufficient, given the dynamics of the superstructure, to yield a solution to the complete soil-structure interaction problem.

To find the foundation impedance matrix $[K(\omega)]$, which describes the steady-state response of the foundation, a corresponding transient problem is solved to obtain an "impulse response matrix" $[\tilde{K}(t)]$. $[K(\omega)]$ is related to $[\tilde{K}(t)]$ through Fourier transformation.

Determination of each column of the foundation impulse response matrix $[\tilde{K}(t)]$ requires the solution of a mixed boundary value problem as sketched in Fig. 2.1. A semi-infinite elastic medium V is bounded by the surface $S_\sigma + S_u$, where S_u coincides with the welded foundation contact and S_σ corresponds to the earth's surface. The position vector is denoted by $\underline{x}$. $\underline{n}(\underline{x})$ denotes the unit vector normal to $S_u + S_\sigma$, and is directed out of V. We define a displacement vector $\underline{U}_j(\underline{x})$ which, for $\underline{x}$ on S_u, corresponds to the jth rigid-body mode of S_u. Using $\hat{\underline{x}}$, $\hat{\underline{y}}$, $\hat{\underline{z}}$ to denote unit vectors aligned with the coordinate axes, the functions $\underline{U}_j(\underline{x})$, j = 1,...6, corresponding to Δ_x, Δ_y, Δ_z, ϕ_x, ϕ_y, ϕ_z, are given by

$$\begin{aligned} \underline{U}_1(\underline{x}) &= \hat{\underline{x}} & \underline{U}_4(\underline{x}) &= \underline{x} \times \hat{\underline{x}} \\ \underline{U}_2(\underline{x}) &= \hat{\underline{y}} & \underline{U}_5(\underline{x}) &= -\underline{x} \times \hat{\underline{y}} \\ \underline{U}_3(\underline{x}) &= \hat{\underline{z}} & \underline{U}_6(\underline{x}) &= -\underline{x} \times \hat{\underline{z}} \end{aligned} \tag{2.30}$$

$\underline{u}_j(\underline{x}, t)$ and $\underline{\sigma}_j(\underline{x}, t)$ denote the dispacement vector and stress tensor, respectively, in $V + S_\sigma + S_u$. We require that $\underline{u}_j$ and $\underline{\sigma}_j$ satisfy

$$
\begin{aligned}
&\underline{u}_j(\underline{x},\ t) = \underline{U}_j(\underline{x})\delta(t) && \text{for } \underline{x} \text{ on } S_u \\
&\underline{\sigma}_j(\underline{x},\ t)\quad \underline{n}(\underline{x}) = 0 && \text{for } \underline{x} \text{ on } S_\sigma \\
&\underline{\nabla} \cdot \underline{\sigma}_j(\underline{x},\ t) - \rho(\underline{x})\ \frac{\partial^2}{\partial t^2}\ \underline{u}_j(\underline{x},\ t) = 0 && \text{for } \underline{x} \text{ in } V \\
&\underline{\sigma}_j(\underline{x},\ t) = \underline{E}(\underline{x}) : \underline{\nabla}\ \underline{u}_j(\underline{x},\ t) = \underline{u}_j\underline{\nabla}(\underline{x},\ t)
\end{aligned}
\tag{2.31}
$$

where ρ is the density, $\underline{E}$ is the fourth-order elastic tensor, and $\delta(t)$ is the Dirac delta function. The first equation represents displacement boundary conditions on the foundation contact, applied as an impulse in time. The second equation is the boundary condition on the free surface. The third is momentum conservation, and the fourth is the stress-strain relationship.

Once Eqs. (2.31) have been solved for $\underline{\sigma}_j$, $j = 1,\ldots 6$, the components of an impulse response matrix $[\tilde{K}(t)]$ are given by

$$
\tilde{K}_{ij}(t) = \int_{S_u} \underline{U}_i(\underline{x}) \cdot \underline{\sigma}_j(\underline{x},\ t)\quad \underline{n}(\underline{x})dS\ . \tag{2.32}
$$

The impedance matrix $[K(\omega)]$ is obtained by Fourier transforming $[\tilde{K}(t)]$:

$$
[K(\omega)] = \int_{-\infty}^{\infty} [\tilde{K}(t)] e^{-i\omega t} dt\ . \tag{2.33}
$$

The effectiveness of this transient analysis procedure is enhanced by the fact that impulsive displacements are imposed on S_u, rather than impulsive forces. Impulsive displacements yield foundation forces with short transient times, whereas impulsive forces would produce protracted displacement responses. (The damped harmonic oscillator, governed by $\ddot{u} + 2\gamma\dot{u} + \omega^2 u = f$, exemplifies this behavior: the force response to an impulsive displacement is simply $\delta''(t) + 2\gamma\delta'(t) + \omega^2\delta(t)$, while the displacement in response to an impulsive force is $\frac{H(t)}{(\omega^2 - \gamma^2)^{\frac{1}{2}}} e^{-\gamma t}\sin(\omega^2 - \gamma^2)^{\frac{1}{2}}t)$. $[K(t)]$ is therefore nearly zero, except

over a short time interval; thus a relatively short time sample of $[K(t)]$ gives $[K(\omega)]$ accurately, evan at very low frequencies.

The input motion $\{\Delta^*\}$ associated with a particular seismic disturbance is found by determining the generalized forces $\{\Gamma^*\}$ required to hold S_u stationary in the presence of the incident disturbance. Once $\{\Gamma^*\}$ is known, $\{\Delta^*\}$ is obtained from the relationship

$$\{\Delta^*(\omega)\} = -[K(\omega)]^{-1}\{\Gamma^*(\omega)\} \ . \tag{2.34}$$

To find $\{\Gamma^*(\omega)\}$, which corresponds to a steady-state seismic disturbance, we solve a transient problem, as in the previous section. A transient generalized force $\{\Gamma^*(t)\}$ is found, and Fourier transformed to obtain $\{\Gamma^*(\omega)\}$.

The seismic disturbance is described by the "free-field" displacement and stress $\underline{u}_f(\underline{x}, t)$, $\underline{\sigma}_f(\underline{x}, t)$. These are the displacement and stress which would occur in the absence of the structure and foundation. We assume that $\underline{u}_f$ and $\underline{\sigma}_f$ are known and that they obey the equations of motion in V and the free surface condition on S_σ.

The "scattered field," denoted by $\underline{u}_s(\underline{x}, t)$ and $\underline{\sigma}_s(\underline{x}, t)$, is defined as the difference between the total field and free field:

$$\begin{aligned} \underline{u}_s &= \underline{u} - \underline{u}_f \\ \underline{\sigma}_s &= \underline{\sigma} - \underline{\sigma}_f \ . \end{aligned} \tag{2.35}$$

The total displacement is required to vanish on S_u, so the scattered field satisfies the equations

$$
\begin{aligned}
&\underline{u}_s = -\underline{u}_f && \text{on } S_u \\
&\underline{\sigma}_s \quad \underline{n} = 0 && \text{on } S_\sigma \\
&\underline{\nabla} \cdot \underline{\sigma}_s - \rho \frac{\partial^2}{\partial t^2} \underline{u}_s = 0 && \text{in V} \\
&\underline{\sigma}_s = \underline{E} : (\underline{\nabla}\, \underline{u}_s + \underline{u}_s \underline{\nabla}) \quad .
\end{aligned}
\tag{2.36}
$$

Once Eqs. (2.36) have been solved for $\underline{\sigma}_s$, the components of $\{\Gamma^*(t)\}$ are computed from the equation:

$$
\tilde{\Gamma}_i^*(t) = \int_{S_u} \underline{U}_i(\underline{x}) \cdot (\underline{\sigma}_s + \underline{\sigma}_f) \cdot \underline{n}(\underline{x}) dS \tag{2.37}
$$

for $i = 1,\ldots 6$. $\{\Gamma^*(\omega)\}$ is obtained by Fourier transformation of $\{\tilde{\Gamma}^*(t)\}$.

An explicit time stepping finite element algorithm based on that described by Frazier and Petersen [H.1] is used to obtain an approximate solution to Eqs. (2.31) and (2.36). An important feature of this explicit method is that waves propagate in the finite element grid without losing energy, when no material viscosity is employed in the calculation. The finite element discretization causes high frequency waves to propagate at reduced phase velocities, however. As a result, the Fourier transform of the numerical solution is reliable only for angular frequencies ω less than approximately $2\pi\beta/6\Delta x$, where β is the shear wave speed in V and Δx is the characteristic dimension of an individual element in the numerical grid. It should be pointed out out that although higher frequency components in the numerical computations do not correctly represent high frequency components of the exact solution, it is unnecessary and undesirable, in the case of linear problems, to introduce artificial damping to suppress these components. Such damping reduces the maximum frequency at which the Fourier transform of the numerical solution accurately represents the continuum solution.

In order for the explicit integration method to be stable, the time step Δt must be less than $2/\omega_{max}$, where ω_{max} is the highest resonant frequency of the grid. Provided this stability criterion is met, the choice of Δt has negligle effect on the accuracy of the numerical solution. We have found that a time step of $.4\ \Delta x/\alpha$, where α is the P wave speed in V, is sufficiently small to insure stability.

In order to prevent the "artificial" grid boundaries (that is, boundaries of the finite element grid other than S_u or S_σ) from influencing $[\tilde{K}(t)]$ or $\{\Gamma^*(t)\}$, the numerical grid is extended sufficiently far from the foundation that no reflected wave from an artificial boundary reaches S_u over the duration of the transient calculation. If the computation runs from $t = 0$ to $t = T$, then the artifical boundaries must be a distance d greater than $\frac{T\alpha}{2}$ from every portion of S_u. In practice, $d \geq .6\ T\alpha$ gives results for $[\tilde{K}(t)]$ and $\{\Gamma^*(t)\}$ free of contamination by spurious reflected waves. (We have generally allowed the artificial boundaries to be traction-free; however, the above considerations insure that any homogeneous boundary conditions are acceptable).

When the elastic structure of the soil and the geometry of the foundation are both axisymmetric, the above three-dimensional problems can be simplified. This reduction is accomplished by expanding the cylindrical components of the displacements and applied forces in a series, each term of which has azimuthal dependence of the form $\sin n\theta$ or $\cos n\theta$. Only the $n = 0$ term contributes to the vertical and torsional response of a rigid foundation, and only $n = 1$ terms contribute to horizontal and rocking response.

As a test of the transient finite element method, the torsional impedance for a hemispherical foundation has been obtained by use of the model illustrated in Fig. 3.1 and the results compared with the exact solution obtained by Luco. The comparison shown in Fig. 2.3 indicates excellent agreement at low frequencies. At high frequencies the finite element results are slightly lower than the exact values, the error however does not exceed 5%. Besides the good agreement obtained, the finite element results do not show any of the oscillations that reveal reflections from the boundaries of the finite element model and it properly represents the radiation damping at low frequencies.

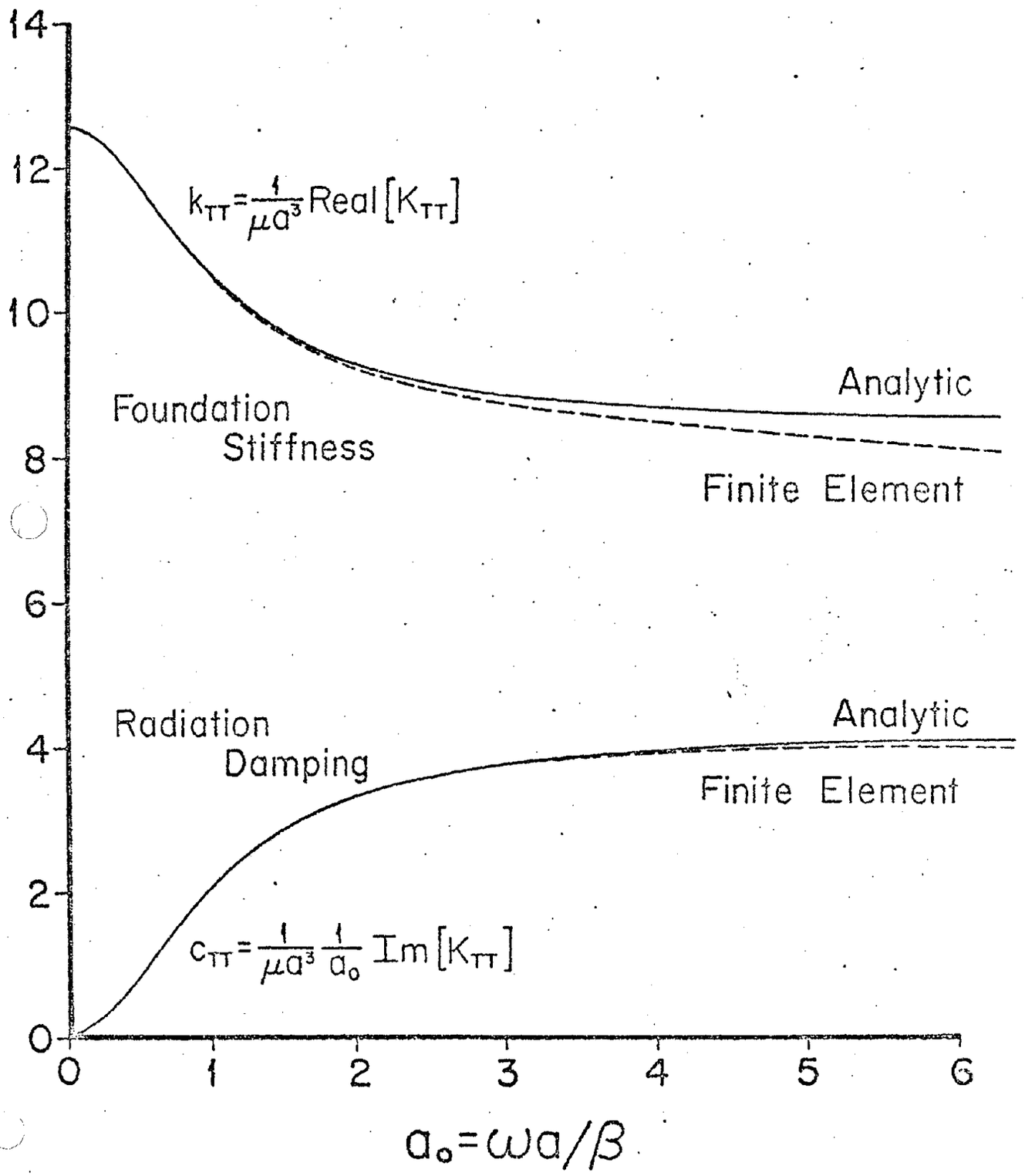
14
12
10
8
6
4
2
0
$k_{TT}=\frac{1}{\mu a^3}\text{Real}[K_{TT}]$
Foundation
Stiffness
Analytic
Finite Element
Radiation
Damping
Analytic
Finite Element
$c_{TT}=\frac{1}{\mu a^3}\frac{1}{a_o}\text{Im}[K_{TT}]$
0
1
2
3
4
5
6
$a_o=\omega a/\beta$

Figure 2.3

3. FOUNDATION RESPONSE TO EXTERNAL FORCES

3.1 Impedance Functions for Hemispherical Foundations

As a first example of the application of the finite element method of solution, the impedance functions for a hemispherical foundation embedded in homogeneous, isotropic, elastic half-space were determined. The rigid hemisphere is characterized by the radius $\underline{a}$, while the elastic half-space is characterized by the shear modulus μ, S-wave velocity β and Poisson's ratio ν. The numerical results correspond to the case of welded contact between the foundation and the soil and to a Poisson's ratio of $\nu = 0.25$. The origin of the system of coordinates was taken at the center of the hemisphere as shown in Fig. 3.1.

Due to the symmetry of the problem geometry about the vertical z-axis, the impedance matrix can be written in the form

$$[K] = \begin{bmatrix} K_{HH} & 0 & 0 & 0 & K_{HM} & 0 \\ 0 & K_{HH} & 0 & -K_{HM} & 0 & 0 \\ 0 & 0 & K_{VV} & 0 & 0 & 0 \\ 0 & -K_{MH} & 0 & K_{MM} & 0 & 0 \\ K_{MH} & 0 & 0 & & K_{MM} & 0 \\ 0 & 0 & 0 & & 0 & K_{TT} \end{bmatrix} \tag{3.1}$$

where $K_{MH} = K_{HM}$. To describe the results it is convenient to introduce the stiffness coefficients k_{HH}, k_{VV}, k_{MM}, k_{HM}, k_{TT} and the damping coefficients c_{HH}, c_{VV}, c_{MM}, c_{HM}, c_{TT}. These coefficients, which are real and dimensionless, are defined by

$$K_{HH} = \mu a(k_{HH} + i a_o c_{HH})$$

$$K_{VV} = \mu a(k_{VV} + i a_o c_{VV})$$

$$K_{MM} = \mu a^3(k_{MM} + i a_o c_{MM}) \qquad (3.2)$$

$$K_{MH} = \mu a^2(k_{MH} + i a_o c_{MH})$$

$$K_{TT} = \mu a^3(k_{TT} + i a_o c_{TT})$$

where $a_o = \omega a/\beta$ is a dimensionless frequency.

A portion of the grid used in the computation is illustrated in 3.1. A total of 1000 axisymmetric elements, with 20 elements adjacent to the foundation surface, were used. The computation run from $t = 0$ to $t = 6a/\alpha$ where α is the P-wave velocity in the half-space.

The torsional impedance function obtained by the finite element have been compared with the exact analytical solution in Fig. 2.3. The results for c_{TT} agree to within 3% in the frequency range from $a_o = 0.2$ to $a_o = 6$. Those for k_{TT} agree within 5% in the same frequency intervall. The differences increase as the frequency increases.

The five stiffness coefficients for the hemisphere are plotted versus a_o in Fig. 3.2a while the five damping coefficients are plotted in Fig. 3.2.b. The coefficients k_{HH}, k_{VV}, k_{MH}, c_{HH}, c_{VV} are nearly independent of frequency, while k_{TT} and k_{MM} are decreasing functions of a_o and c_{TT} and c_{MM} are increasing functions of frequency. The coupling terms k_{MH} and c_{MH}, which are very small for a disk foundation, are, for the hemisphere, comparable in amplitude to the diagonal coefficients. The diagonal coefficients are larger than their corresponding

values for a disk foundation by factors of between 1.5 and 3 (the exception being k_{VV} which is only 25% larger for the hemisphere).

As a further test of the accuracy of the results presented, the damping coefficients at $a_o = 6$ are compared in Table 3.1 with the asymptotic values obtained by considering plane P and S waves radiating normal to the surface of the hemisphere.

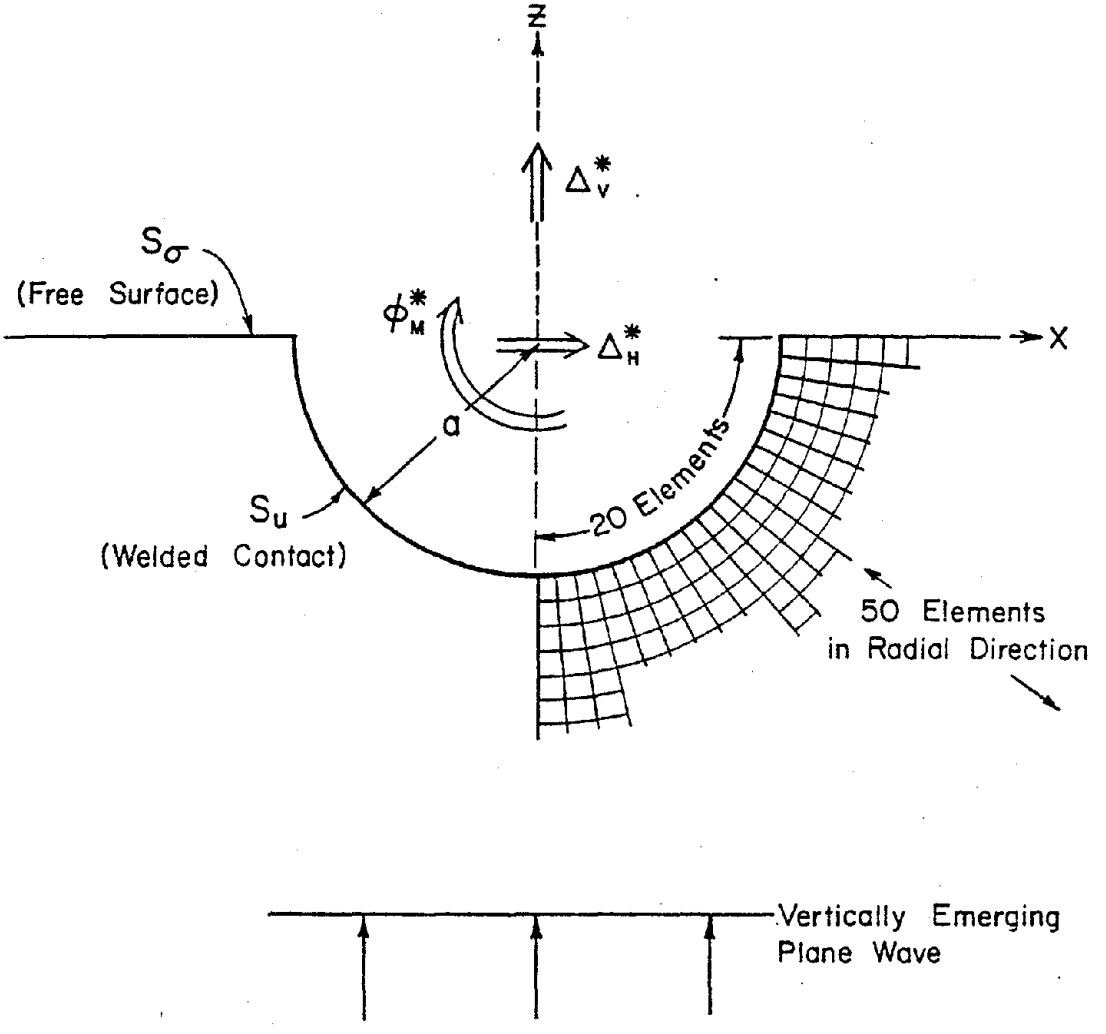

Figure 3.1. Problem formulation and finite element grid for embedded hemisphere.

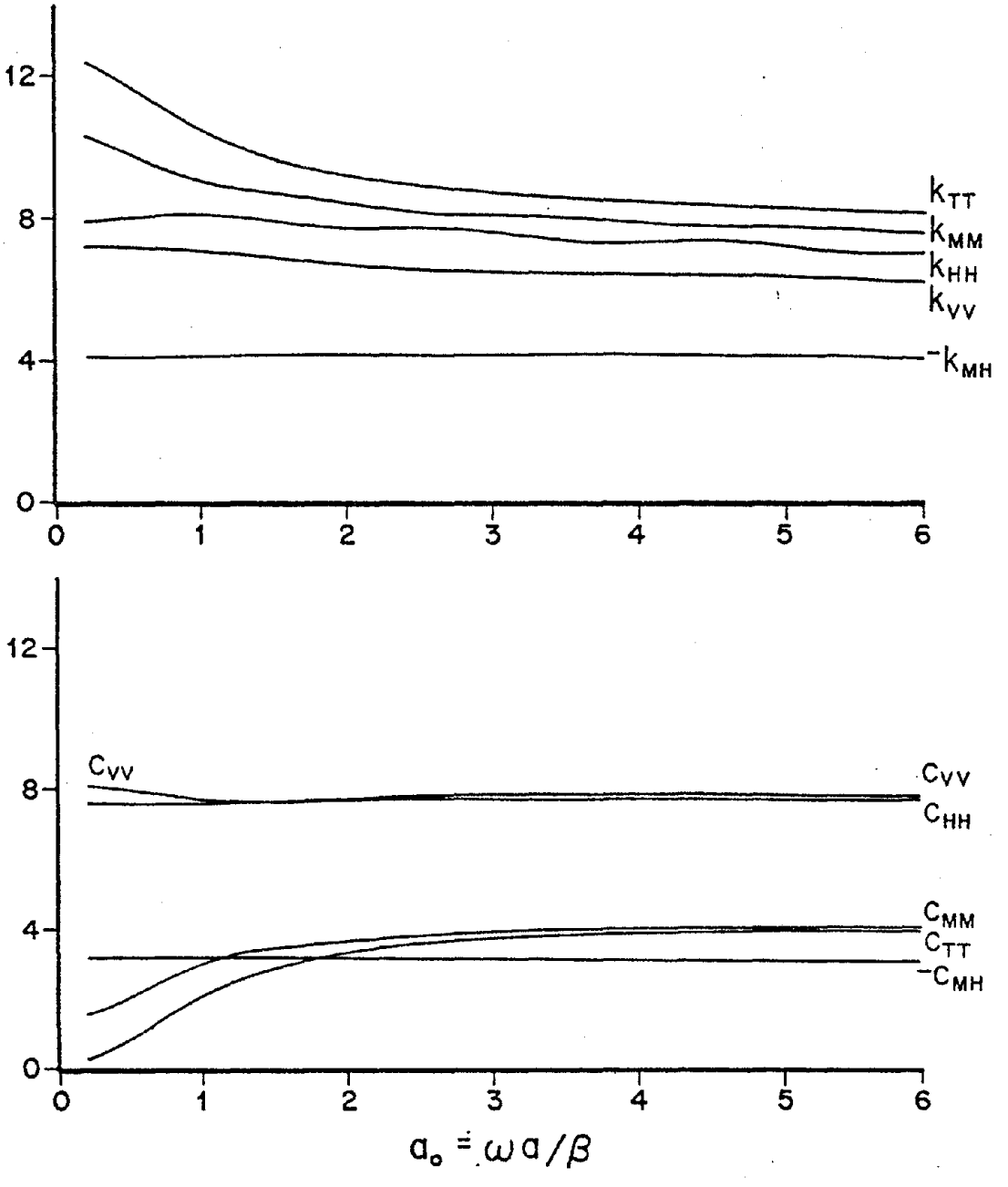

Figure 3.2. a) Stiffness coefficients, and b) radiation damping coefficients for the embedded hemisphere.

TABLE 3.1

HIGH FREQUENCY VALUES OF RADIATION DAMPING FOR HEMISPHERE

Radiation Damping Coefficient	Analytic Solution [lim $a_o \to \infty$]	Finite Element Solution [$a_o = 6$]
c_{MM}	4.19	4.04
c_{TT}	4.19	3.98
c_{HH}	7.81	7.72
c_{VV}	7.81	7.78

3.2 Impedance Functions for Cylindrical Foundations.

As a second example of the finite element method of solution, the impedance functions for cylindrical foundations embedded in a homogeneous, isotropic half-space were determined. The rigid cylindrical foundation is characterized by the radius a, the embedment depth ha, while the elastic half-space is characterized by the shear modulus μ, S wave velocity β and Poisson's ratio ν. The numerical results correspond to the case of welded contact between the foundation and the soil and to a Poisson's ratio of $\nu = 0.25$. The origin of the system of coordinates was taken at the center of the base of the cylinder as shown in Fig. 3.3.

Fig. 3.3 illustrates the grids used for embedment ratios h of 0, 0.5, 1.0 and 2.0. For h = 0, 0.5 and 1, the grid contains 10 elements along the foundation radius; for h = 2.0, seven elements along the radius were used.

The calculated impedance functions are plotted versus the dimensionless frequency $a_o = \omega a/\beta$ in Figs. 3.4 to 3.8 for embedment ratios h = 0, 0.5, 1.0 and 2.0. Solid lines correspond to the stiffness coefficients, while dashed lines represent the damping coefficients defined as in Eq. (3.2).

The results presented in Figs. 3.4 to 3.8 indicate that the embedment ratio h has a marked effect on the stiffness and damping coefficients. The torsional stiffness and damping coefficients increase almost linearly with embedment depth; the vertical and horizontal damping coefficients also increase almost linearly with embedment depth, while the corresponding stiffness coefficients also increase with embedment depth but not in the same proportion as the damping coefficients. The frequency dependence of the impedance

functions in the embedded case is similar to that for flat foundations.

A measure of the accuracy of the finite element method is obtained by comparing the static values of the torsional stiffness coefficients with those obtained by Luco (1976) by use of an integral equations approach. The comparisons presented in Table 3.2 indicates that the finite element solution is highly accurate in the low frequency range. To test accuracy of the finite element at high frequencies, the damping coefficients obtained are compared with the exact asymptotic values in Table 3.3. Again, close agreement is obtained.

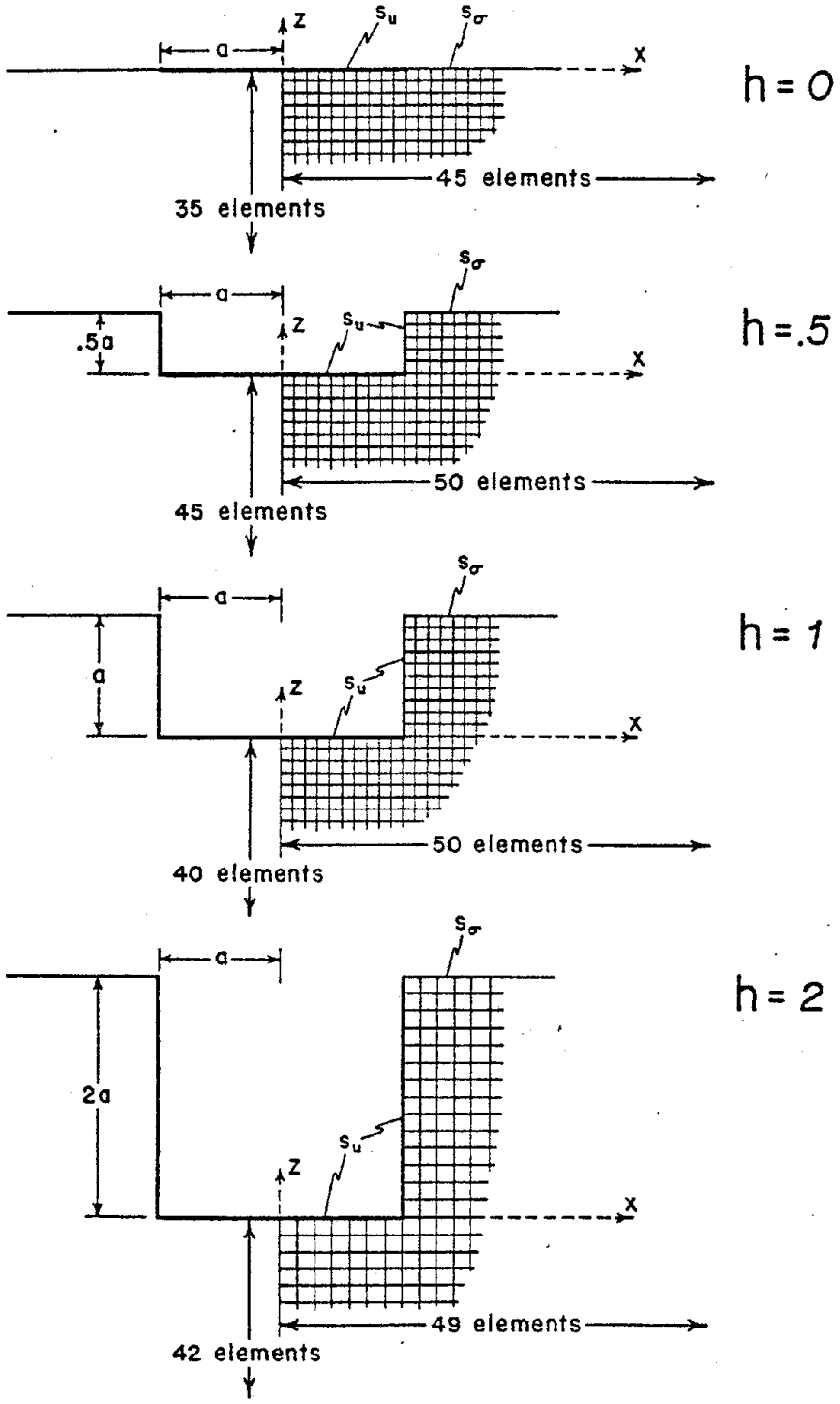

Figure 3.3. Boundary geometries, coordinate systems, and numerical grids used for analysis of cylindrical foundations.

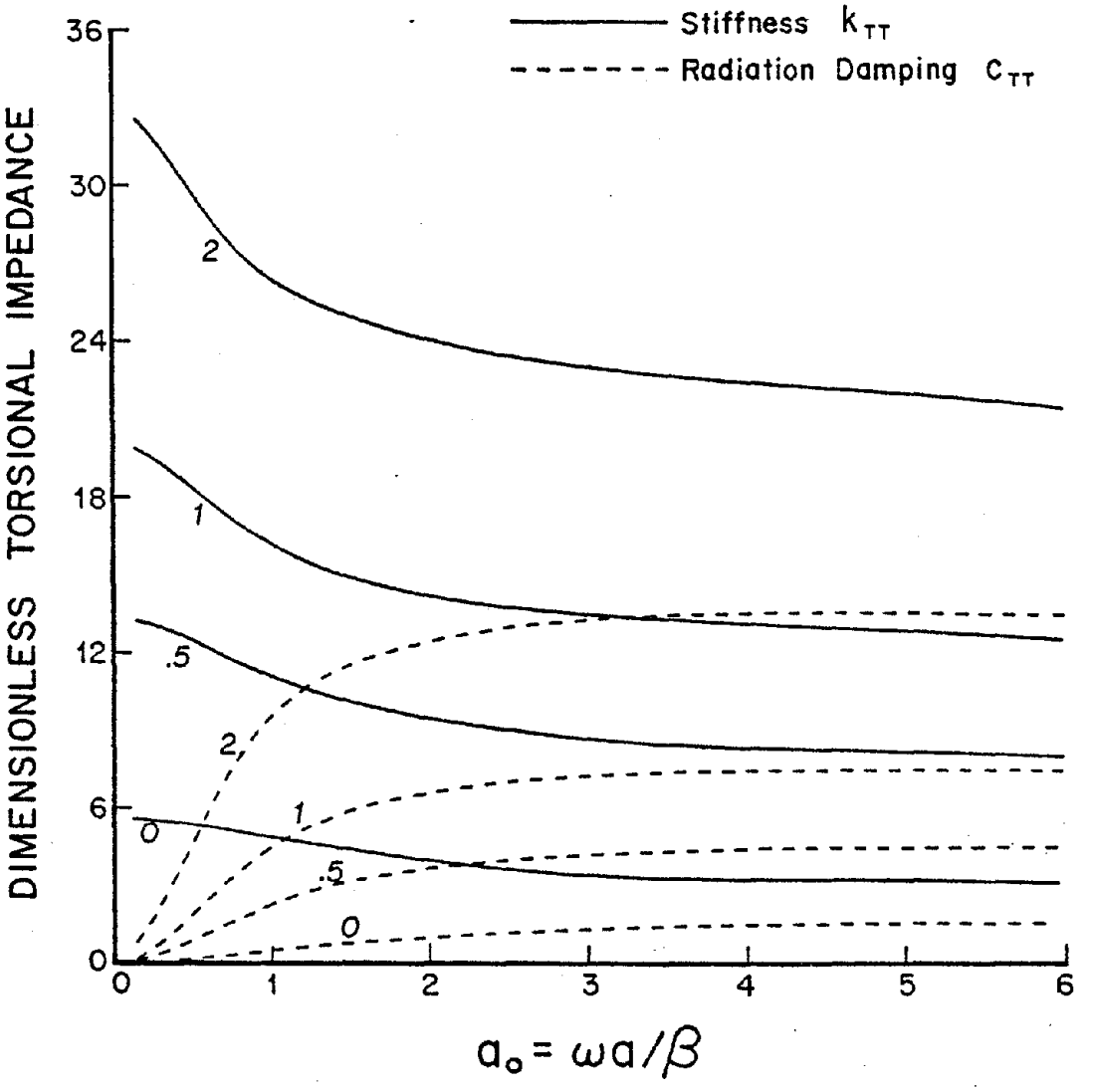

Figure 3.4. Torsional stiffness and radiation damping for embedded cylinders. The parameter is h, the ratio of depth to radius of the cylinder.

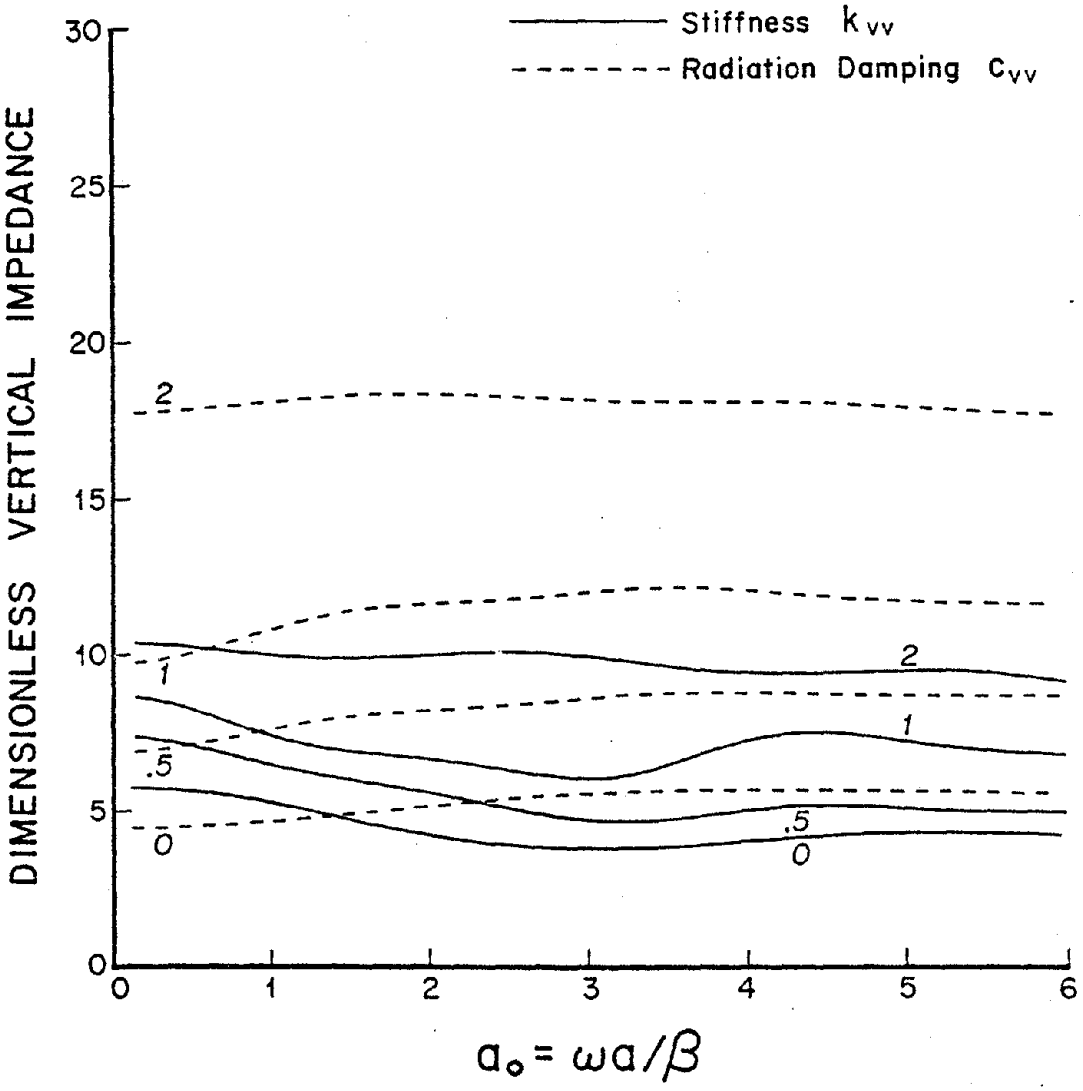

Figure 3.5. Vertical stiffness and radiation damping for embedded cylinders. The parameter is h, the ratio of depth to radius of the cylinder.

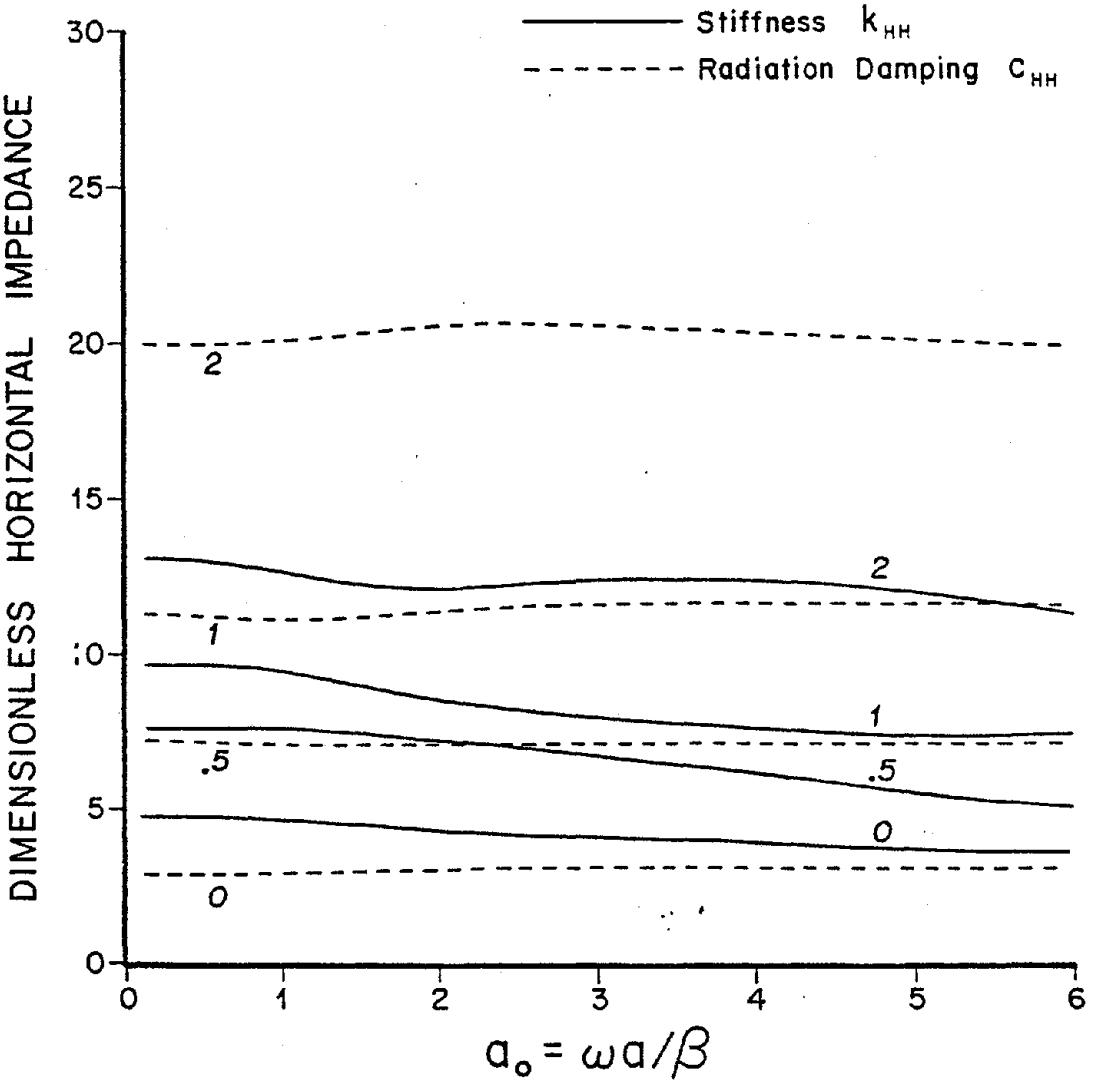

Figure 3.6. Horizontal stiffness and radiation damping for embedded cylinders. The parameter is h, the ratio of depth to radius of the cylinder.

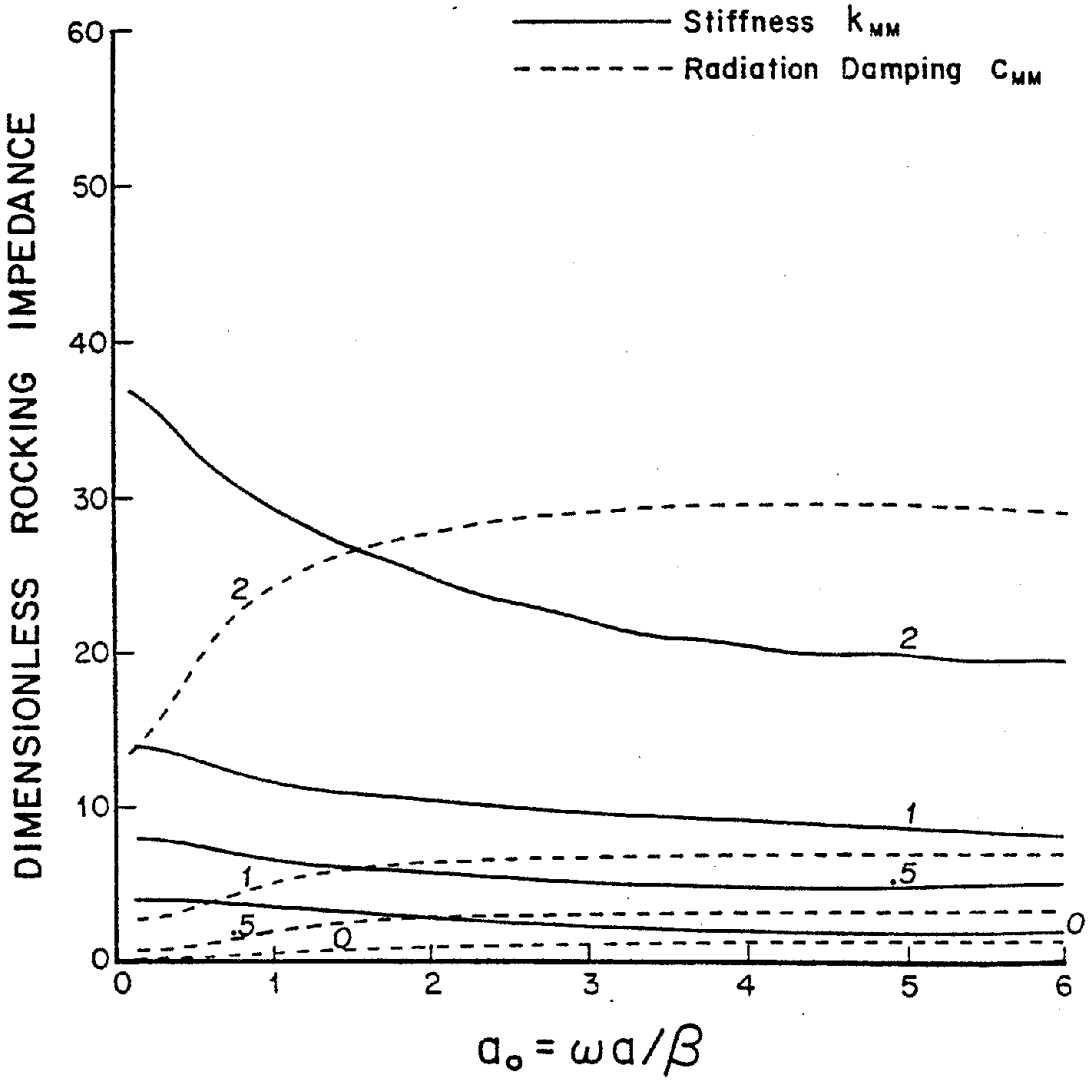

Figure 3.7. Rocking stiffness and radiation damping for embedded cylinders. The parameter is h, the ratio of depth to radius of the cylinder.

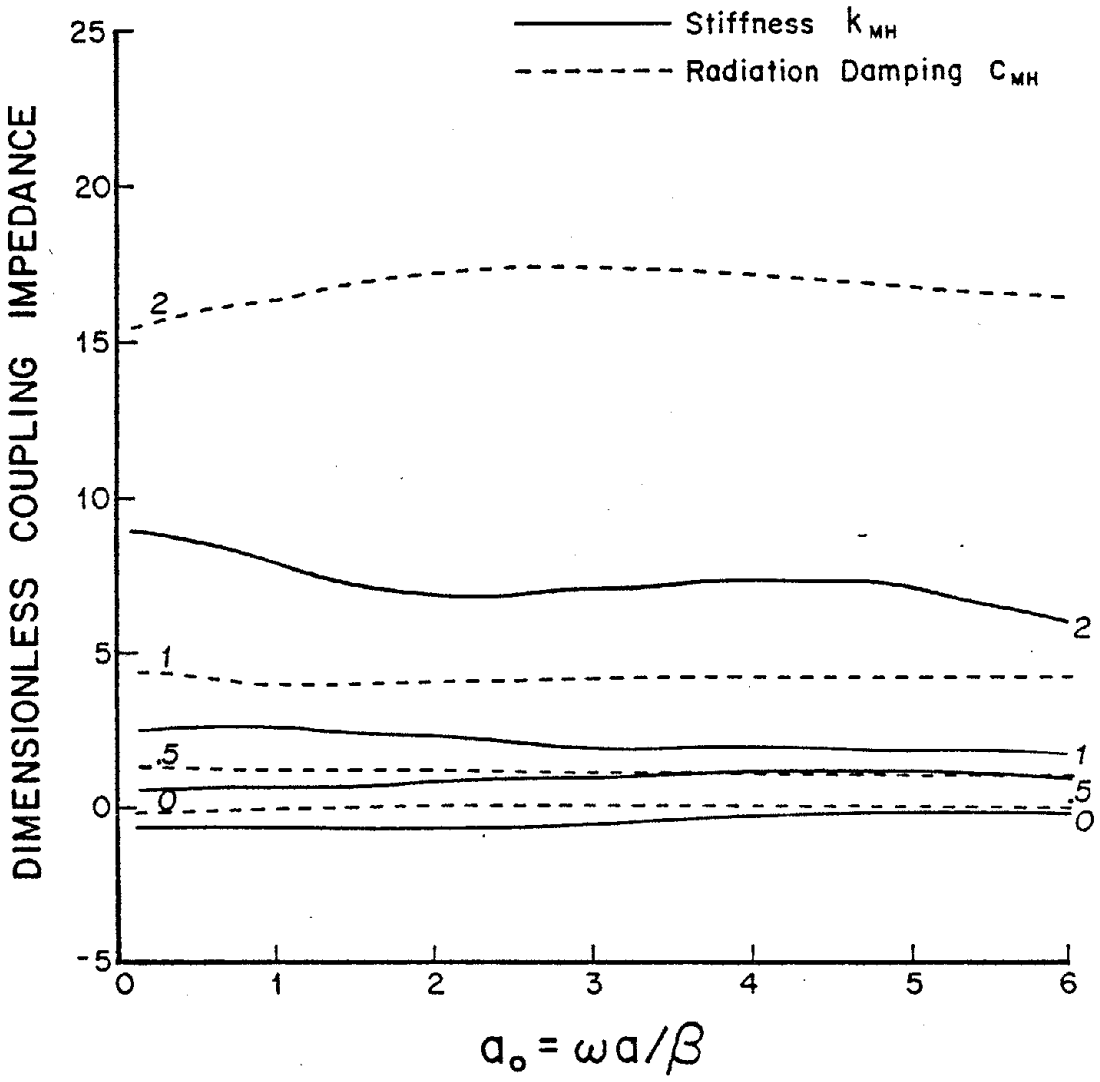

Figure 3.8. Coupling stiffness and radiation damping for embedded cylinders. The parameter is h, the ratio of depth to radius of the cylinder.

TABLE 3.2

STATIC TORSIONAL IMPEDANCE FOR CYLINDRICAL FOUNDATIONS

h	Numerical Solution Via Integral Equations (Luco, 1976c)	Numerical Solution Via Finite Element Method
0	5.33	5.53
0.5	13.23	13.17
1.0	19.89	19.65
2.0	32.75	32.03

TABLE 3.3

HIGH FREQUENCY VALUES OF RADIATION DAMPING FOR EMBEDDED CYLINDERS

	C_{MM}		C_{TT}		C_{HH}		C_{VV}	
h	Analytic $a_o \to \infty$	F.E. $a_o = 6$	Analytic $a_o \to \infty$	F.E. $a_o = 6$	Analytic $a_o \to \infty$	F.E. $a_o = 6$	Analytic $a_o \to \infty$	F.E. $a_o = 6$
0.0	1.36	1.43	1.57	1.51	3.14	3.12	5.44	5.52
0.5	3.29	3.27	4.71	4.44	7.43	7.18	8.58	8.59
1.0	7.36	7.01	7.85	7.40	11.72	11.54	11.72	11.49
2.0	30.51	28.81	14.14	13.34	20.29	19.85	18.00	17.54

3.3 Comparison of the Impedance Functions Obtained by the Finite Element and the Integral Equation Methods.

To investigate the adequacy of the integral equation method of solution, the impedance functions for rigid cylindrical foundations embedded in a uniform half-space were calculated and compared with those obtained by use of the finite element method.

The geometry of the foundations considered are shown in Figs. 3.9 and 3.10 and correspond to embedment ratios of 0.25, 0.5, 1.0 and 2.0. The integral equations were discretized by considering a number M of observation points on the contact between the foundation and the soil (M varies from 31 to 61 depending on the embedment ratio). The number N of ring source points used in each case is also shown in the Figures (N varies from 12 to 27 depending on embedment ratio). The contact between the foundation and the soil was assumed to be of the welded-type . The soil was represented as a viscoelastic half-space characterized by a shear wave velocity β, a compressional wave velocity $\alpha = \sqrt{3}\beta$ and material damping constants of 0.01 and 0.005 for shear and compressional waves, respectively (specific attenuation factors: $Q_\beta = 50$ and $Q_\alpha = 100$).

The impedance functions, referred to the center of the base of the foundation and normalized as in Eq. 3.2, are compared with those obtained by the finite element method in Figs. 3.11 to 3.20. In interpreting these comparisons it must be kept in mind that the finite element results were obtained for a perfectly elastic soil model (no attenuation) while the integral equation results include a small amount of material damping.

Figs. 3.11 and 3.12 show the comparisons for the torsional stiffness and damping coefficients. The solid lines represent the

integral equation results while the dashed lines correspond to the finite element results (the same convention is used in the subsequent figures). It may be seen in Fig. 3.11 that there is close agreement between both sets of results, the only significant differences appear at high frequencies where the integral equation results are slightly higher than those obtained by the finite element method. Since comparisons of the finite element results with exact solutions reveal that the finite element method tends to underestimate the stiffness coefficients at high frequencies, it may be concluded that the integral equation results are highly accurate.

The comparison of the torsional damping coefficients shown in Fig. 3.12 indicates again good agreement except at the low frequency end where the effects of material damping included in the integral equation solution lead to higher values for the damping coefficients. At high frequencies, it seems that the integral equation values are closer to the exact asymptotic values. These results also indicate that the integral equation method of solution leads to slightly better accuracy.

The comparisons for the other impedance functions lead to similar conclusions. In general, the agreement between the two sets of results is good. The most significant differences occur for the vertical and horizontal stiffness coefficients at high frequencies and are probably associated with shortcomings of the finite element method for small wavelengths.

The results obtained indicate that both the transient finite element solution and the integral equation solution provide sufficiently accurate results for most practical applications.

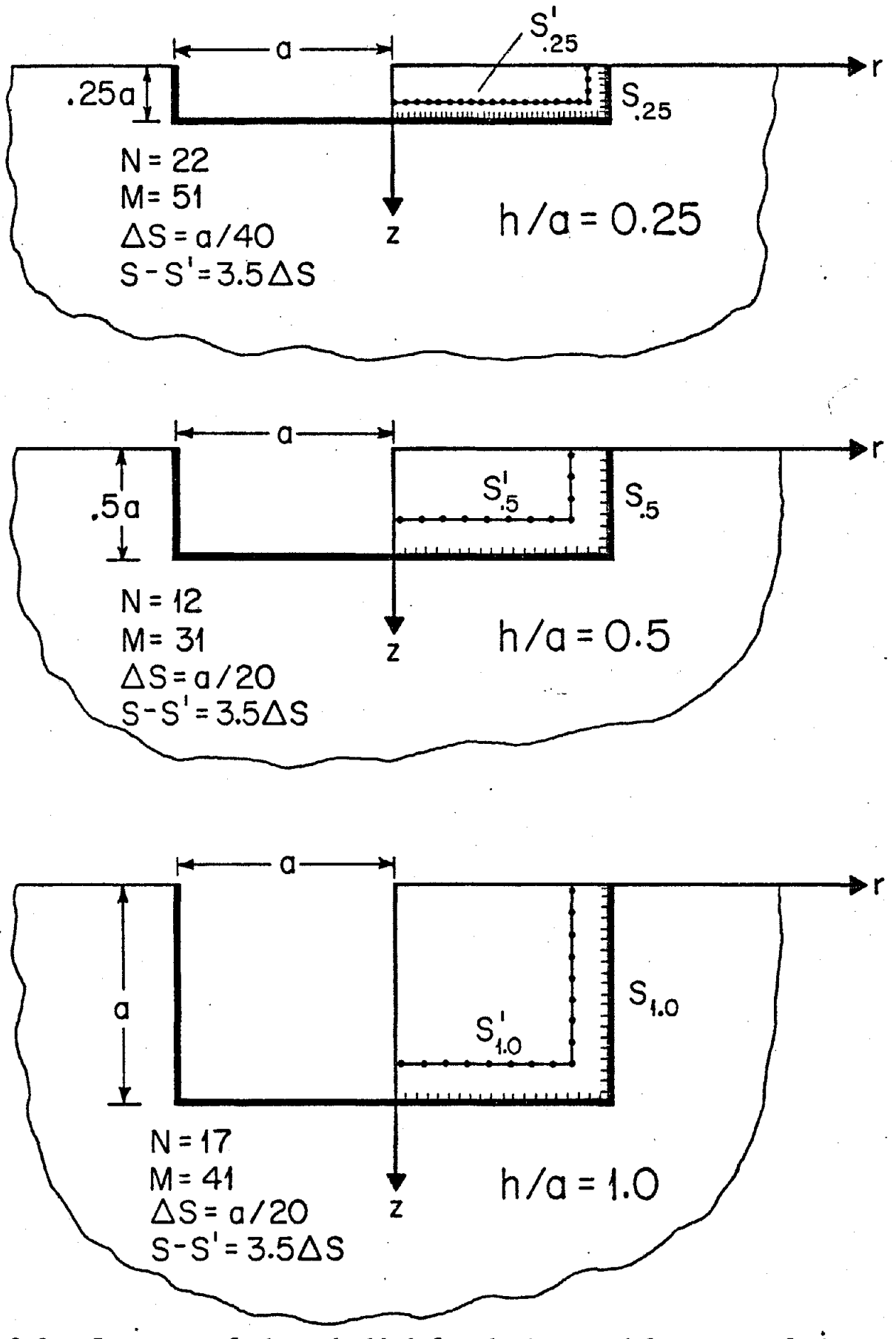

Figure 3.9. Geometry of the embedded foundations and location of the source and observation points.

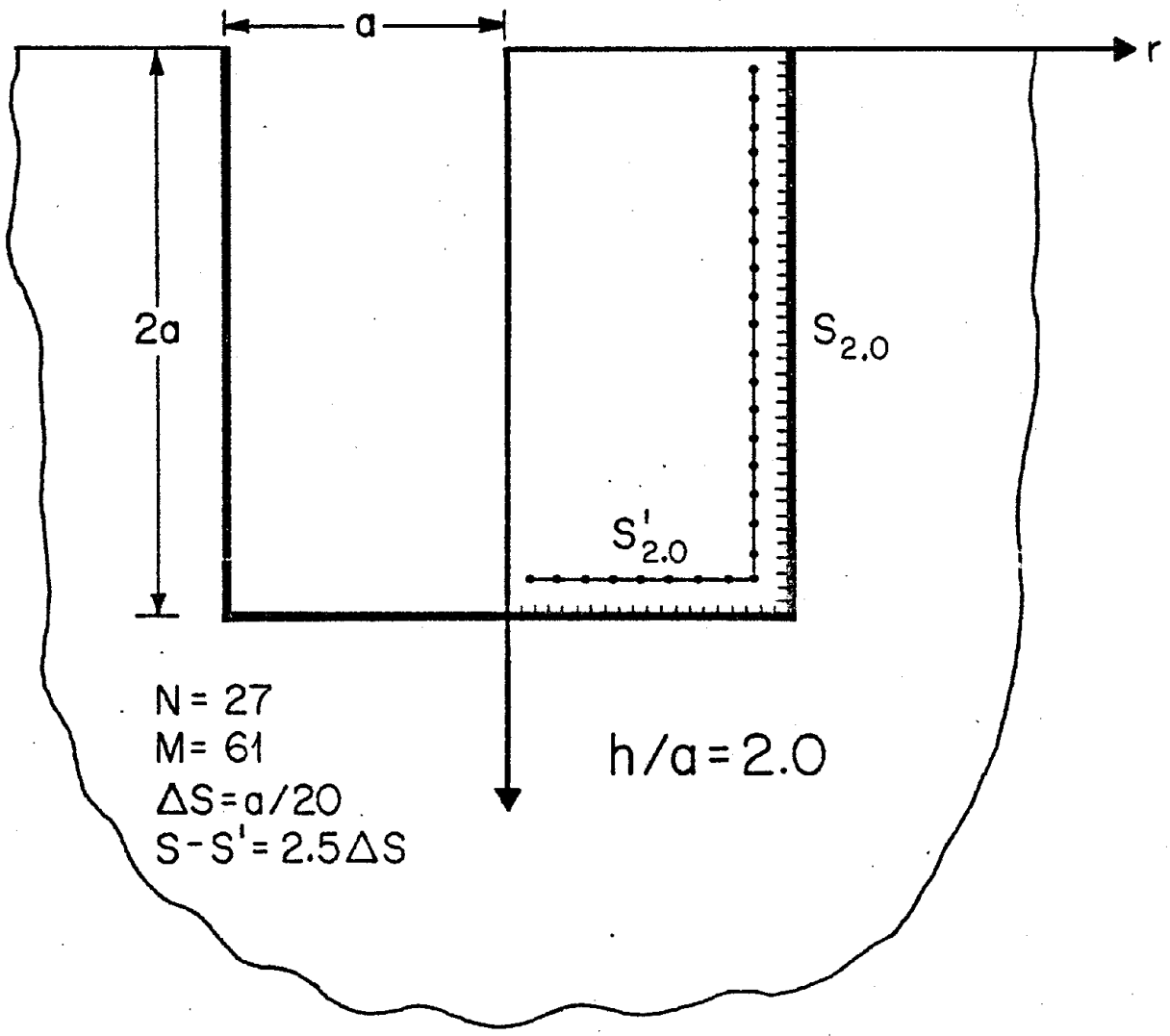

Figure 3.10. Geometry of the embedded foundations and location of the source and observation points.

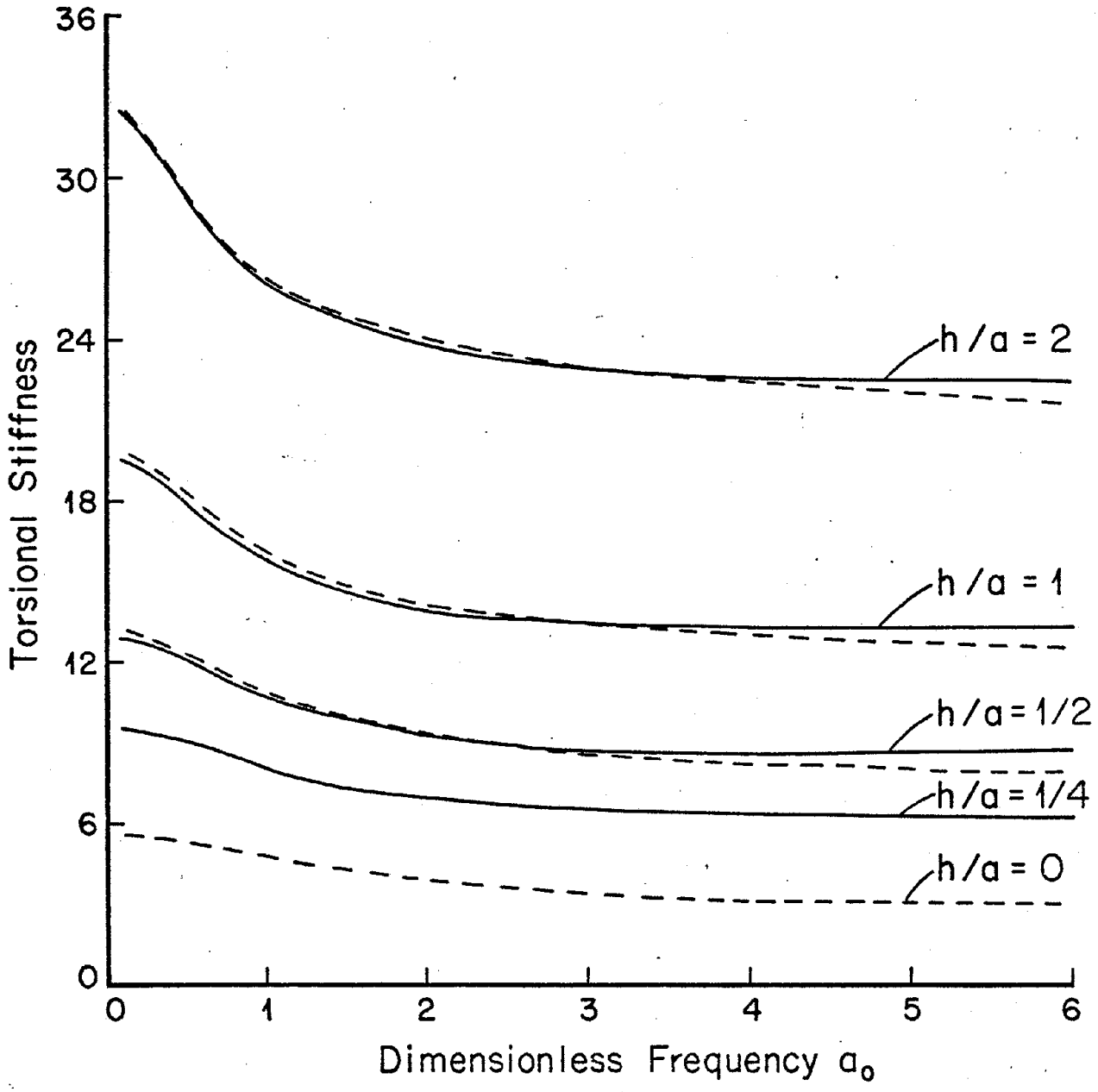

Figure 3.11. Torsional stiffness coefficients for embedded cylindrical foundations (solid line: integral equation method; dashed line: finite element method).

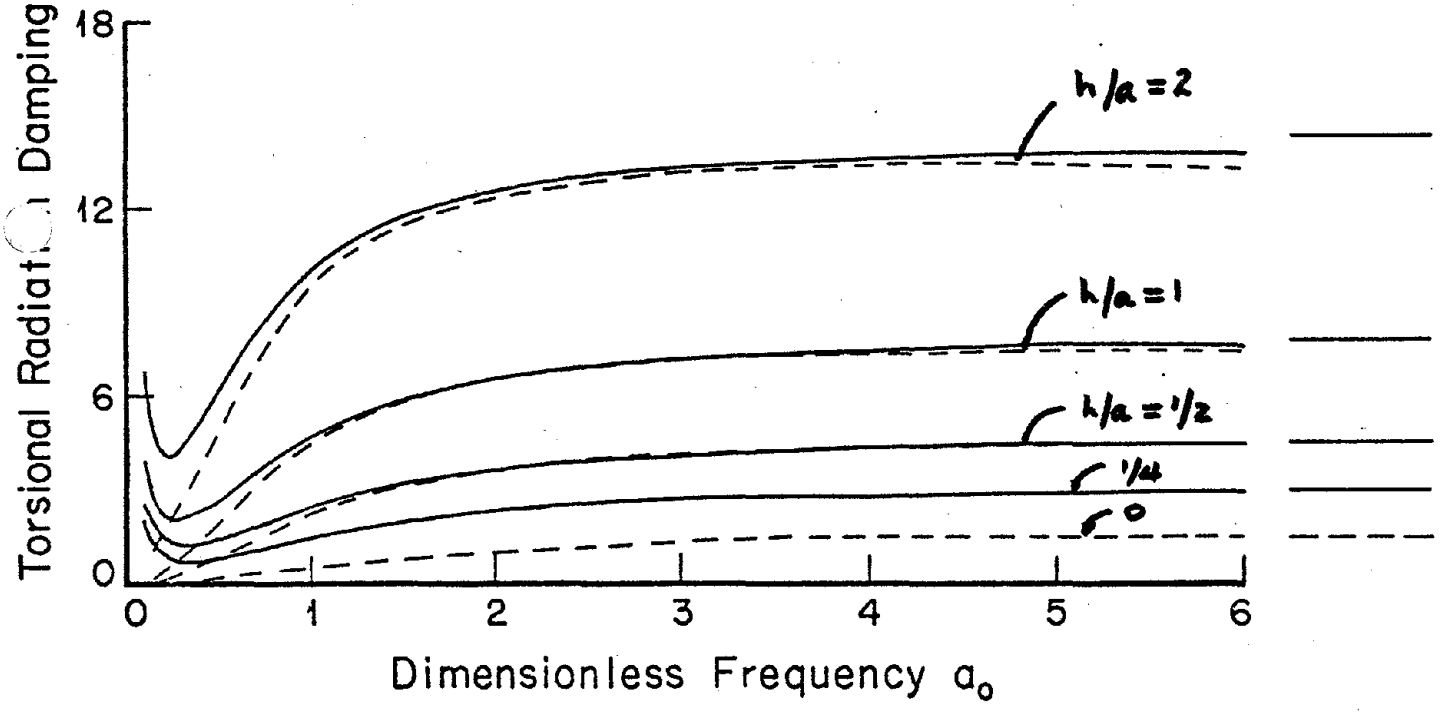

Figure 3.12. Torsional damping coefficient for embedded cylindrical foundations (solid line: integral equation method; dashed line: finite element method).

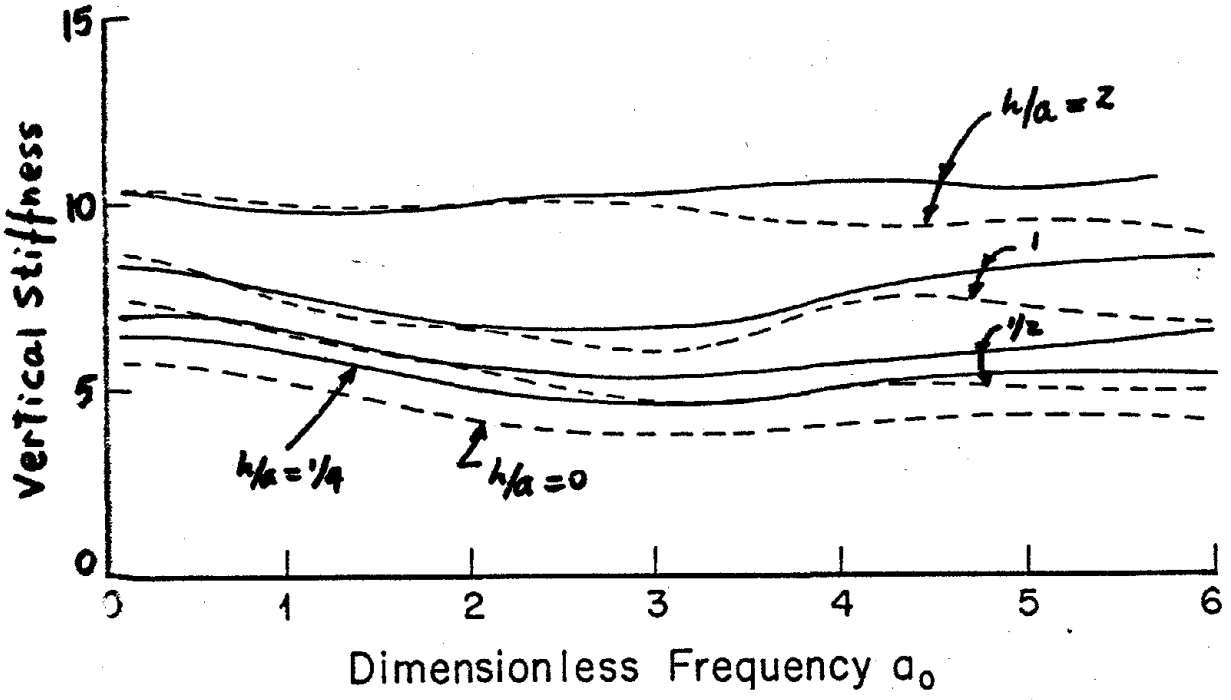

Figure 3.13. Vertical stiffness coefficients for embedded cylindrical foundations (solid line: integral equation method; dashed line: finite element method).

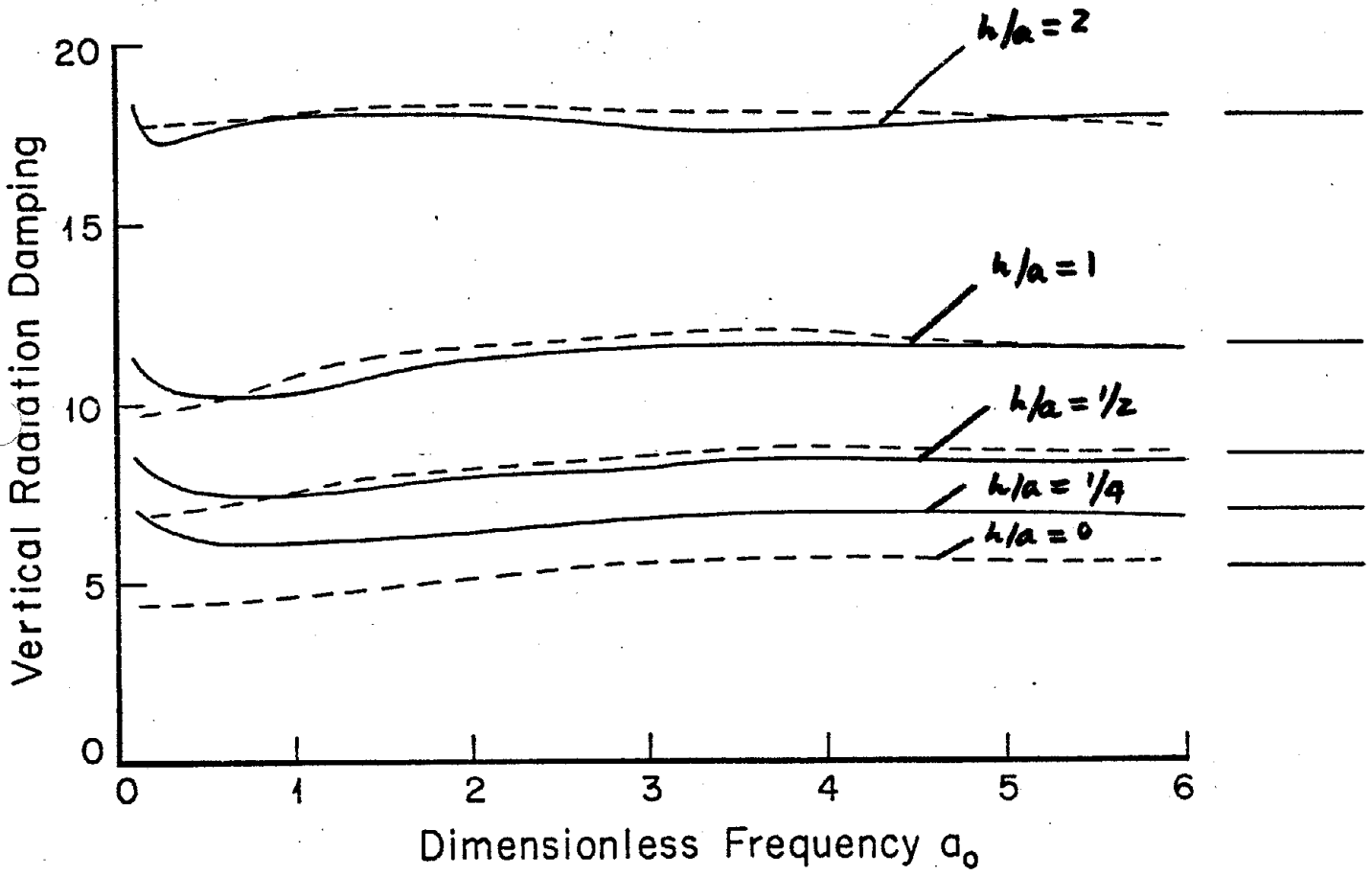

Figure 3.14. Vertical damping coefficient for embedded cylindrical foundations (solid line: integral equation method; dashed line: finite element method).

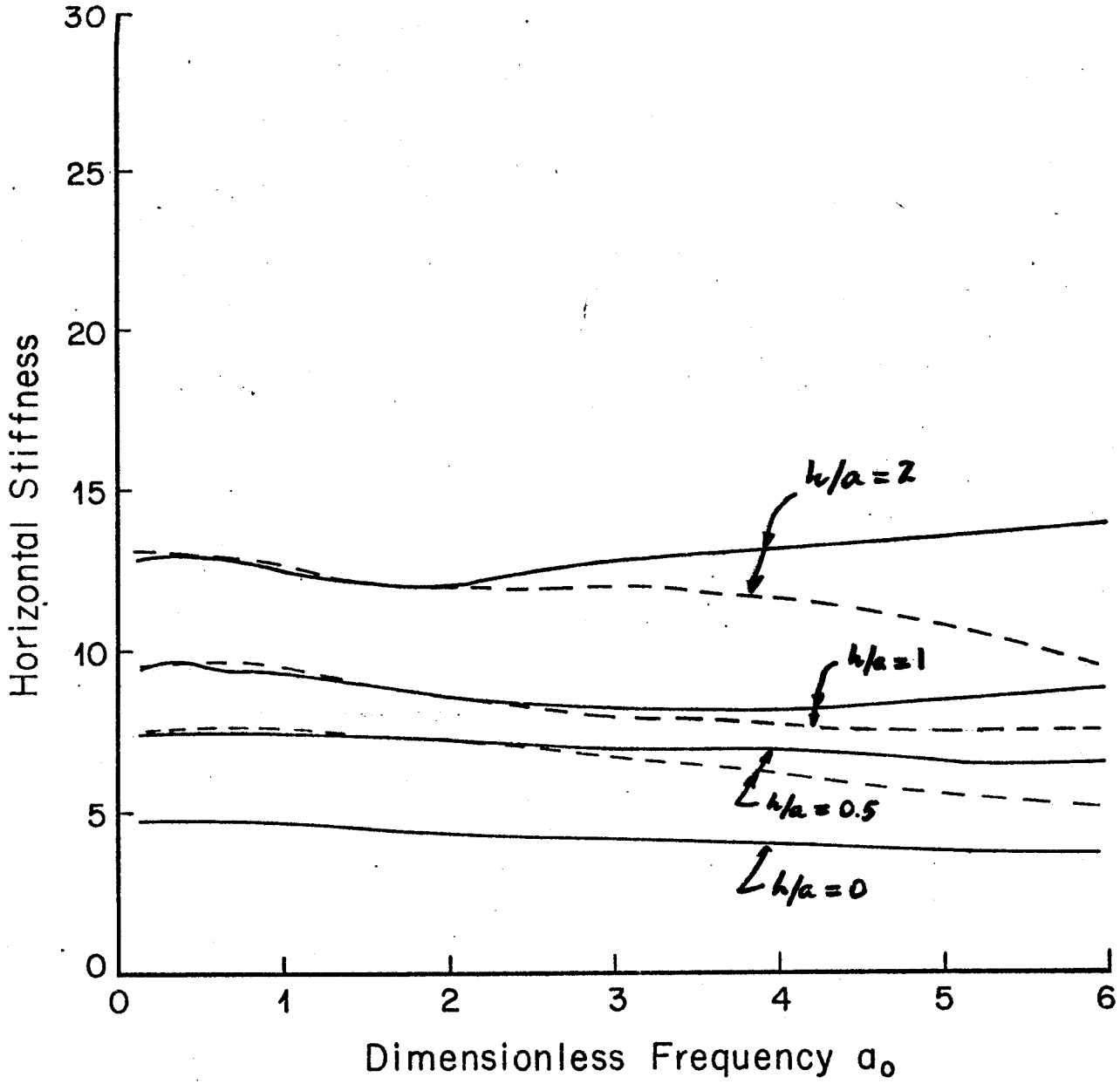

Figure 3.15. Horizontal stiffness coefficients for embedded cylindrical foundations (solid line: integral equation method; dashed line: finite element method).

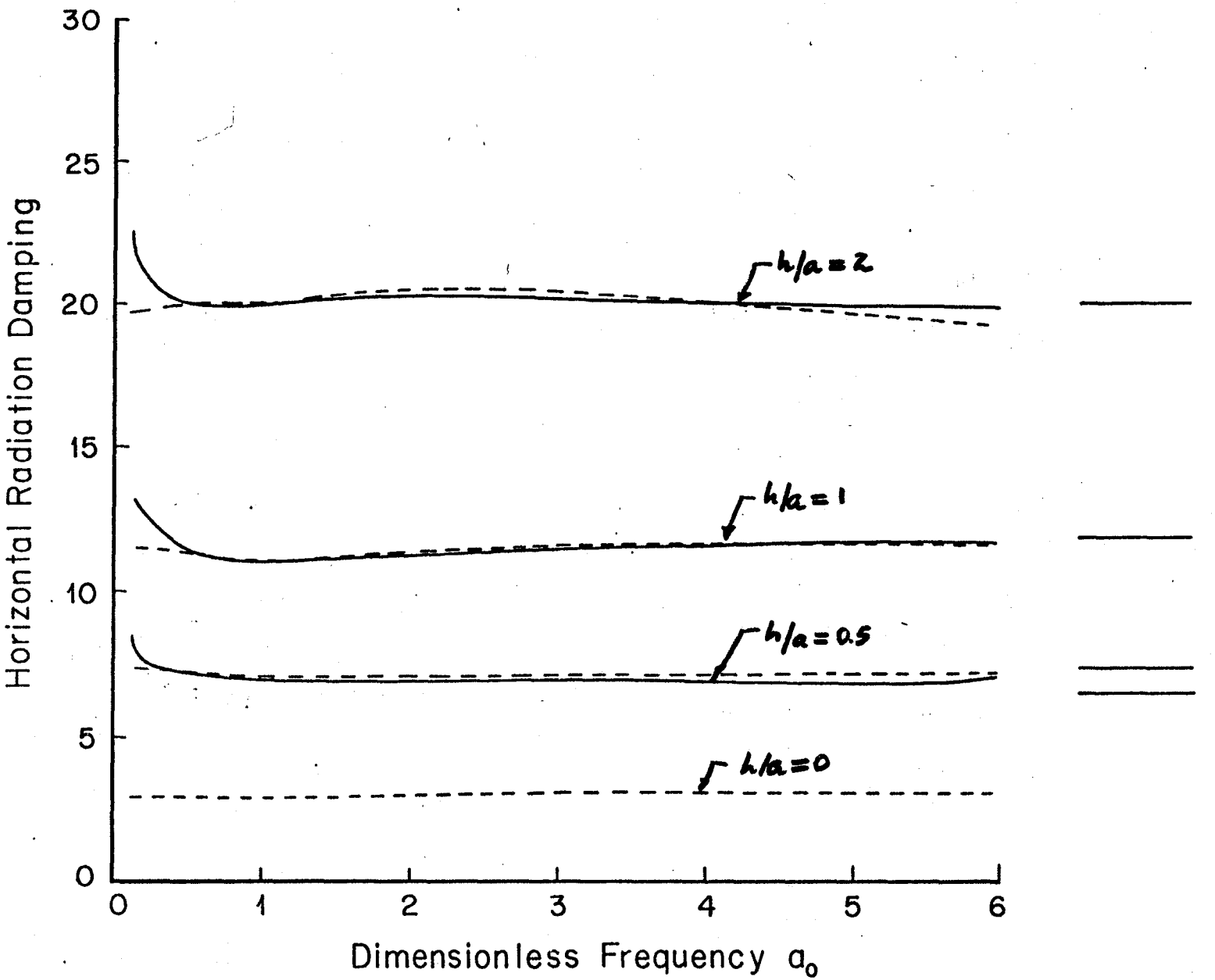

Figure 3.16. Horizontal damping coefficients for embedded cylindrical foundations (solid line: integral equation method; dashed line: finite element method).

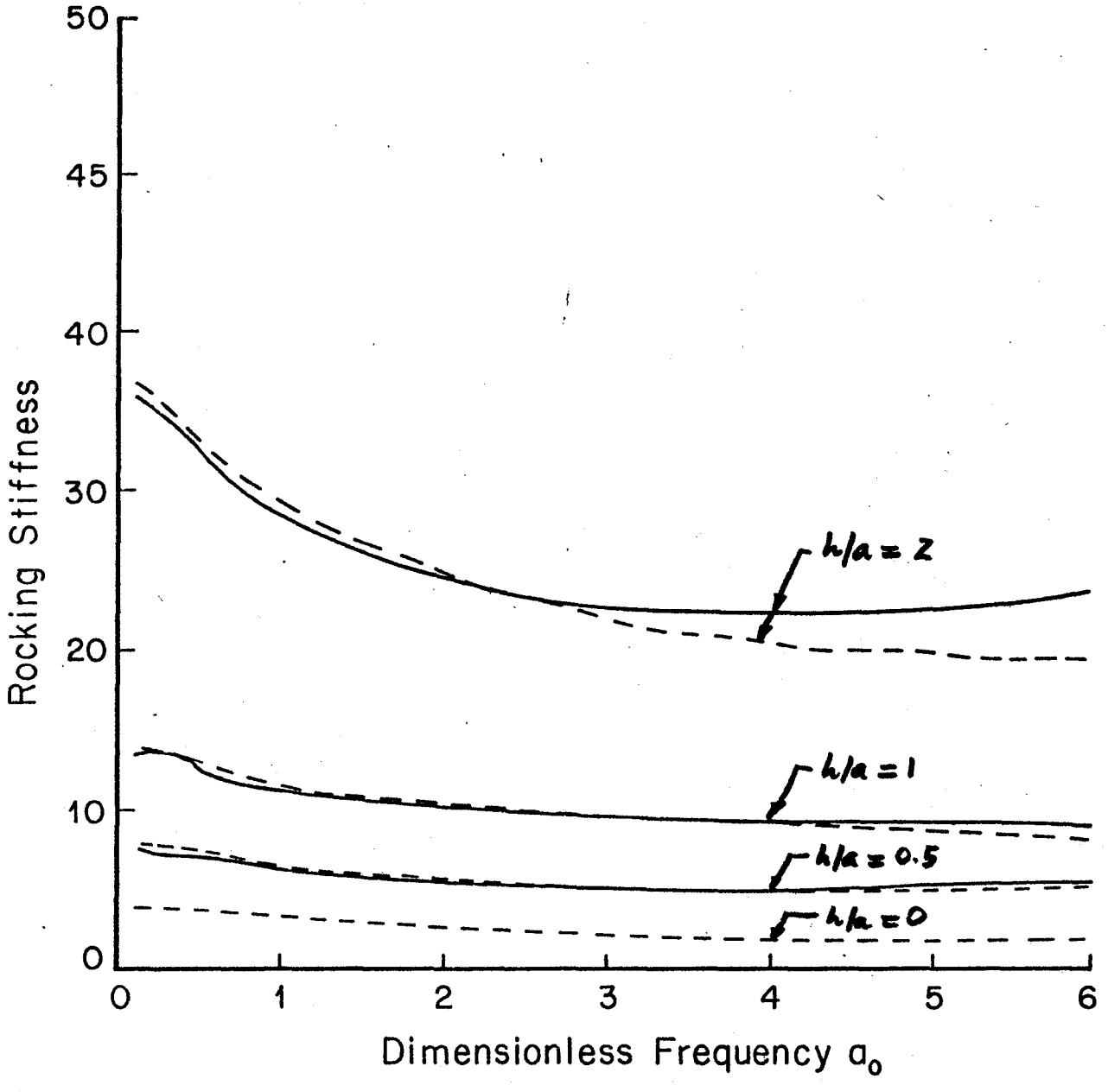

Figure 3.17. Rocking stiffness coefficients for embedded cylindrical foundations (solid line: integral equation method; dashed line: finite element method).

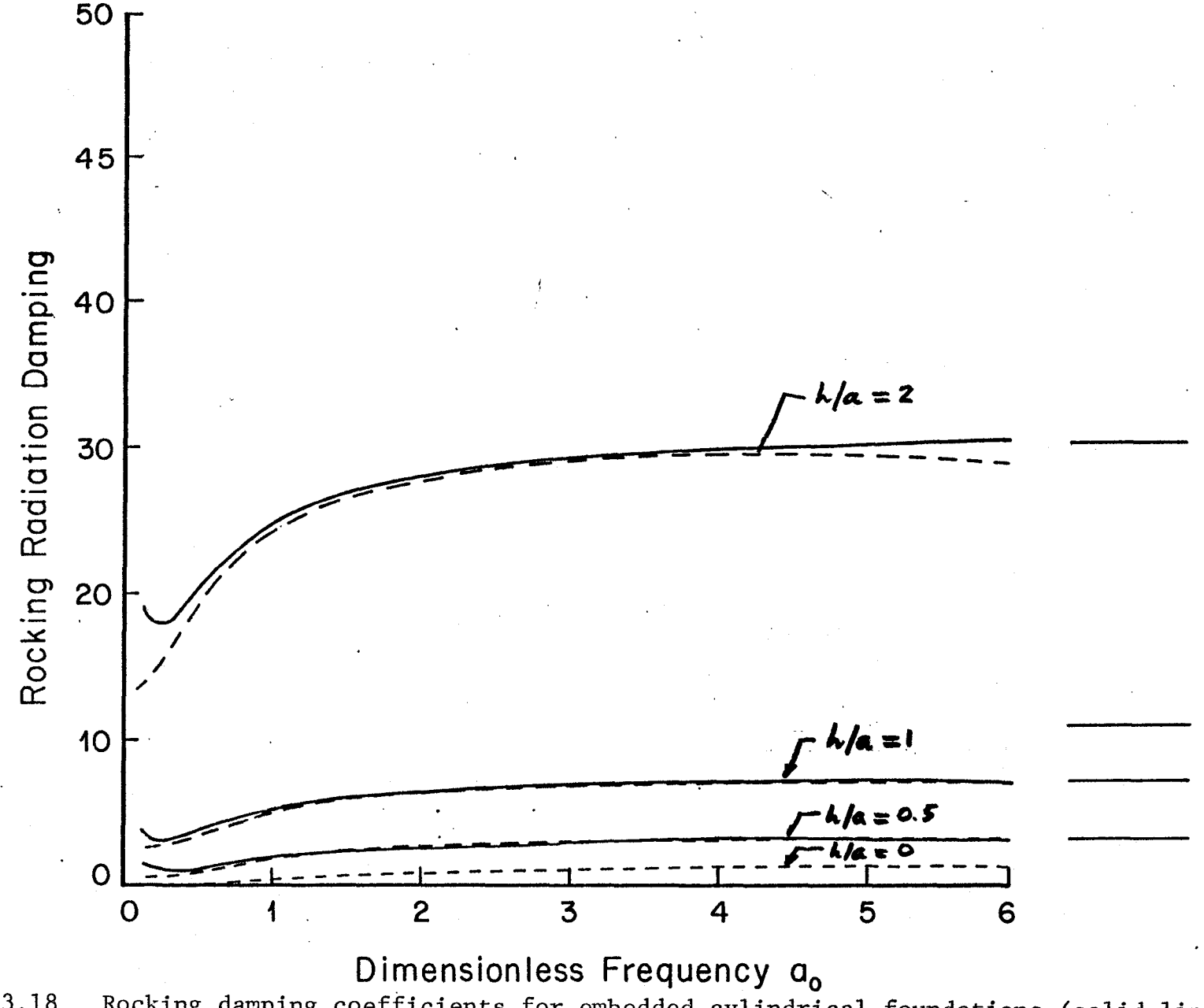

Figure 3.18. Rocking damping coefficients for embedded cylindrical foundations (solid line: integral equation method; dashed line: finite element method).

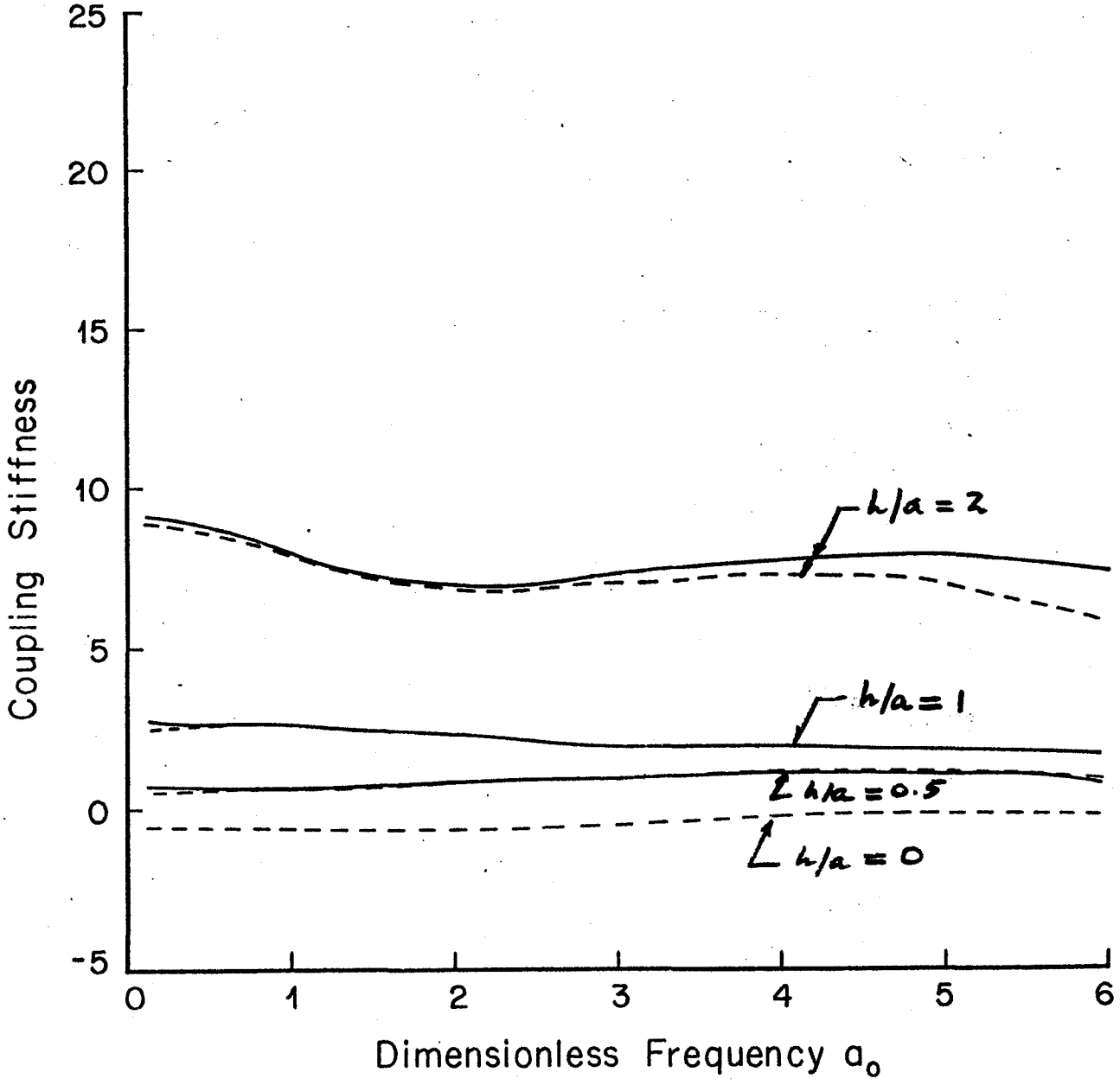

Figure 3.19. Coupling stiffness coefficients for embedded cylindrical foundations (solid line: integral equation method; dashed line: finite element method).

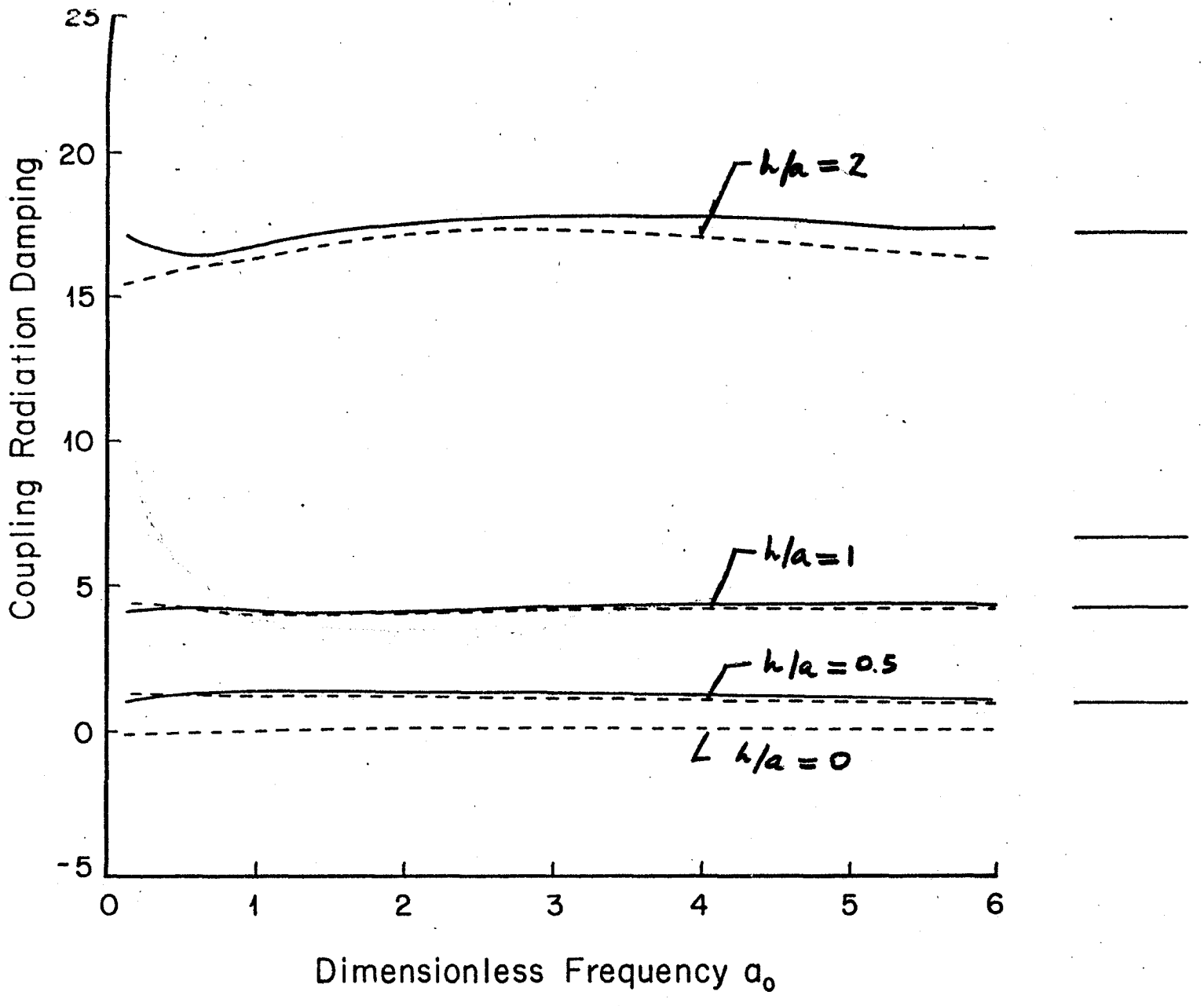

Figure 3.20. Coupling damping coefficients for embedded cylindrical foundations (solid line: integral equation method; dashed line: finite element method).

3.4 Effect of Material Damping on the Impedance Functions for Cylindrical Foundations

The effects of material damping on the response of cylindrical foundations embedded in a uniform viscoelastic half-space were investigated by considering a cylindrical foundation with an embedment ratio of 0.25. Material damping was assumed to be of the hysteretic-type. The integral equation formulation was employed for the model shown in Fig. 3.9 ($h/a = 0.25$, $\alpha/\beta = \sqrt{3}$).

The impedance functions were evaluated for shear wave material damping ratios of 1, 5 and 10 percent. (Specific attenuation factors for shear waves $Q_\beta = 50$, 10 and 5, respectively. For compressional waves the corresponding attenuation factors used were $Q_\alpha = 100$, 20 and 10, respectively). The results obtained are shown in Figs. 3.21 to 3.30.

In general, the results obtained indicate that material damping tends to reduce the stiffness coefficients at high frequencies. At low frequencies, the effects of material damping on the stiffness coefficients are negligible (Figs. 3.21, 3.23, 3.25, 3.27, 3.29). On the other hand, the effects of material damping on the damping coefficients are quite marked at low frequencies and decrease as the frequency increases (Figs. 3.22, 3.24, 3.26, 3.28, 3.30).

It is important to mention that the integral formulation employed can also be used to investigate other attenuation mechanisms in addition to the hysteretic-type just discussed.

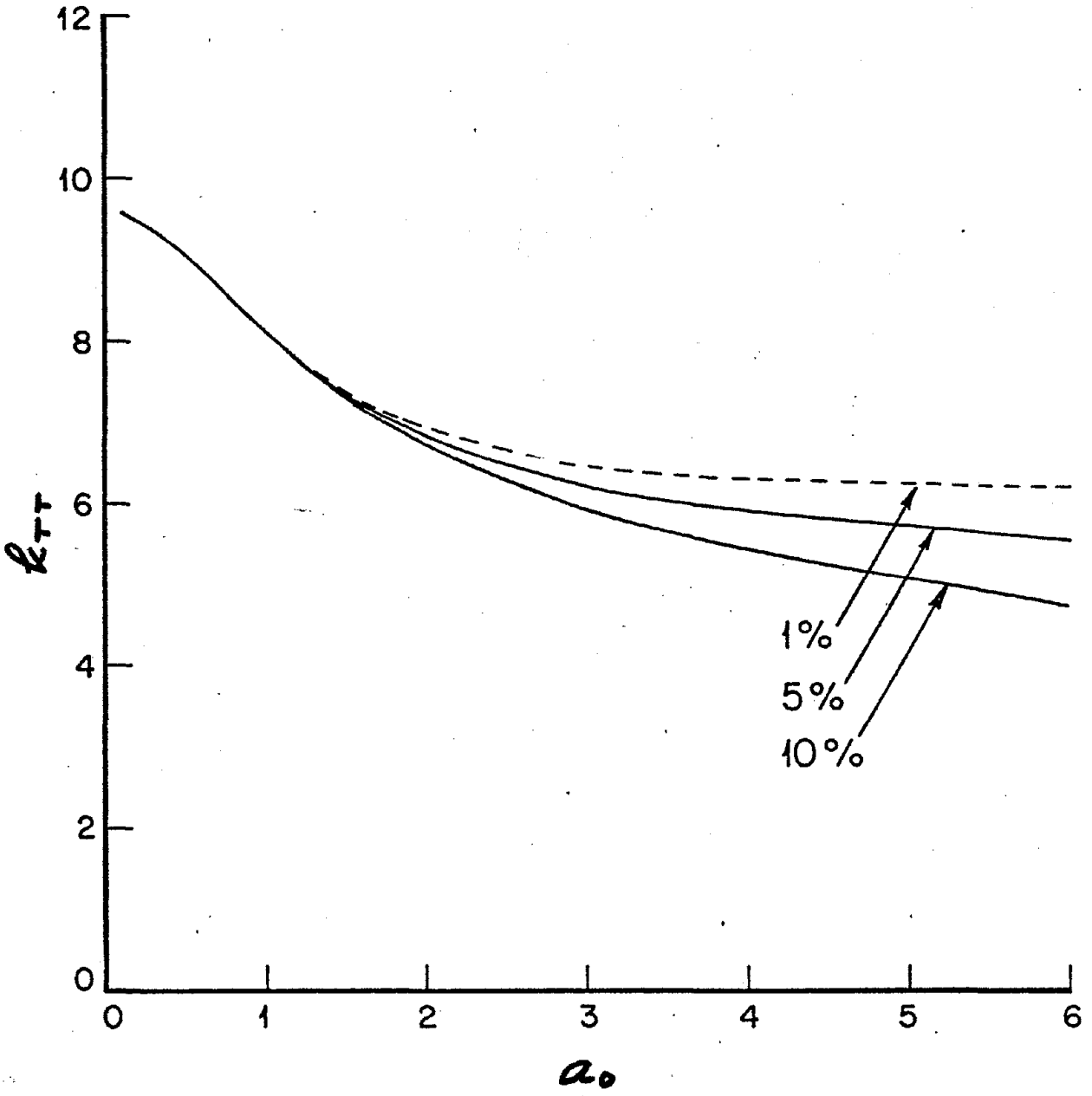

Figure 3.21. Effect of material damping on the torsional stiffness coefficient (h/a = 0.25).

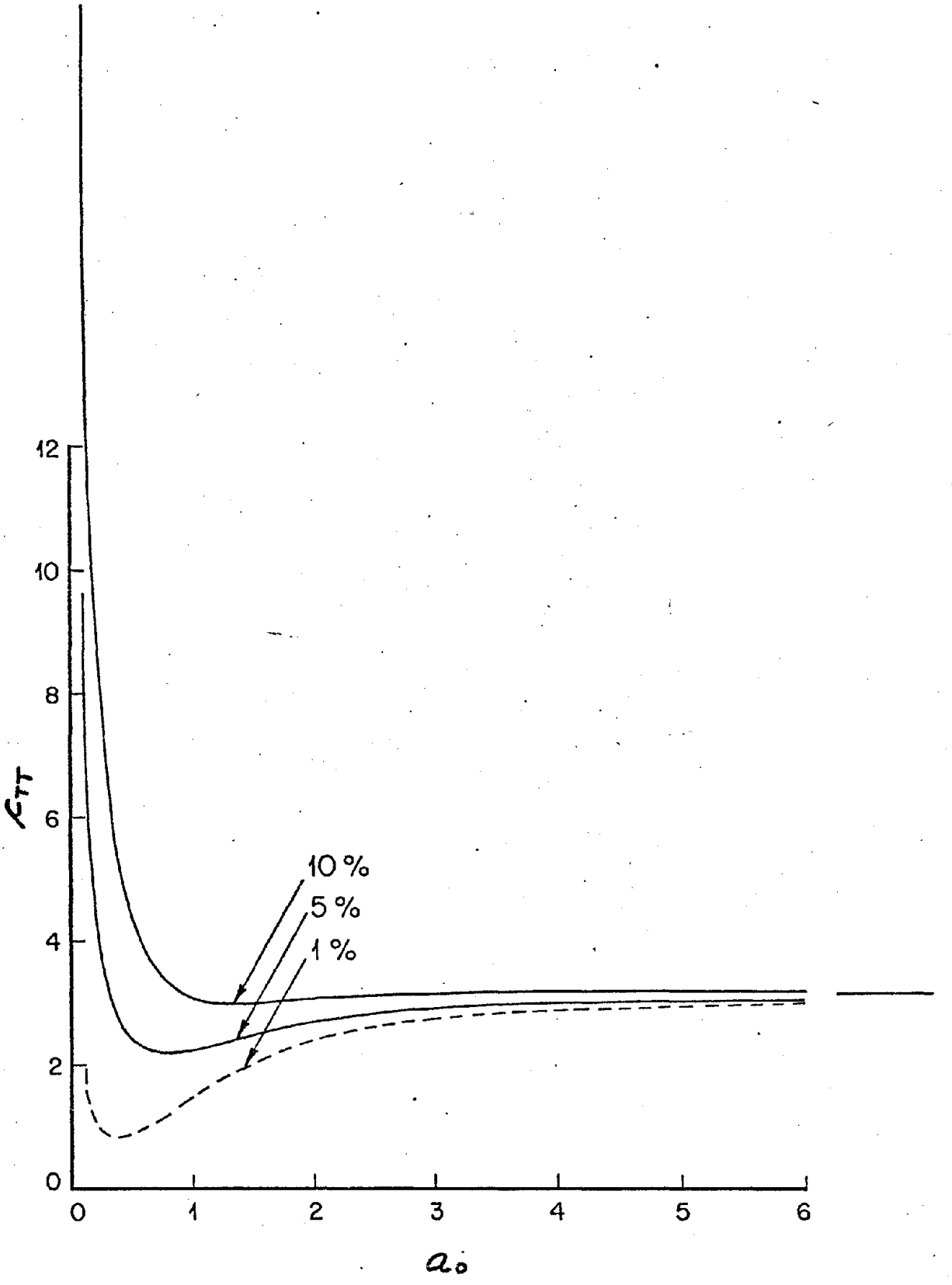

Figure 3.22. Effect of material damping on the torsional damping coefficient (h/a = 0.25).

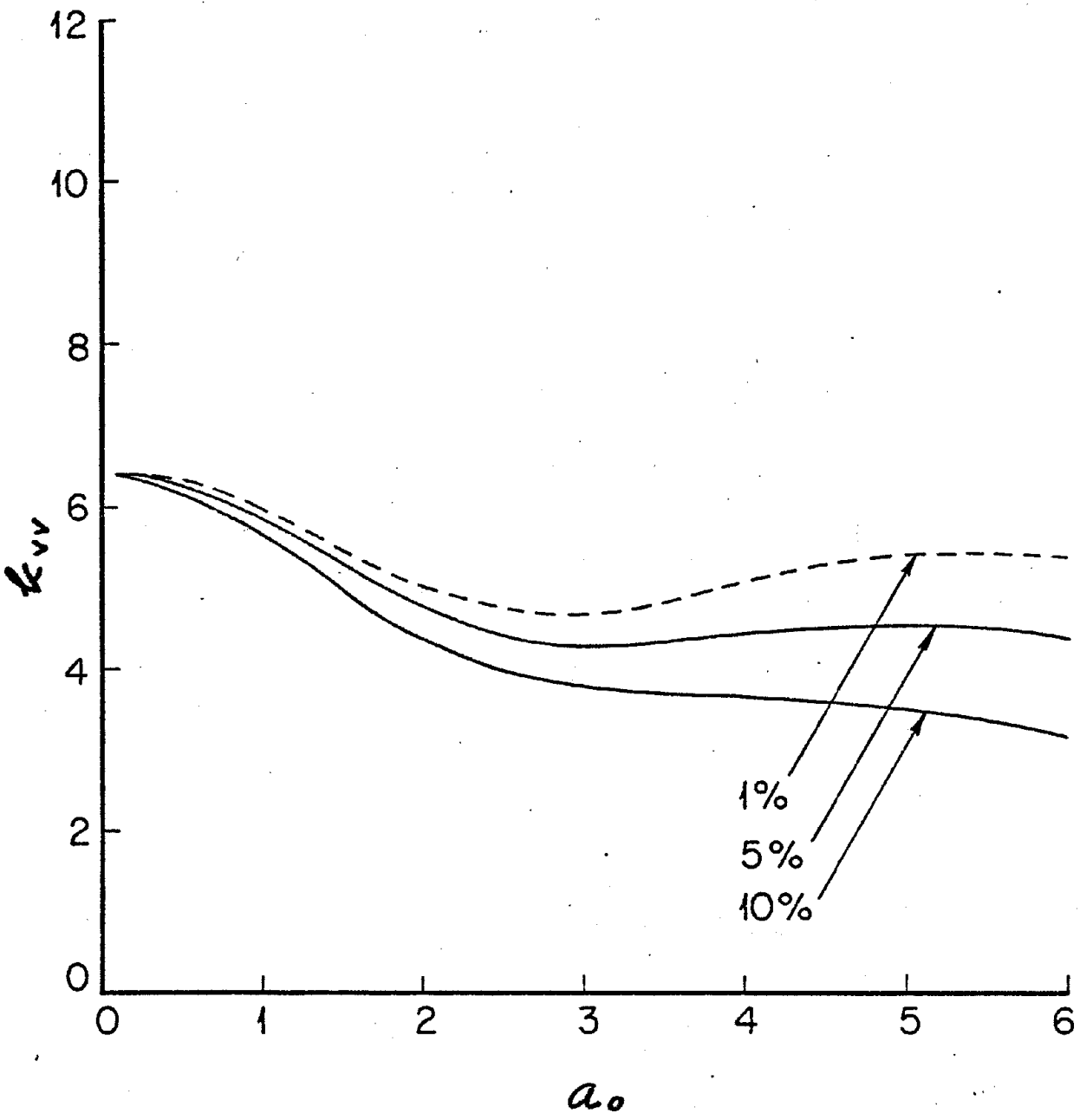

Figure 3.23. Effect of material damping on the vertical stiffness coefficient (h/a = 0.25).

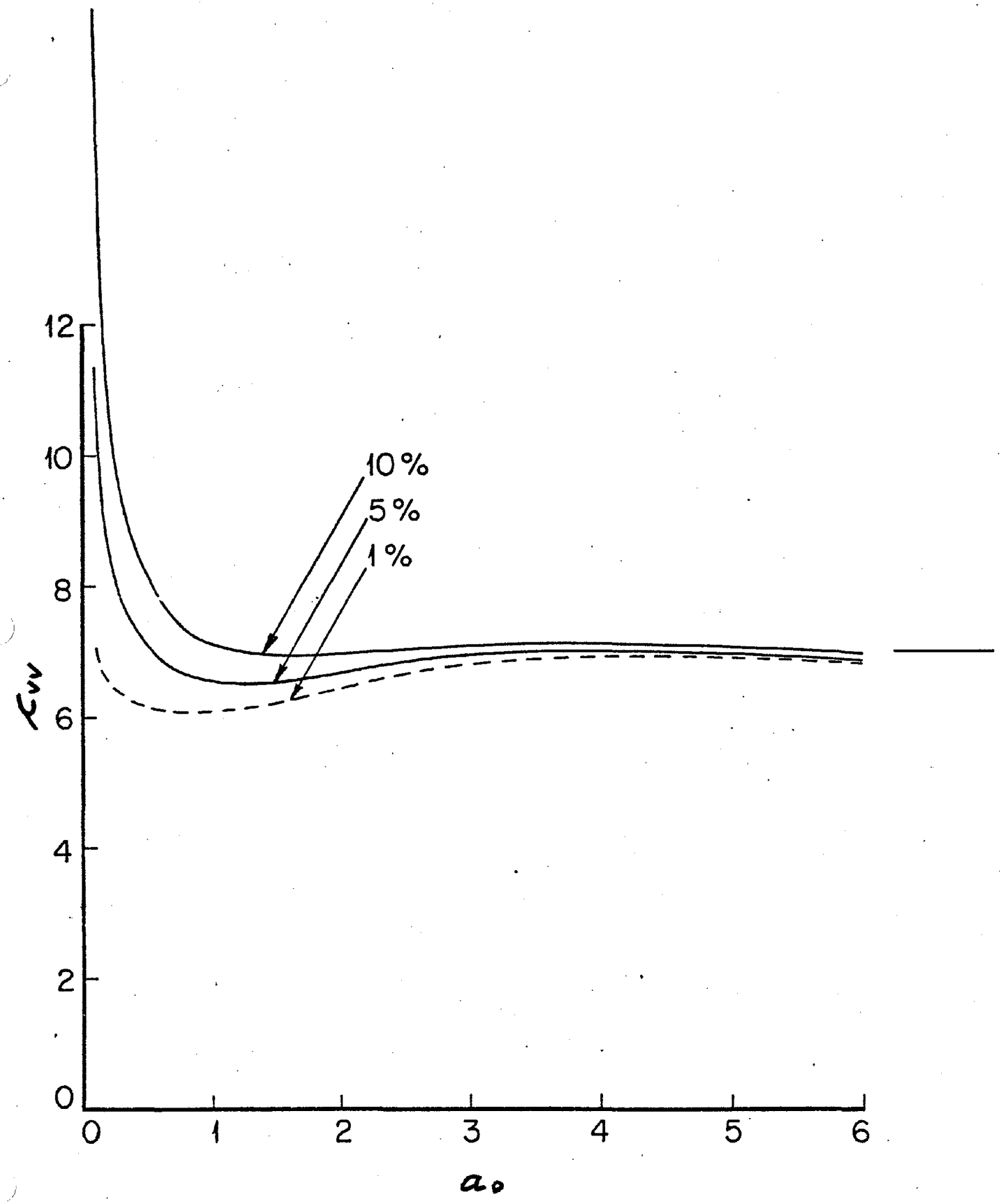

Figure 3.24. Effect of material damping on the vertical damping coefficient (h/a = 0.25).

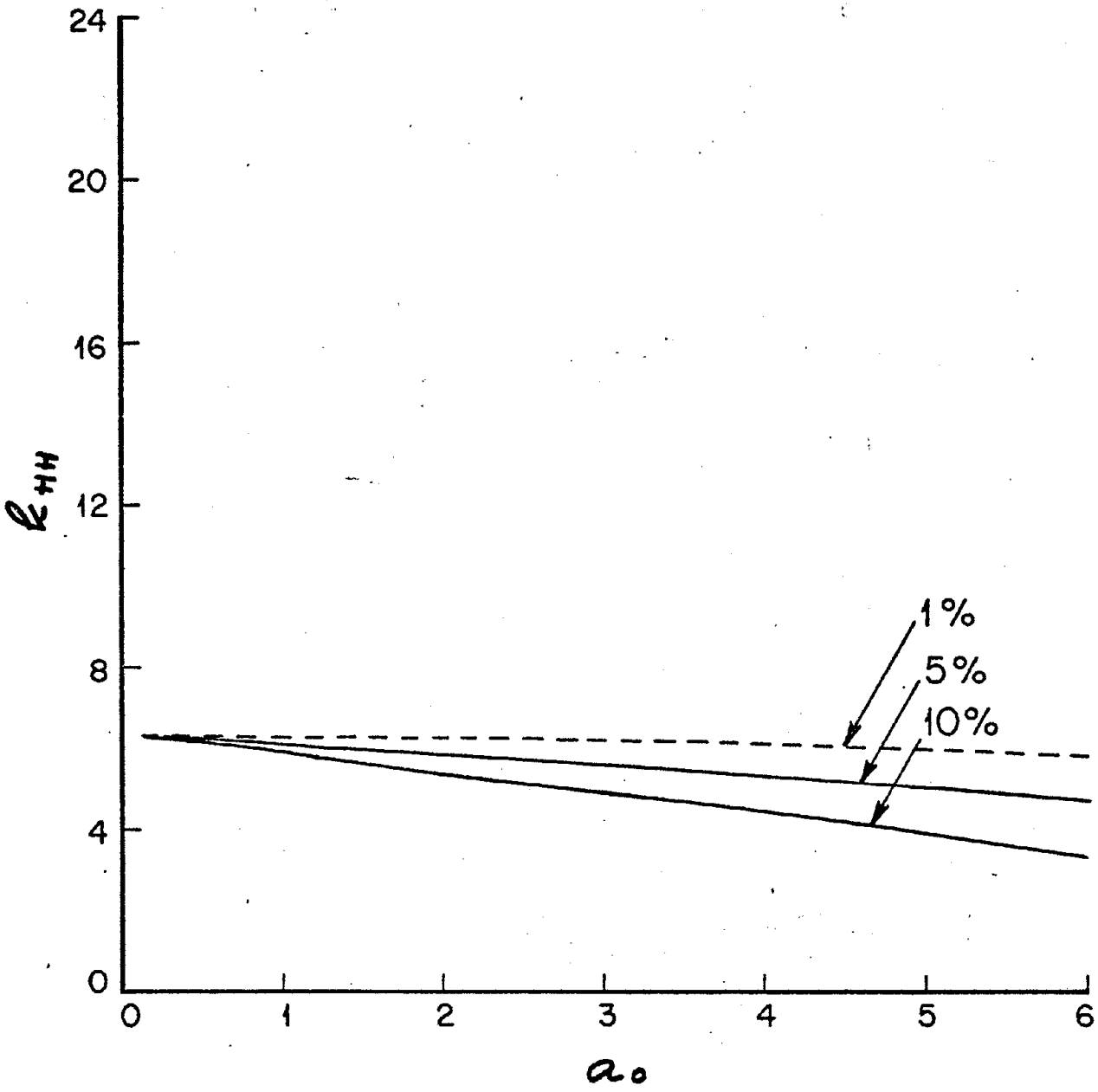

Figure 3.25. Effect of material damping on the horizontal stiffness coefficient (h/a = 0.25).

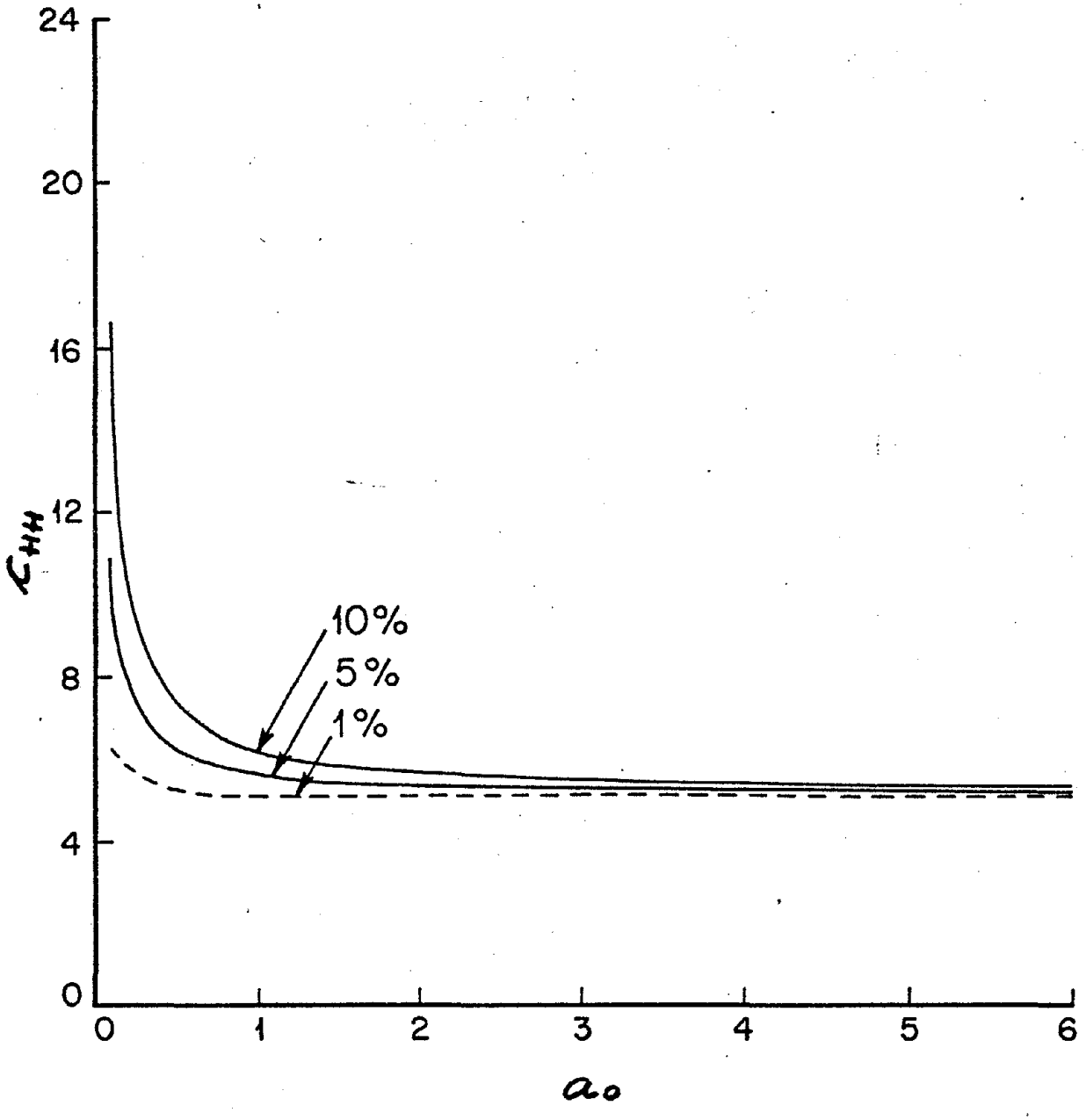

Figure 3.26. Effect of material damping on the horizontal damping coefficient (h/a = 0.25).

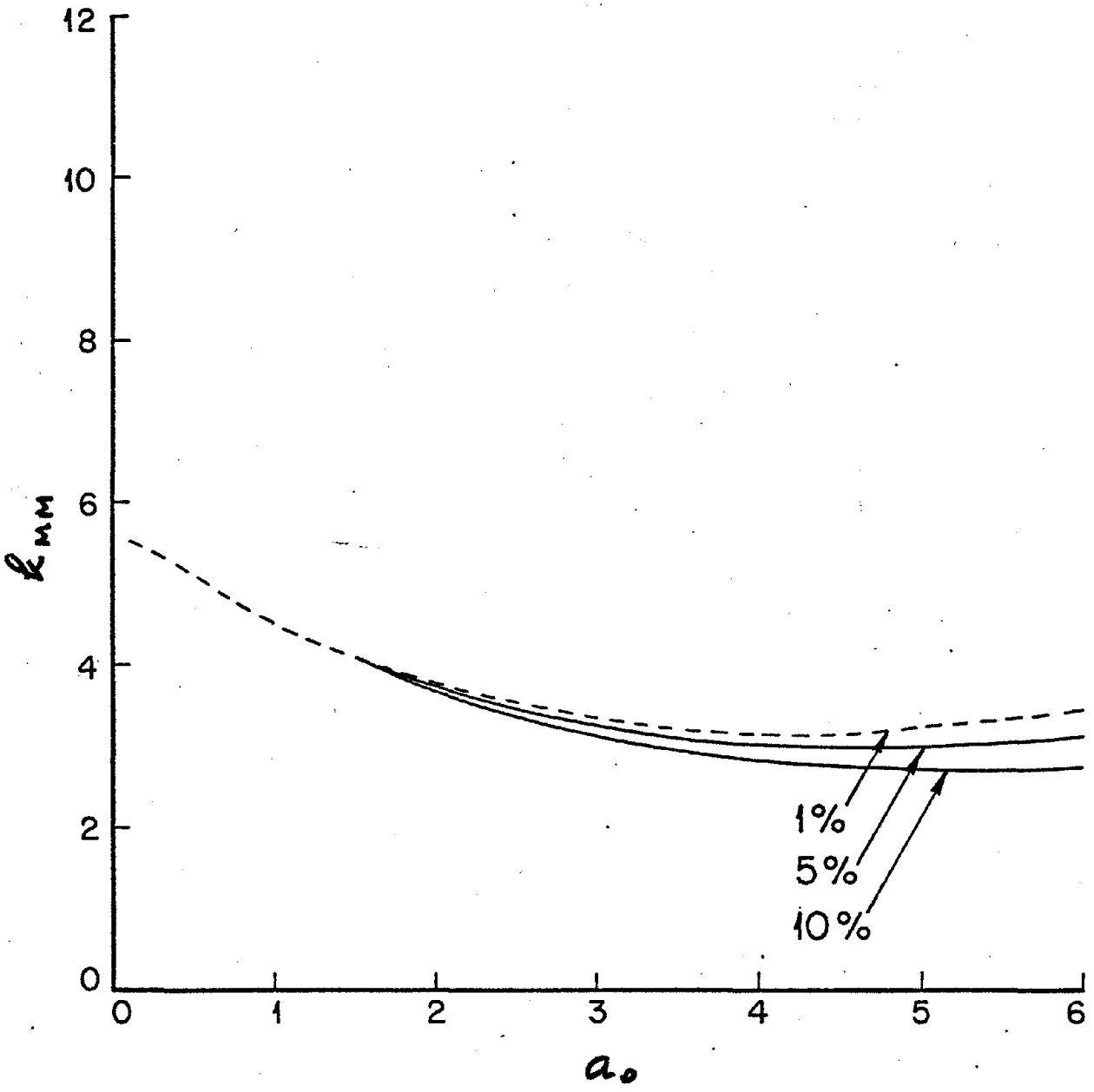

Figure 3.27. Effect of material damping on the rocking stiffness coefficient (h/a = 0.25).

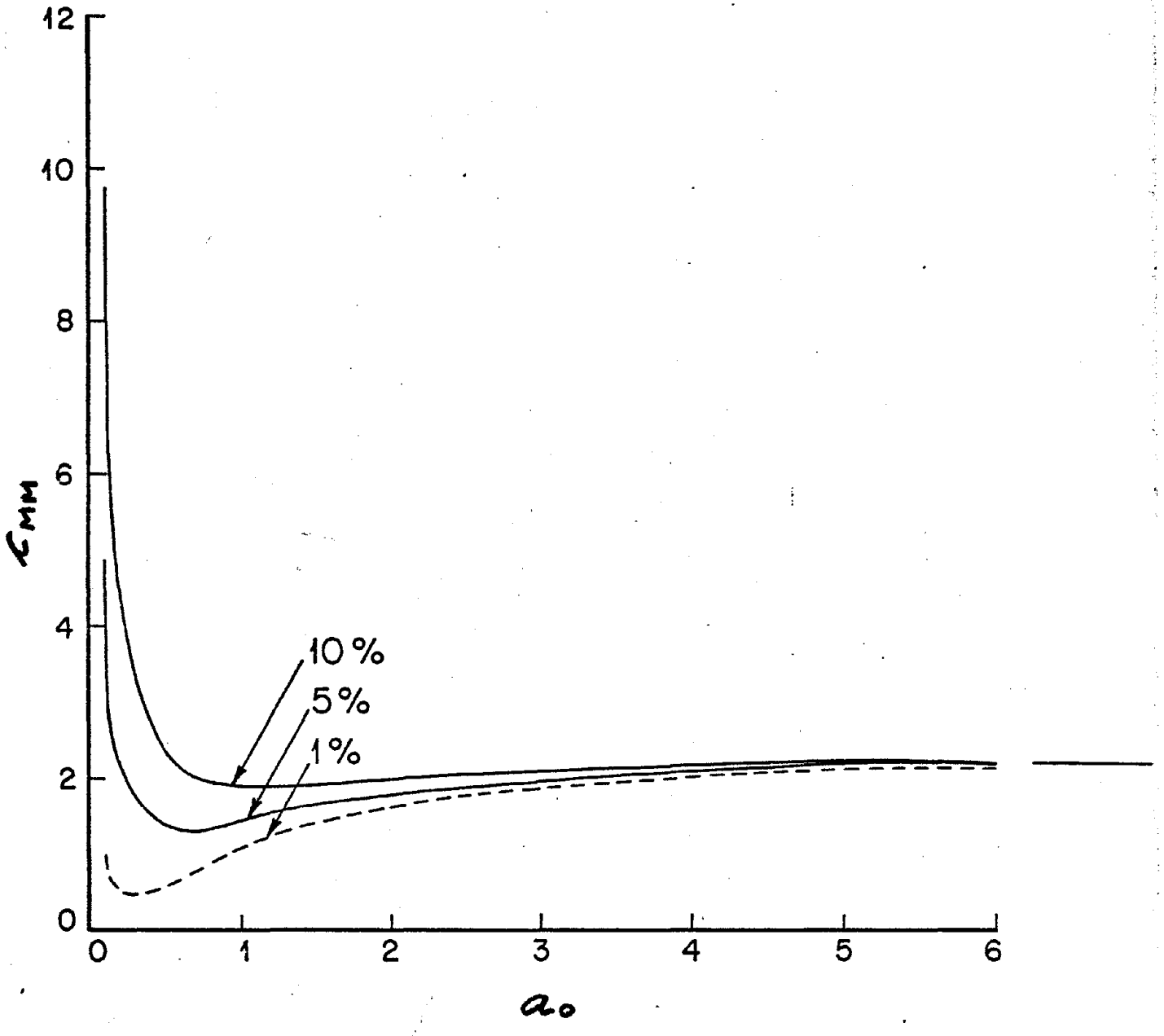

Figure 3.28. Effect of material damping on the rocking damping coefficient (h/a = 0.25).

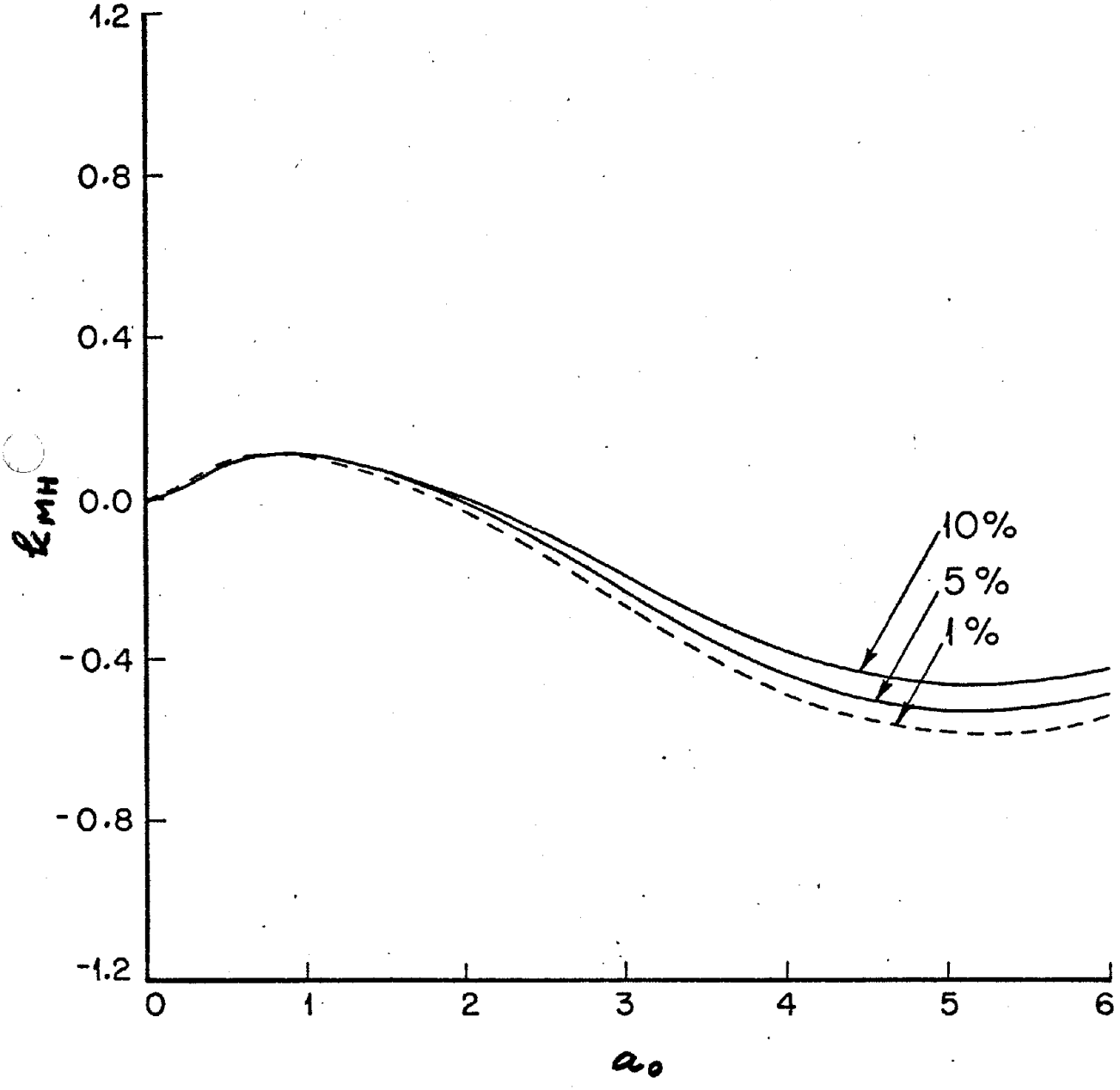

Figure 3.29. Effect of material damping on the coupling stiffness coefficient (h/a = 0.25).

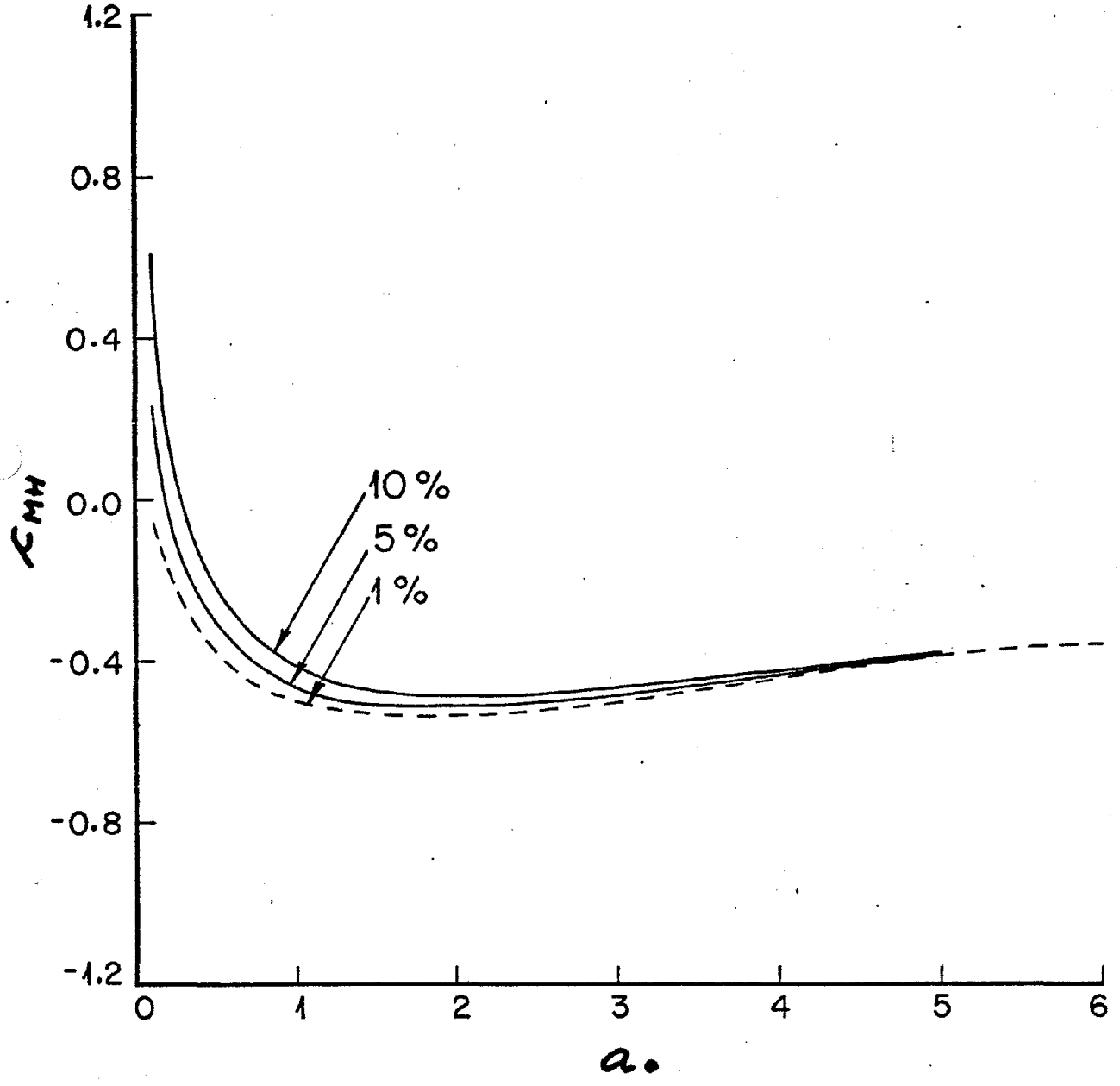

Figure 3.30. Effect of material damping on the coupling damping coefficient (h/a = 0.25).

3.5 Effect of Lateral Separation on the Impedance Functions for Cylindrical Foundations

In many practical situations it is not possible to assume that the foundation is in welded contact with the surrounding soil. The presence of backfill or the possible inelastic deformation of the top soil layers suggest that a more realistic model for the contact conditions must allow for the lateral separation between the foundation and the soil. The effects of the lateral separation were investigated by considering a cylindrical foundation embedded in a uniform viscoelastic half-space ($h/a = 2.0$, $\xi = 0.01$, $\alpha/\beta = \sqrt{3}$). Four cases were considered: in the first case, the foundation was perfectly welded to the surrounding soil (0% separation); in the second case, the top 25% of the lateral boundary of the foundation was assumed to act independently from the soil while the rest of the foundation remained in welded contact (25% separation); the third and fourth cases correspond to 50 and 75% separation.

Some typical results obtained by use of the integral equation formulation are shown in Figs. 3.31 and 3.32. In Fig. 3.31 the effects of lateral separation of the torsional stiffness coefficients are shown. The corresponding effects on the torsional damping coefficients are presented in Fig. 3.32. The results obtained indicate that lateral separation has a marked effect on the impedance functions. The effect corresponds to a reduction of the stiffness and damping coefficients. In particular, the damping coefficients for a cylindrical foundation with an embedment ratio $h/a = 2.0$ and with lateral separation on the top 50% of the mantle are very close to the corresponding damping coefficients for a foundation welded to the soil and with an "effective"

embedment ratio of h/a = 1 (refer to Figs. 3.32 and 3.11).

In addition to the reduction of the impedance functions just described, the presence of lateral separation increases the frequency dependence of the impedance functions as may be seen in Figs. 3.31 and 3.32.

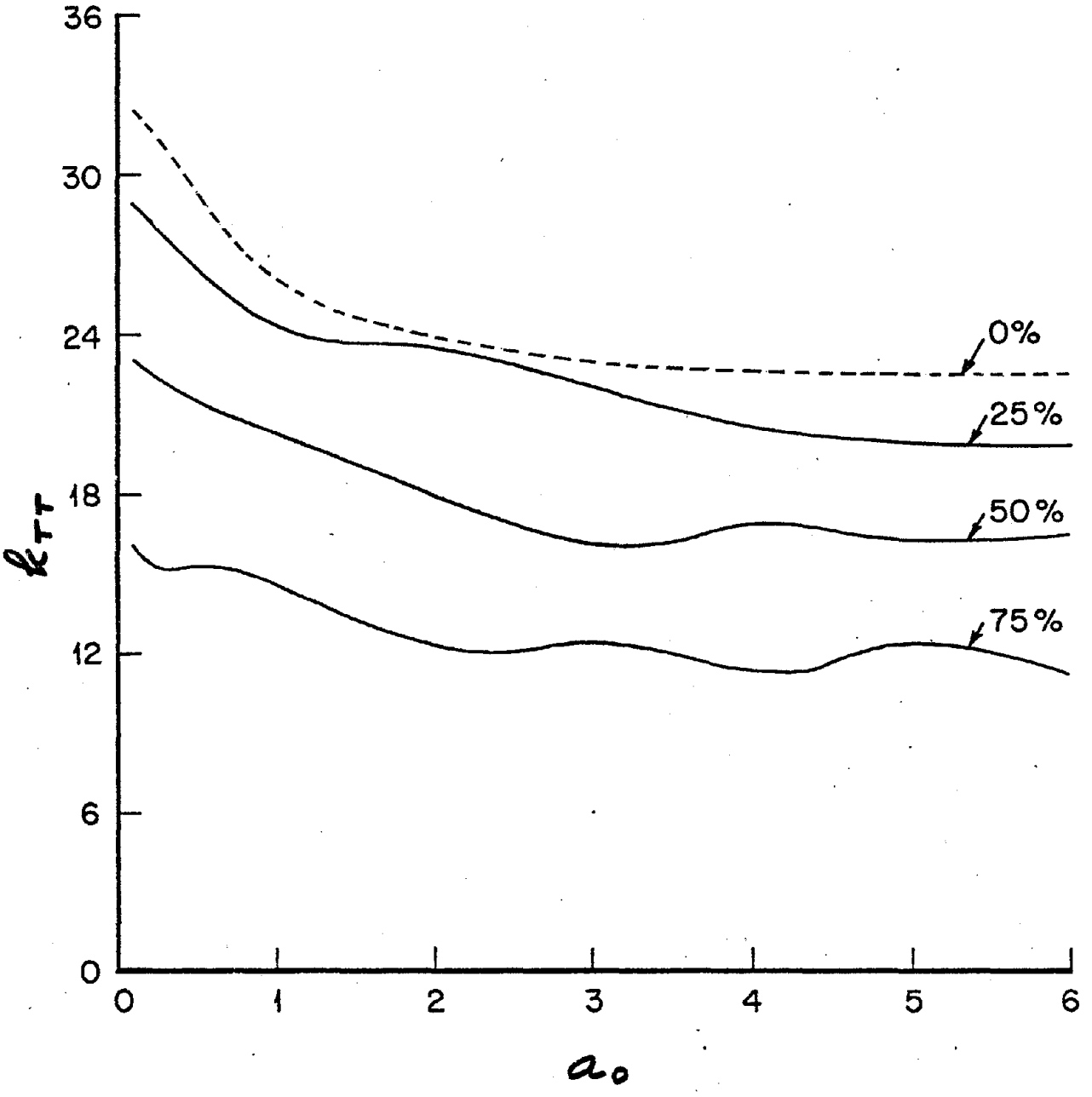

Figure 3.31. Effect of lateral separation on the stiffness coefficient for an embedded cylindircal foundation (h/a = 2.0).

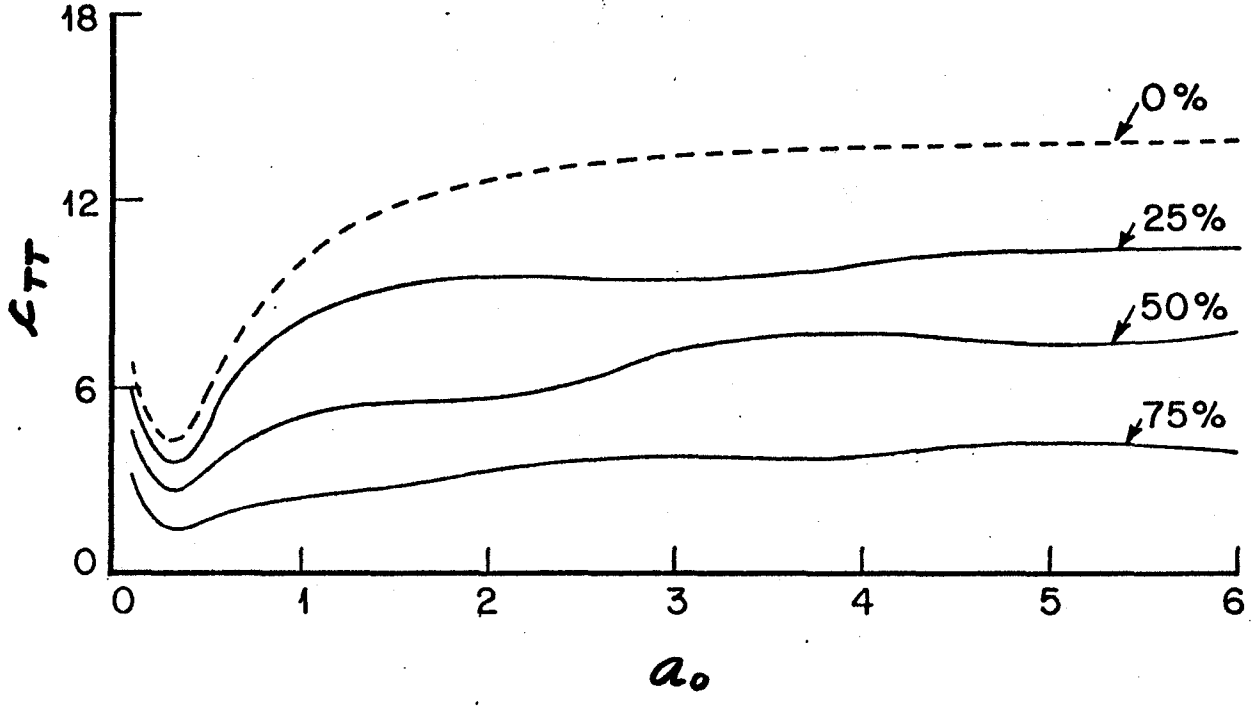

Figure 3.32. Effect of lateral separation on the torsional damping coefficient for an embedded cylindrical foundation (h/a = 2.0).

3.6 Impedance Functions for Cylindrical Foundations in Layered Media

As an example of application of the integral equation approach to foundations embedded in layered viscoelastic media, the case of a rigid cylindrical foundation of radius a = 40 ft embedded in the soil to a depth h = 18 ft has been analyzed. The soil deposit consists of six parallel viscoelastic layers overlying a uniform viscoelastic half-space. The soil properties are listed in Table 3.1.

The horizontal, rocking and coupling impedances functions referred to the center of the base of the foundation are shown in Fig. 3.3. The stiffness and damping coefficients have been normalized as in Eq. (3.2) by the shear modulus and shear wave velocity of the top layer. The layering introduces a more pronounced frequency dependence than in the case of a uniform soil deposit. Also, due to the presence of stiffer soils at depth, the damping coefficients at low frequencies are lower than those for a uniform soil deposit.

These results indicate that the integral formulations used in conjunction with the Green functions for layered viscoelastic media provides an excellent technique to obtain the response of foundations embedded in layered viscoelastic media.

TABLE 3.1 SOIL PROPERTIES

Layer	Depth (ft)	Shear Wave Velocity (ft/sec)	P-Wave Velocity (ft/sec)	Unit Weight (lb/ft^3)	Material Damping Ratio (Shear)
1	0- 6	630	1260	115	0.01
2	6- 18	1110	2220	115	0.01
3	18- 32	1380	2760	115	0.01
4	32- 66	1600	3200	115	0.01
5	66-336	2000	4000	115	0.01
6	336-389	2500	5000	115	0.01
7	389-	3100	6200	115	0.01

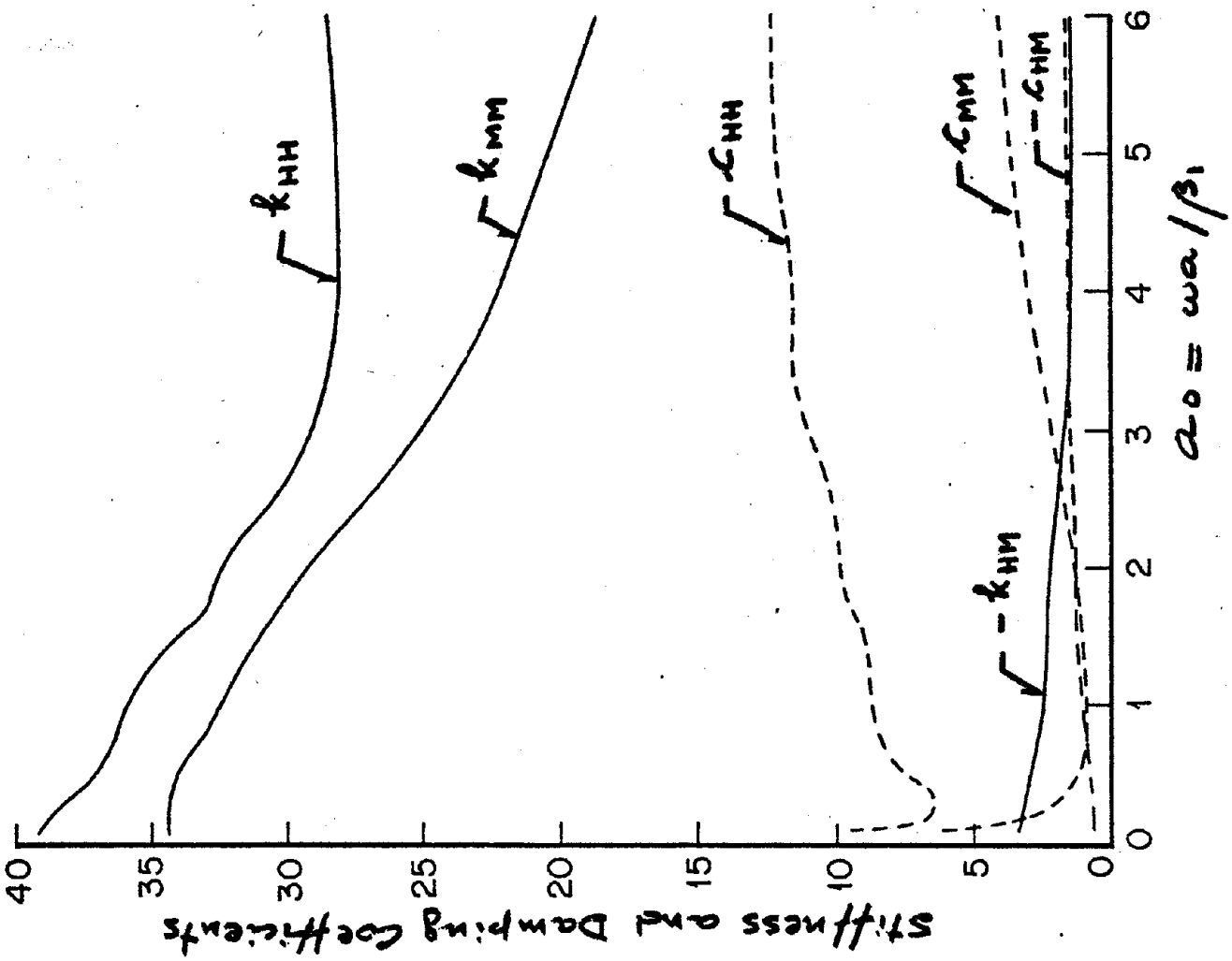

Figure 3.33. Impedance functions for a rigid cylindrical foundation (a = 40 ft, h = 18 ft) embedded in a layered viscoelastic half-space with properties listed in Table 3.1. (Solid lines: stiffness coefficients; dashed lines: damping coefficients).

4. FOUNDATION RESPONSE TO SEISMIC WAVES

4.1 Response of Hemispherical Foundation to Vertically Incident Waves

The finite element method was used to obtain the dynamic response of a rigid hemispherical foundation embedded in a uniform half-space ($\nu = 0.25$) and subjected to vertically incident plane S and P waves. The amplitude of the particle motion in both cases was taken to be $u_o/2$ so that the amplitude of motion on the free surface of the half-space in absence of the foundation is u_o. The geometry of the problem and the finite element grid used are illustrated in Fig. 3.1.

For vertically incident S-waves the response of the foundation, assumed massless and in welded contact with the soil, consists of a translation Δ_H^* and of a rotation ϕ_H^* about a horizontal axis. The response of the foundation is referred to the center of the hemisphere as shown in Fig. 3.1. The real imaginary parts as well as the amplitude of the response are presented in Fig. 4.1 versus the dimensionless frequency a_o. The dimensionless rocking response $\phi_H^* a/u_o$ is presented at the top, while the second figure corresponds to the dimensionless translational response Δ_H^*/u_o.

The results obtained indicate that the embedment of the foundation leads to a marked rocking response which is absent in the case of flat foundations. Also, the scattering of the seismic wave by the embedded foundation leads to a marked reduction of the translational response at high frequencies. These results have important implications in the analysis of the response of structures to seismic excitation.

For vertically incident P-waves the response of the foundation consists of pure translation in the vertical direction Δ_V^*. The real and imaginary parts as well as the amplitude of the normalized response

Δ_V^*/v_o are shown in the last figure of Fig. 4.1. Again the scattering by the embedded foundation leads to a marked reduction of the foundation response at high frequencies. This reduction does not occur for flat foundations excited by vertically incident waves.

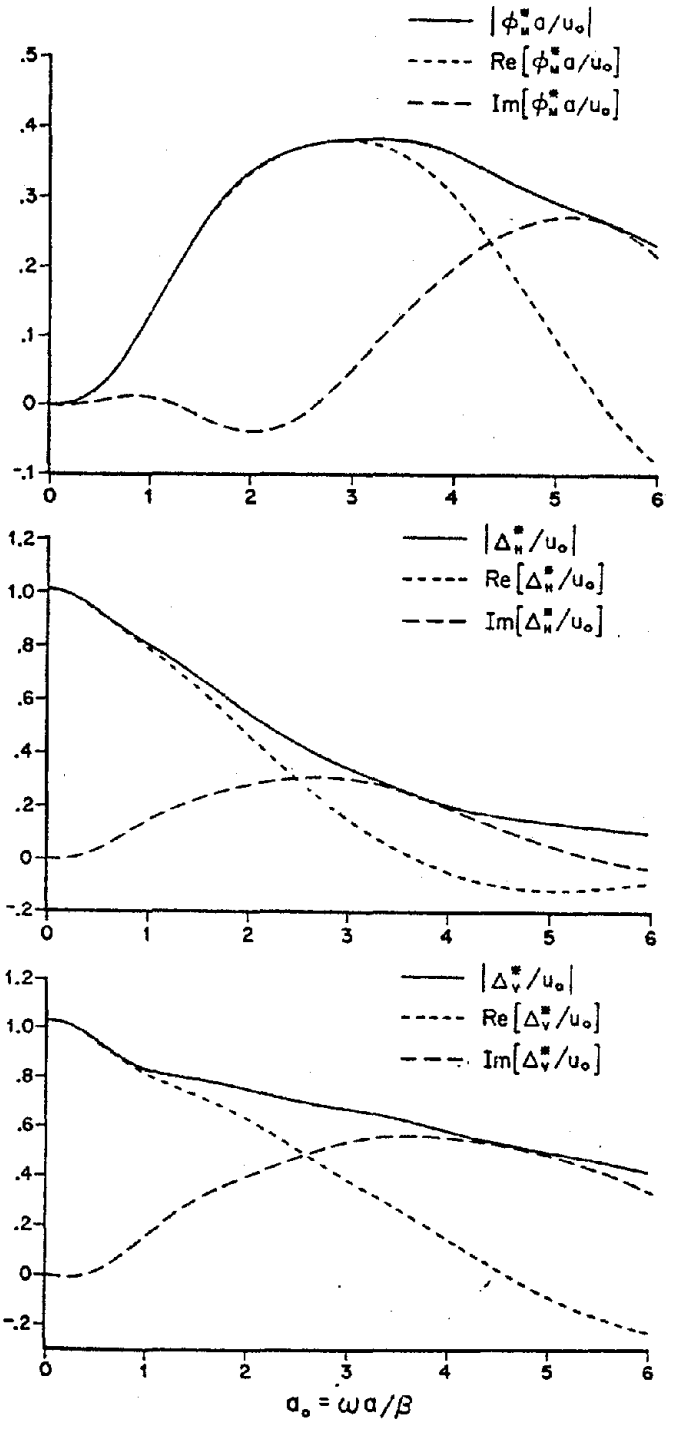

Figure 4.1. Input motion of the embedded hemisphere due to vertically incident plane waves: a) rocking due to incident S waves; b) horizontal translation due to incident S waves; and c) vertical translation due to incident P waves.

4.2 Response of Hemispherical Foundation to Horizontally Incident SH-Waves

The dynamic response of a rigid massless hemispherical foundation embedded in a uniform elastic half-space ($\nu = 0.25$) and subjected to horizontally incident SH-waves of amplitude u_o was obtained by use of the finite element method. The geometry of the problem and the grid used are illustrated in Fig. 3.1.

For horizontally incident SH-waves the response of the foundation consists of a translation Δ_H^*, rocking about a horizontal axis ϕ_M^* and rotation about a vertical axis ϕ_T^*. The results obtained plotted versus the dimensionless frequency a_o are shown in Figs. 4.2 and 4.3. The normalized rocking response $\phi_M^* a/u_o$ and the normalized translational response Δ_H^*/u_o are shown in Fig. 4.2. The results indicate that horizontally incident SH-waves generate a small rocking response and that the scattering of the incoming wave by the rigid foundation leads to a significant reduction of the translational response at high frequencies.

The most important characteristic of the response for horizontally incident SH-waves corresponds to the high torsional response shown in Fig. 4.3. The results shown in Fig. 4.3 indicate that the tangential motion on the perimeter of the foundation ($\phi_T^* a$) associated with the torsional response may be as high as 50 percent of the free-field motion u_o.

A measure of the accuracy of the results obtained is obtained by comparison with the exact solution for the torsional response obtained by Luco (1976). The comparison shown in Fig. 4.3 validates the finite element results in a wide frequency range.

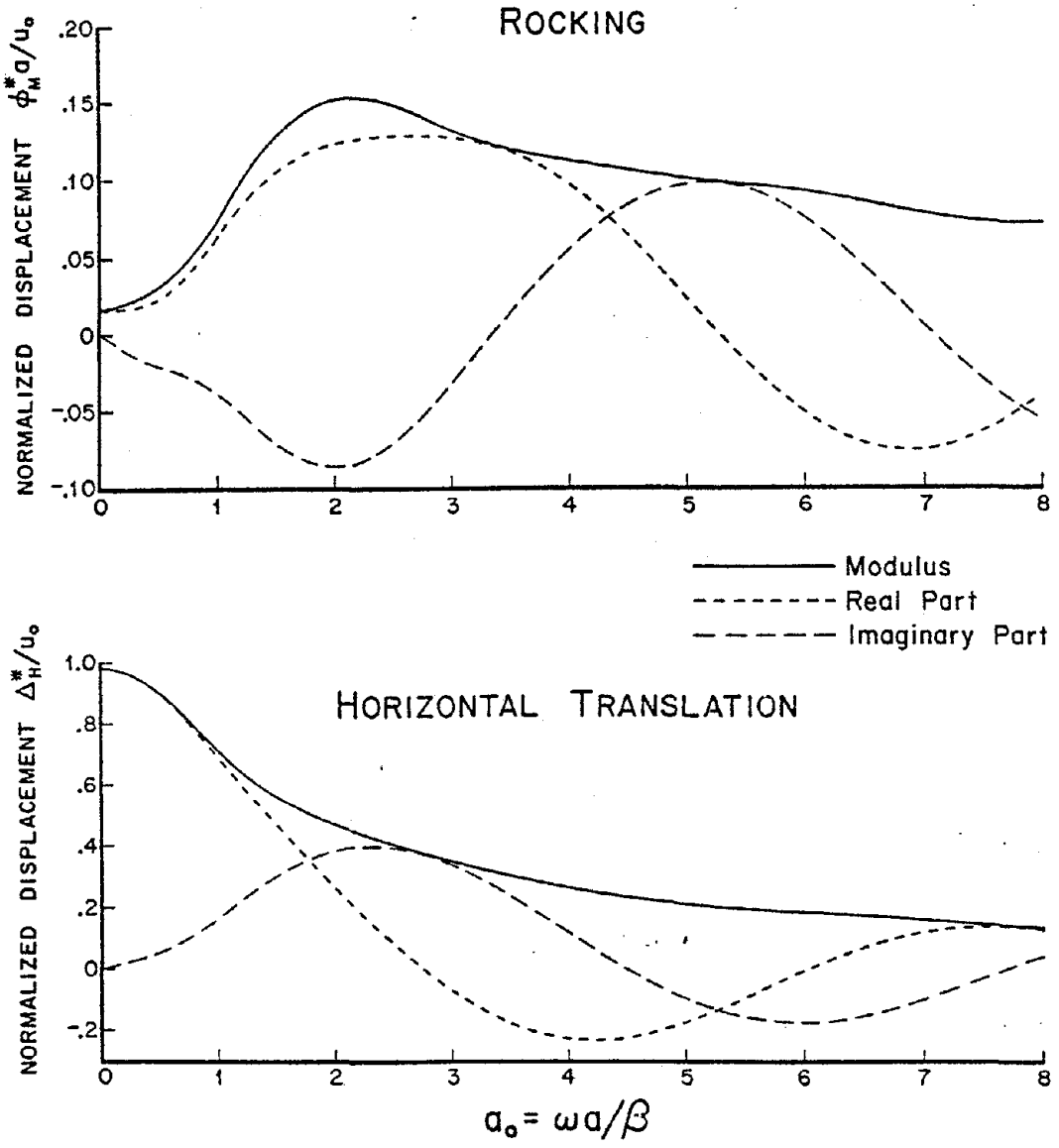

Figure 4.2. Rocking and horizontal components of input motion of the embedded hemisphere, due to horizontally incident, plane SH waves.

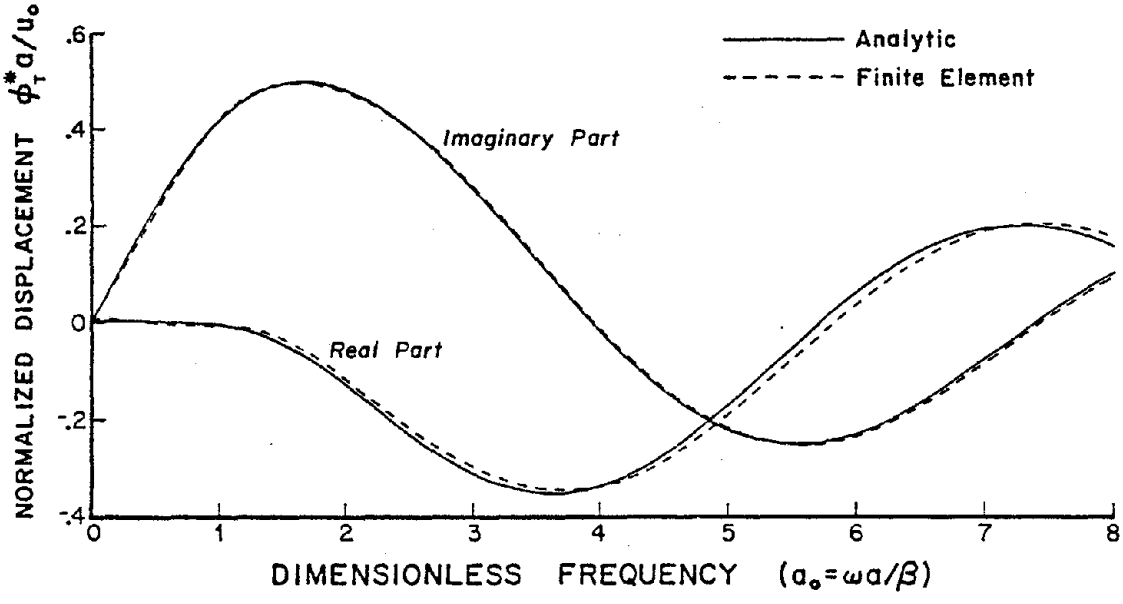

Figure 4.3. Comparison of finite element solution with continuum solution for the torsional input motion of the embedded hemisphere due to horizontally incident, plane SH waves.

4.3 Response of Cylindrical Foundations to Vertically Incident Waves

The response of rigid massless cylindrical foundations embedded in a uniform elastic half-space ($\nu = 0.25$) and subjected to vertically incident S-waves has been studied by use of the finite element method of solution. The geometry of the problem and the grid used are presented in Fig. 3.3. Embedment ratios of 0.5, 1.0 and 2.0 were considered and the foundation was assumed to be in welded contact with the surrounding soil. The amplitude of the incoming S-wave was taken to be $u_o/2$ so that the amplitude of the free-field motion on the soil surface corresponds to u_o.

The response of the cylindrical foundations to vertically incident S-waves consists of a translational component Δ_H^* and a rocking component about a horizontal axis ϕ_M^*. The response of the foundation is referred to the center of the base of the cylinder.

The normalized horizontal response Δ_H^*/u_o is shown in Fig. 4.4 versus the dimensionless frequency a_o for three values of the embedment ratio. The normalized rocking response $\phi_M^* a/u_o$ is shown in Fig. 4.5. A comparison of the effect of embedment on the amplitude of the rocking and horizontal responses is presented in Fig. 4.6. The results obtained indicate that the embedment of the foundation causes a significant reduction of the translational response at high frequencies. The deeper the embedment, the more significant the reduction in translational response. The embedment of the foundation causes a significant rocking response. The rocking response at low frequency becomes more pronounced for deeper foundations.

These results have important implications in the analysis of the response of structures to vertically incident SH-waves. The scattering

effects tend to reduce the structural response while the rocking response has the opposite effect.

The results shown in Fig. 4.6 show that at the extreme low-frequency end the finite element results show an error of about 5 percent (for $a_o = 0$, the ratio Δ_H/u_o should be exactly one).

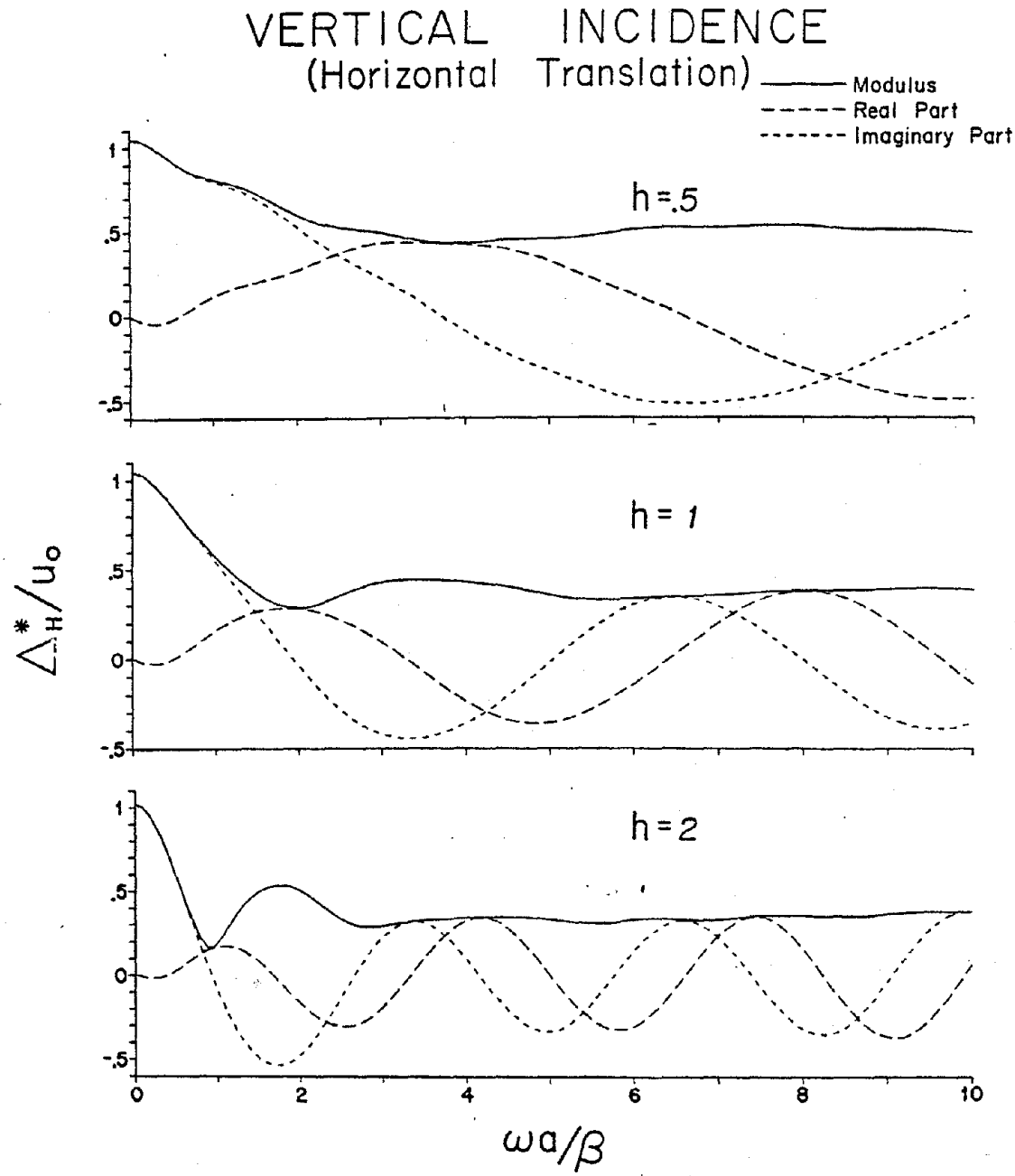

Figure 4.4. Horizontal translational component of the input motion of embedded cylinders, for the case of vertically incident, plane S waves.

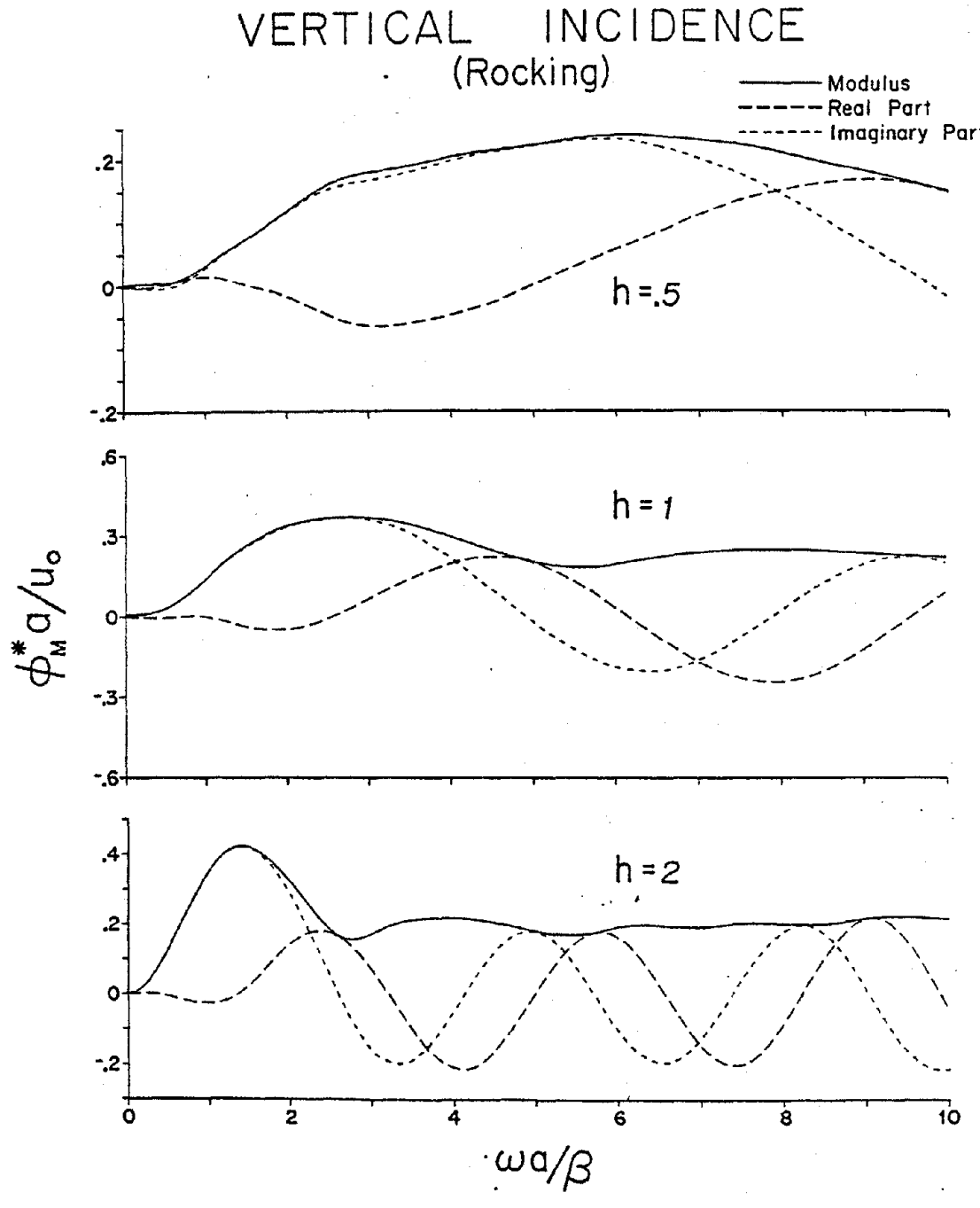

Figure 4.5. Rocking component of the input motion of embedded cylinders for the case of vertically incident, plane S waves.

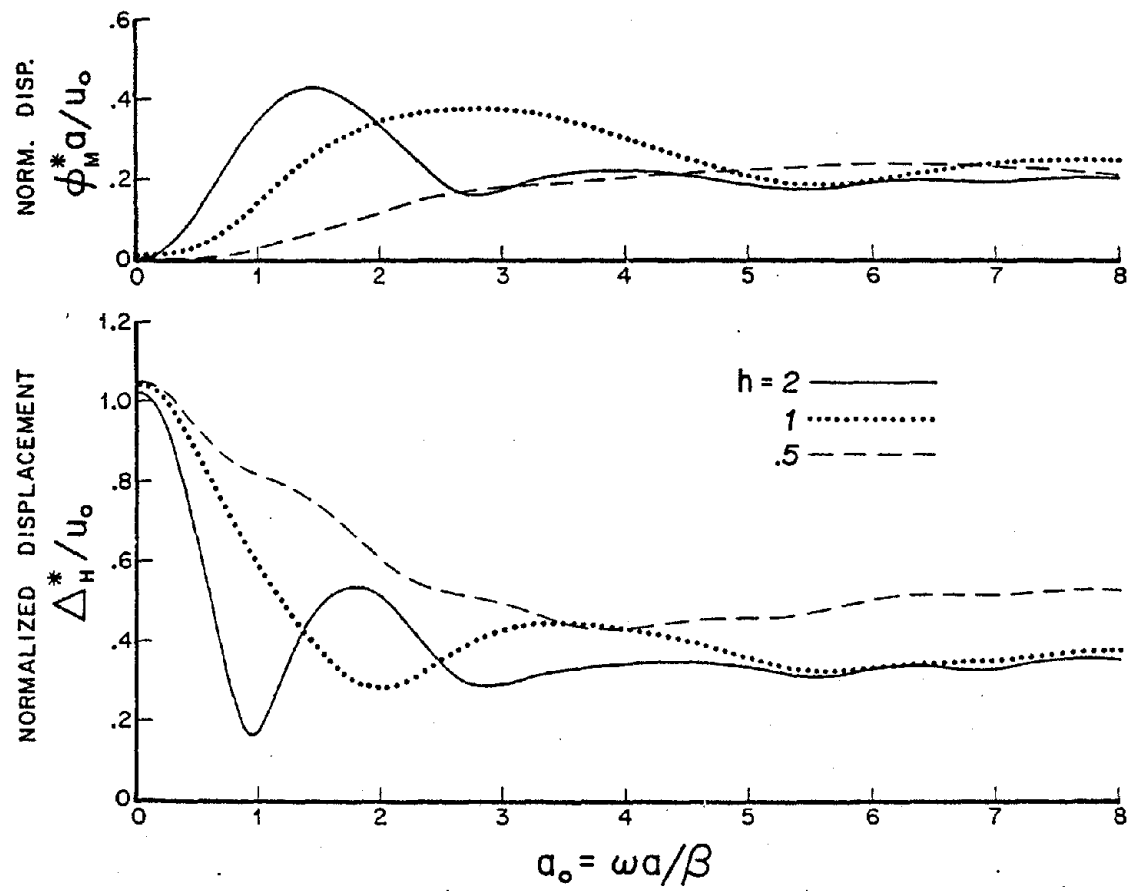

Figure 4.6. Input motion amplitudes of cylinders due to vertically incident, plane S waves: a) rocking; and b) horizontal translation. h is the ratio of depth to radius of the cylinder.

4.4 Response of Cylindrical Foundations to Horizontally Incident SH-Waves

The response of rigid massless cylindrical foundations embedded in a uniform elastic half-space ($\nu = 0.25$) and subjected to horizontally incident SH-waves was investigated. In particular, the effects of the embedment on the response were analyzed by considering foundations with embedment ratios of 0, 0.5, 1.0 and 2.0. The foundations were assumed to be in welded contact with the surrounding soil. The finite element grid considered are shown in Fig. 3.3.

The response of cylindrical foundations to horizontally incident SH-waves of amplitude u_o consists of translation Δ_H^* in the direction of the particle motion, rotation Δ_M^* about a horizontal axis in the direction of propagation of the wave and torsion ϕ_T^* about a vertical axis. The horizontal, rocking and torsional components of the response plotted versus the dimensionless frequency a_o are shown in Figs. 4.7, 4.8 and 4.9, respectively, for embedment ratios of 0, 0.5, 1.0 and 2.0. The amplitudes of the response for different embedment ratios are compared in Fig. 4.10.

The results obtained indicate that the rocking response for horizontally incident SH-waves is quite small and can be neglected for most practical applications. The translational response shows a marked reduction for high frequencies and is almost independent of the embedment depth. As in the case of hemispherical foundation excited by horizontally incident SH-waves, the torsional response of cylindrical foundations to horizontally incident SH-waves is quite significant. The amplitude of the torsional response is almost independent of the embedment for embedment ratios higher than 0.5 in agreement with the results of Apsel and Luco (1977) for semi-ellipsoidal foundations.

The tangential displacement $\phi_T^* a$ on the perimeter of the foundation associated with the torsional response may have an amplitude of 0.4 to 0.6 of the free-field motion amplitude u_o. These high values for the torsional response indicate that present analyses of structrues which are based on the assumption of vertically incident waves need to be reviewed.

Finally, the normalized amplitudes of the response of a cylindrical foundation with an embedment ratio of 1.0 for different types of excitation are compared in Fig. 4.11. The normalized translational response $|\Delta_H^*/u_o|$ (curve (a)) for vertically incident S-waves is compared with the corresponding quantity for horizontally incident SH-waves (curve (b)). The normalized rocking response $|\phi_M^* a/v_o|$ for vertically incident S-waves (curve (c)) is compared with the corresponding quantity for horizontal excitation (curve (d)). The normalized torsional response $|\phi_T^* a/v_o|$ for horizontally incident SH-waves is shown in Fig. 4.11 as curve (e). These results indicate that the angle of incidence of the seismic excitation has an important effect in both the nature and the amplitude of the foundation response.

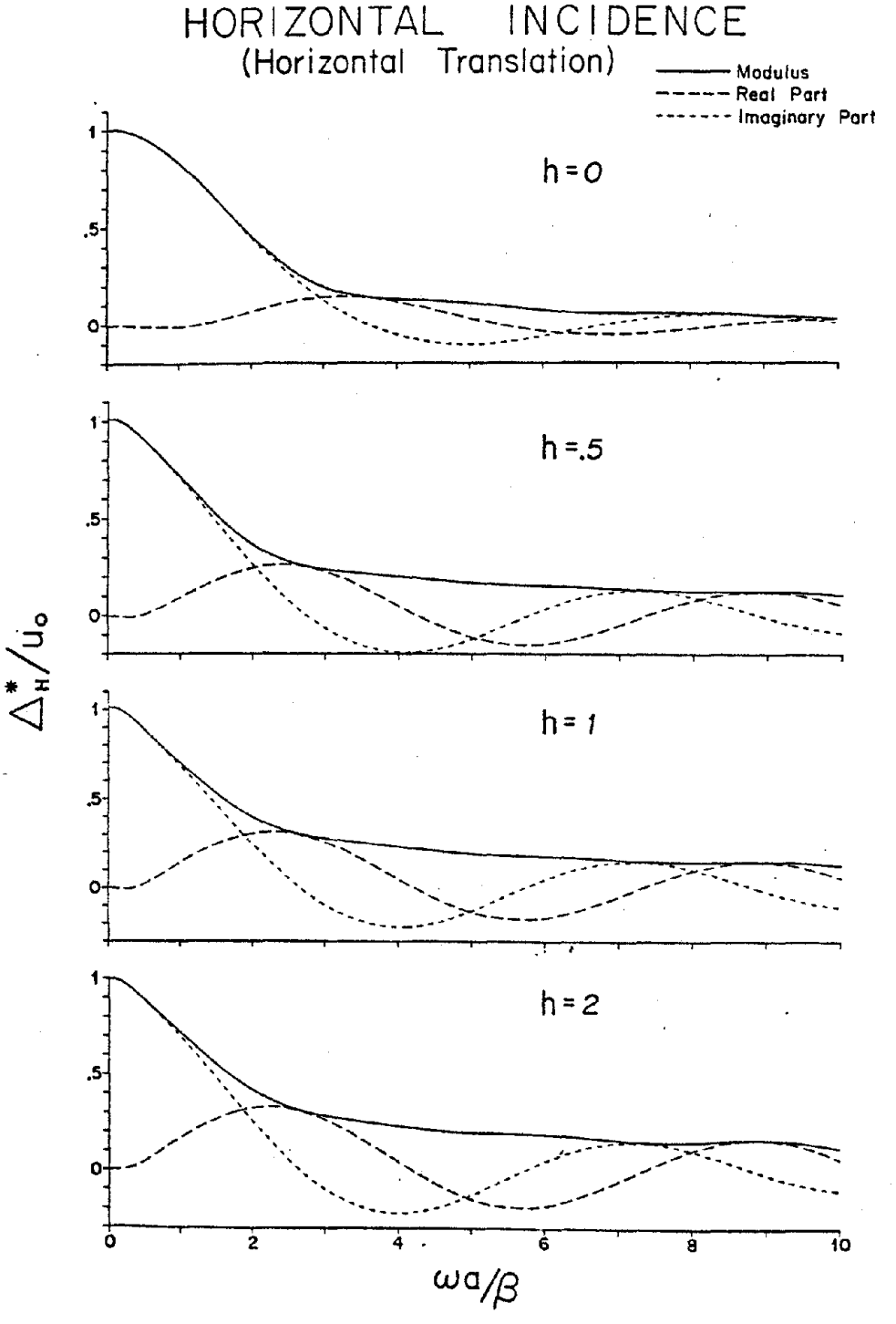

Figure 4.7. Horizontal component of the input motion of embedded cylinders, for the case of horizontally incident, plane SH-waves.

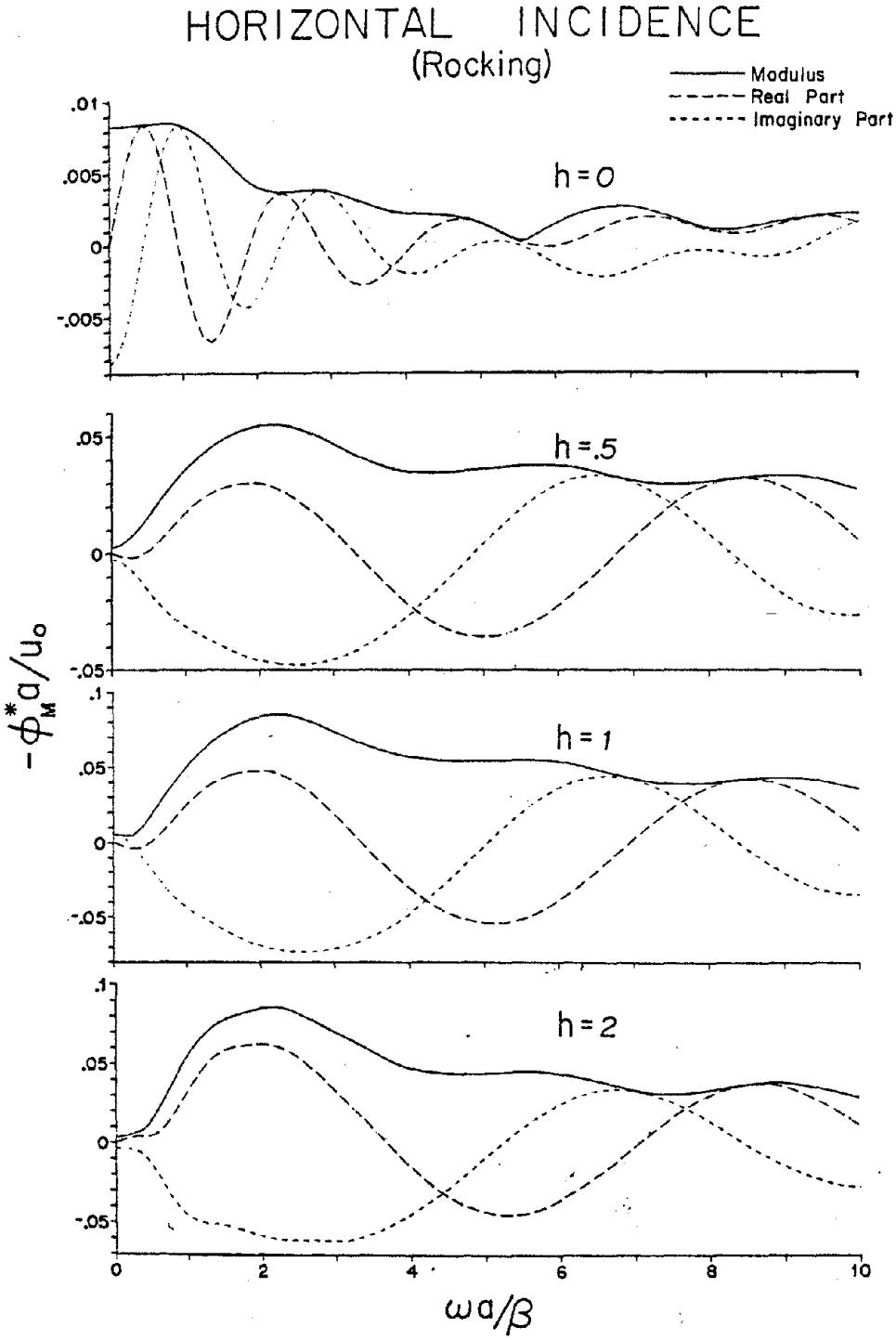

Figure 4.8. Rocking translational component of the input motion of embedded cylinders, for the case of horizontally incident, plane SH waves.

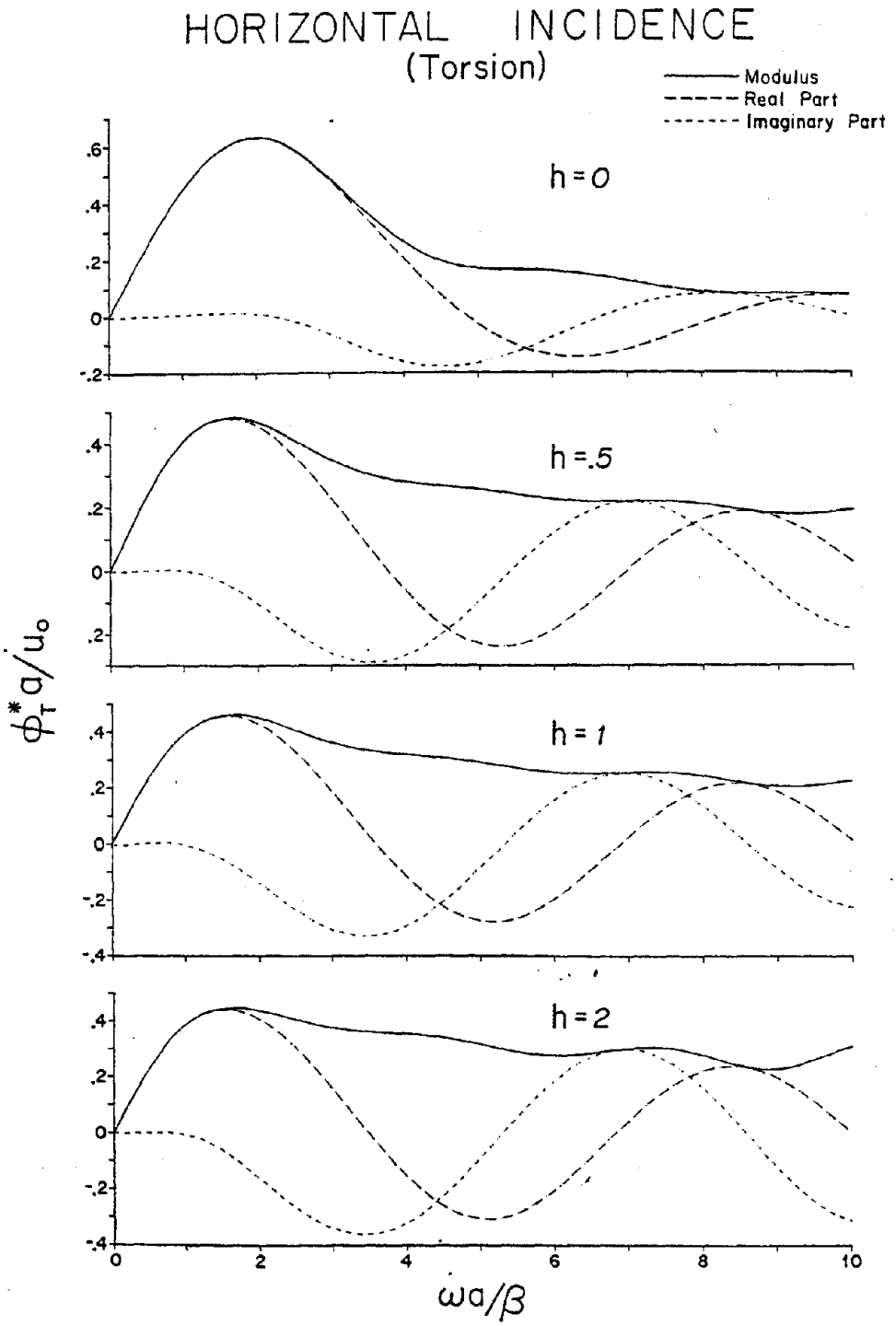

Figure 4.9. Torsional component of the input motion of embedded cylinders, for the case of horizontally incident, plane SH waves.

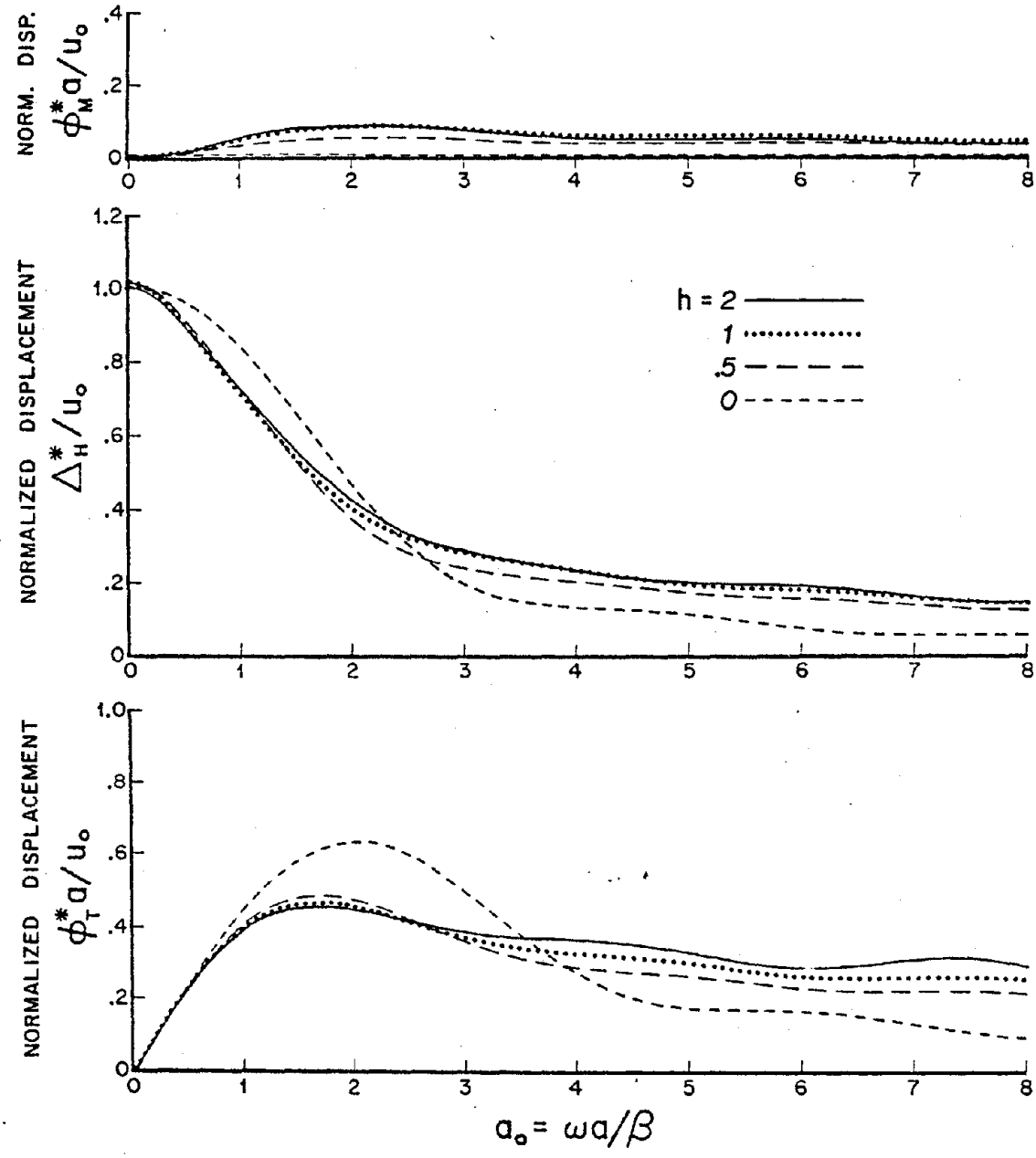

Figure 4.10. Input motion amplitudes of cylinders due to horizontally incident, plane SH waves: a) rocking; b) horizontal translation; and c) torsion. h is the ratio of depth to radius of the cylinder.

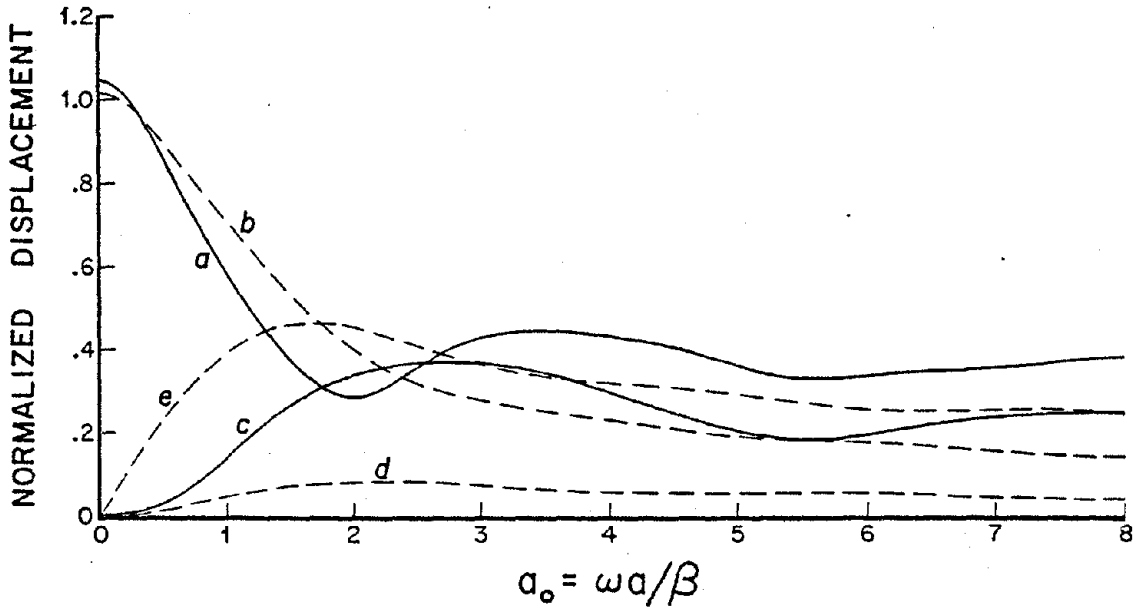

Figure 4.11. Amplitudes of the input motion components of a cylinder with h = 1, due to both horizontally and vertically incident waves.

5. SUMMARY AND CONCLUSIONS

The first objective of this research project was to develop methods to obtain the dynamic response of rigid foundations embedded in layered viscoelastic media and excited by external forces and by obliquely incident seismic waves. A second objective was to generate particular results for different types of foundation geometries, contact conditions, soil deposits and excitation. Finally, it was expected that a general understanding of the dynamic response of embedded foundations would emerge out of a detailed study of the particular results obtained.

From the methodological point of view, two methods to obtain the dynamic response of foundations were developed and tested. The first method is based on performing a transient finite element analysis for a set of impulsive motions of the foundation. The impedance functions and the foundation input motion in the frequency domain are obtained via numerical Fourier transformations. The transient finite element analysis eliminates the nonphysical reflections from the model's boundaries, and it is more efficient than finite element analyses in the frequency domain. The accuracy of the method was documented by comparisons with available analytical solutions.

The second method is based on an integral equation formulation of the boundary-value problem which employs the Green's functions for layered viscoelastic media. Discretization of the integral equations describing the boundary conditions provides a very flexible and efficient method to obtain the dynamic response of foundations in the frequency domain. The accuracy of method was established by comparisons with the results obtained by use of the transient finite element method.

Comparison of the relative advantages of the two procedures indicates that the integral equation approach is more efficient in the case in which the physical properties of the soil change significantly from layer to layer. The integral equation approach is also more flexible in its capability of representing a variety of attenuation mechanisms. The transient finite element method, on the other hand, is capable of considering nonparallel layers while the integral equation approach is limited to the case of parallel horizontal layers.

In terms of particular results, the impedance functions for rigid hemispherical and cylindrical foundations embedded in a uniform half-space have been obtained. The effects of embedment depth, material attenuation constants and types of bond between the foundation and the soil have been investigated. The results obtained indicate that the embedment depth has a marked effect on the amplitude of the impedance functions while the frequency dependence is not significantly affected by the embedment depth. Both the stiffness and radiation damping coefficients increase with increasing embedment depth. The effects are more pronounced on the radiation damping coefficients. The introduction of material attenuation in the soil has the effect of reducing the stiffness coefficients at high frequencies while increasing the damping coefficients at low frequencies. The consideration of partial bonding between the foundation and the soil leads to marked reductions of the impedance functions while at the same time increasing the frequency dependency.

The response of rigid hemispherical and cylindrical foundations embedded in a uniform half-space and subjected to the action of seismic waves has been obtained. The effects on the response of the

angle of incidence of the seismic waves and of embedment depth have been analyzed. For vertically incident SH-waves, the rocking components of the response (which is zero for flat foundations) attains significant values which become more pronounced as the embedment depth increases. The horizontal component (which equals the free-field motion for flat foundations) suffers a marked reduction in amplitude as a consequence of the embedment of the foundation. For horizontally incident SH-waves, the response of the foundation includes horizontal, rocking and torsional components. The rocking response increases with embedment depth but is small compared with the other components. The horizontal components of the response for horizontal incidence also shows a significant reduction, particularly, at high frequencies. The torsional response is quite significant. Both the horizontal and torsional response for horizontally incident SH-waves decrease with embedment at low frequencies, but embedment ratios higher than 0.5 have little effect on these components.

The values obtained in this study completely characterize the response of embedded foundations subjected to external forces and seismic waves and will make possible detailed studies of the interaction between structures and the soil for seismic and wind excitation. The results will also prove useful in the analysis of vibrations of machine foundations.

Some important by-products of the research project must be mentioned. In the process of developing the integral equation method described above, it was necessary to formulate new techniques to determine the Green's functions for layered viscoelastic media. The computer programs developed to compute Green's functions are being extensively

used in strong motion seismology and ocean bottom seismology. The methods developed in this project are also applicable to a variety of radiation and scattering problems encountered in studies of wave propagation. The dynamic response of piles embedded in layered viscoelastic media and excited by external forces and by seismic waves has also been studied by use of the methods developed in this project.

REFERENCES

A1. Luco, J. E.,"Dynamic Interaction of a Shear Wall with the Soil," J. Engrg. Mech. Div., ASCE, Vol. 95, 1969, pp. 333-346.

A2. Trifunac, M. D., "Interaction of a Shear Wall with the Soil for Incident Plane SH waves," Bull. Seism. Soc. Am., Vol. 62 1972, pp. 63-83.

A3. Wong, H. L. and Trifunac, M. D., "Interaction of a Shear Wall with the Soil for Incident Plane SH waves: Elliptical Rigid Foundation," Bull. Seism. Soc. Am., Vol. 64, 1974, pp. 1825-1842.

A4. Luco, J. E., Wong, H. L. and Trifunac, M. D., "A Note on the Dynamic Response of Rigid Embedded Foundations," Earthquake Engrg. and Structural Design, Vol. 4, 1975, pp. 119-127.

A5. Wong, H. L., "Dynamic Soil-structure Interaction," Report EERL 75-01, Earthquake Engineering Research Lab., California Institute of Technology, Pasadena, California, 1975.

A6. Thau, S. A. and Umek, A., "Transient Response of a Buried Foundation to Antiplane Shear Waves," J. Applied Mechanics, Vol. 40, N. 4, Trans. ASME, Vol. 95, Series E, Dec. 1973, pp. 1061-1066.

A7. Dravinski, M., "Multiple Diffractions of Elastic Waves by a Rigid Rectangular Foundation," Ph.D. Thesis, Illinois Institute of Technology, May 1975.

A8. Dravinski, M. and S. A. Thau, "Multiple Diffractions of Elastic Shear Waves by a Rigid Rectangular Foundation Embedded in an Elastic Half Space," J. Applied Mechanics, ASME, Vol. 43, 1976, pp. 295-299.

A9. Umek, A., "Dynamic Responses of a Building Foundation to Incident Elastic Waves, Ph. D. Thesis, Illinois Institute of Technology, Dec. 1973.

A10. Thau, S. A., and Umek, A., "Coupled Rocking and Translating Vibrations of a Buried Foundation," J. Applied Mechanics, Vol. 41, N. 3, Trans. ASME, Vol. 96, Series E, Sept. 1974, pp. 697-702.

A11. Dravinski, M. and S. A. Thau, "Multiple Diffractions of Elastic Waves by a Rigid Rectangular Foundation: Plane-strain Model," J. Applied Mechanics, ASME, Vol. 43, 1976, pp. 291-294.

A12. Luco, J. E., "Torsional Response of Structures for SH Waves: the case of Hemispherical Foundations," Bull. Seism. Soc. Am., Vol. 66, No. 1, Feb. 1976, pp. 109-124.

A13. Apsel, R. J. and Luco, J. E., "Torsional Response of a Rigid Embedded Foundation," J. Engrg. Mech. Div., ASCE, Vol. 102, EM6, 1976. pp. 957-970.

A14. Luco, J. E., "Torsion of a Rigid Cylinder Embedded in an Elastic Half-space," J. Applied Mechanics, Vol. 43, 1976, pp. 419-423.

B1. Baranov, V. A., "On the Calculation of Excited Vibrations of an Embedded Foundation," (in Russian), Voprosy Dynamiki: Prochnocti, No. 14, Polytechnical Institute of Riga, 1967, pp. 195-209.

B2. Novak, M. and Beredugo, Y. O., "The Effect of Embedment on Footing Vibrations," Proceedings of the First Canadian Conference on Earthquake Engineering Research, University of British Columbia, Vancouver, B. C., May 1971, pp. 111-125.

B3. Beredugo, Y. O., "Vibrations of Embedded Symmetric Footings," Ph. D. Dissertation University of Western Ontario, London, Canada, 1971, 247 pp.

B4. Beredugo, Y. O. and Novak, M., "Coupled Horizontal and Rocking Vibration of Embedded Footings," Canadian Geotechnical J., Vo. 9, No. 4, November 1972.

B5. Novak, M. and Beredugo, Y. O., "Vertical Vibration of Embedded Footings," Soil Mech. Found. Div., ASCE, Vol. 98, No. SM12, Dec. 1972, pp. 1291-1310.

B6. Novak, M., "Vibrations of Embedded Footings and Structure," Preprint 2029, ASCE National Structural Engineering Meeting, April 1973, San Francisco, California.

B7. Novak, M. and Sachs, K., "Torsional and Coupled Vibrations of Embedded Footings," Int. Jour. Earthq. Engrg. Struct. Dyn., Vol. 2, No. 1, July-Sept., 1973, pp. 11-33.

B8. Novak, M., "The Effect of Embedment on Vibration of Footings and Structures," Proceedings, Fifth World Conference on Earthquake Engineering, Rome 1973.

B9. Cheng, S., "Soil-Structure Interaction Lumped Parameter Representation for Partially Embedded Footings," San Francisco Power Division, Bechtel Power Corporation, May 1973.

C1. Tajimi, H., "Dynamic Analysis of a Structure Embedded in an Elastic Stratum," Proceedings, Fourth World Conference on Earthquake Engineering, Santiago, Chile, 1969.

C2. Masao, T. and Tajimi, H.,"Earthquake Response of Multi-Story Building Considering Surface Layer — Basement Interaction," Proceedings, Fifth World Conference on Earthquake Engineering, Rome 1973.

C3. Yasui, Y. and Nakagawa, K., "Sway-Rocking Vibration of Rigid-Structure Embedded in an Elastic Stratum," Proceedings, Fifth World Conference on Earthquake Engineering, Rome 1973.

C4. Abe, T. and Ang, A. H. S., "Seismic Response of Structures Buried Partially in a Multi-Layered Medium," Proceedings, Fifth World Conference on Earthquake Engineering, Rome 1973.

D1. Ohsaki, Y., "On Movements of a Rigid Body in semi-infinite Elastic Medium," Proc. Japan Earthquake Engrg. Symp., B-21, August-Sept. 1973, Tokyo, pp. 245-252.

E1. Lysmer, J. and Kuhlemeyer, R. L., "Finite Dynamic Model for Infinite Media," J. Engrg. Mech. Div., ASCE, Vol. 95, No. EM4, August, 1969, pp. 859-877. Closure to Discussions, February 1971, pp. 129-131.

E2. Kuhlemeyer, R. L., "Vertical Vibrations of Footings Embedded in Layered Media," Ph.D. Dissertation, Univ. of California, Berkeley, 1969, 253 pp.

E3. Kaldjian, M. J., Discussion of "Design Procedures for Dynamically Loaded Foundations," by R. V. Whitman and F. E. Richart, Jr., Soil Mech. Found. Div., ASCE, Vol. 95, No. SM1, Jan. 1969, pp. 364-366.

E4. Kaldjian, M. J., "Torsional Stiffness of Embedded Footings," Soil Mech. Found. Div., ASCE, Vol. 95, No. SM1, Jan. 1969, pp. 969-980.

E5. Waas, G. and Lysmer, J., "Vibrations of Footings Embedded in Layered Media," Proceedings of the WES Symposium on Applications of the Finite Element Method in Geotechnical Engineering, U. S. Army Engineer Waterways Experiment Station, Vichsburg, Miss., May 1972, pp. 1-24.

E6. Waas, G., "Earthquake Vibration Effects and Abatement for Military Facilities," Tech. Report, S-71-14, U. S. Army Engineer WES, Vicksburg, Miss., Sept. 1972, 182 pp.

E7. Urlich, C. M. and Kuhlemeyer, R. L., "Coupled Rocking and Lateral Vibrations of Embedded Footings," Can. Geotech., Vol. 10, No. 2, May 1973, pp. 145-160

E8. Kausel, K., Roesset, J. M., and Waas, G., "Dynamic Analysis of Footings on Layered Media," J. of the Engrg. Mech. Div., ASCE, Vol. 101, No. EM5, Oct. 1975, pp. 679-693.

E9. Kausel, K. and Roesset, J. M., "Dynamic Stiffness of Circular Foundations," J. of the Engrg. Mech. Div., ASCE, Vol. 101, No. EM6, Dec. 1975, pp. 771-785.

E10. Lysmer, J. and Waas, G., "Shear Waves in Plane Infinite Structures," J. of the Engrg. Mechs. Div., ASCE, Vol. 98, Feb. 1972, pp. 85-105.

E11. Waas, G., "Linear Two-Dimensional Analysis of Soil Dynamics Problems in Semi-Infinite Layered Media," Thesis presented to the Univ. of California, Berkeley in 1972, in partial fulfillment of the requirements for the degree of Philosophy.

F1. Krizek, R. J., Gupta, D. C., and Parmelee, R. A., "Coupled Sliding and Rocking of Embedded Foundations," J. Soil Mech. Found. Div., ASCE Vol. 98, No. SM12, Dec. 1972, pp. 1347-1358.

F2. Parmelee, R. A. and Weesakul, W., "Soil-Structure Interaction of Embedded Buildings," Structural Dynamics Technical Report No. SD 72-1, Dept. of Civil Engineering, Northwestern University, Evanston, Ill., 1972.

G1. Novak, M., "Vibrations of Massive Foundations on Soil," Int. Assoc. Bridge Struct. Engrg., Publ. No. 20, 1960, pp. 263-281.

G2. Novak, M., "On Some Dynamical Problems of Turbomachinery Frame Foundations," Proc. Int. Symp. Meas. Eval. Dyn. Eff. Vibr. Constr., RILEM, Budapest, Vol. 1, 1963, pp. 215-234.

G3. Fry, Z. B., "Development and Evaluation of Soil Bearing Capacity. Foundations of Structures; Field Vibratory Test Data," Tech. Report No. 3-632, U. S. Army Engineer WES, Vicksburg, Miss., 1963.

G4. Girard, J. and Picard, J., "Experimental Study of the Dynamic Behavior of Machine Foundation Blocks: Verification of Laws of Similitude and Influence of the Embedding Depth," (in French), Ann. Inst. Tech. Bat. Trav., Publ. 23, 1970, 141-156.

G5. Novak, M., "Prediction of Footing Vibrations," J. Soil Mech. Found. Div., ASCE, Vol. 96, No. SM3, May 1970, pp. 337-361.

G6. Chae, Y. S., "Dynamic Behavior of Embedded Foundation-Soil Systems," Highway Research Record, No. 323, 1971, pp. 49-59.

G7. Gupta, B. N., "Effect of Foundation Embedment on the Dynamic Behavior of the Foundation-Soil System," Geot., Vol. 22, No. 1, Mar. 1972, pp. 129-137.

G8. Stokoe, K. H., II, "Dynamic Response of Embedded Foundations," Ph. D. Dissertation, Univ. of Michigan, Ann Arbor, 1972, 251 pp.

G9. Tiedemann, D. A., "Vertical Dynamic Response of Embedded Footings," Bureau of Recl. Report, REC-ERC-72-34, Sept. 1972, 22pp.

H1. Frazier, G. A. and Peterson, C. M., "3-D Stress Wave Code for the ILLIAC IV," Systems, Science and Software Report SSS-R-74-2103, 1974.

H2. Geller, R. J. and Frazier, G. A., "Near Field Modeling of Dislocations in a Heterogeneous Crust: A Dynamic Finite Element Approach," submitted to J. Geophys. Res., 1976.

H3. Lomnitz, C., "Linear Dissipation in Solids," J. of Applied Physics, Vol. 28, No. 2, Feb. 1957, 201-205.

I1. Day, S.M., "Finite Element Analysis of Seismic Scattering Problems," Ph.D. dissertation, University of California, San Diego, 1977.

I2. Apsel, R.J., "Green Functions for Layered Viscoelastic Media," Ph.D. dissertation, University of California, San Diego (in preparation).